NIST-GCR-92-613

Characterization of the Confined Ceiling Jet in the Presence of an Upper Layer in Transient and Steady-State Conditions

V. Motevalli and C. Ricciuti

Grant 60NANBOD1049

United States Department of Commerce
Technology Administration
National Institute of Standards and Technology

ERRATA

NIST-GCR-92-613

Characterization of the Confined Ceiling Jet in the Presence of an Upper Layer in Transient and Steady-State Conditions

V. Motevali and C. Ricciuti

Grant 60NANBOD1049

August 1992

Replace pages 45 and 46

NTIS Order No. PB92-238690

Veldman et al. (1977) derived a similar functional relation for the time constant for an unconfined ceiling using a ceiling element as the control volume. This correlation was used to solve for a time constant to use in equation 5-3. The time constant as developed by Veldman et al. (1977) is given here in a modified form for ΔT_{max} and essentially in the original form for the average upper layer temperature in equation 5-8.

$$\tau = \left(\frac{\rho_c c_{p_c}}{\rho_\infty c_{p_\infty}}\right) \frac{\delta_c}{\sqrt{gH}} Q^{*-1/3} f(r/H)^{-1} \qquad \text{(for } \Delta T^*_{max}\text{)} \quad [5\text{-}7]$$

$$\tau = \left(\frac{\rho_c c_{p_c}}{\rho_\infty c_{p_\infty}}\right) \frac{\delta_c}{\sqrt{gH}} Q^{*-1/3} \qquad \text{(for } \Delta T^*_{ul,avg}\text{)} \quad [5\text{-}8]$$

Equation 5-7 shows that τ is a function of the ceiling properties. This is implied in equation 5-6 as well where h_c has to be determined from an energy balance at the ceiling, which includes conduction heat transfer and reradiation from the ceiling surface (see chapter 7 for details).

Since the average upper layer temperature is not a function of radial location, f(r/H) was dropped from equation 5-7. As shown in equation 5-8 this relation provides a time constant proportional to the experimentally determined time constants for the average upper layer temperature. Figure 5.6 shows the use of Veldman's time constant to correlate the average upper layer temperatures. The result is the same as shown in figure 5.4. Equation 5-7 was used to calculate the value for the time constant for the

maximum ceiling jet temperature where f(r/H) is found in equation 4-4. The substitution of τ developed by Veldman et al. (1977) is shown in figure 5.7. The correlation using the experimentally determined τ is shown in figure 4.19. Figure 4.19 shows a better correlation of the data during the first 10 minutes. Thus, equations 5-9 and 5-10 can be readily used to compute the average upper layer temperature and the maximum ceiling jet temperature (for the confined condition) in conjunction with a value for τ calculated using either equation 5-7 or 5-8, as appropriate.

$$\frac{\Delta T^*_{max}}{f(r/H)} = 1 - e^{(-0.022t/\tau)} \qquad \text{(for } \Delta T^*_{max}\text{)} \quad [5\text{-}9]$$

$$\Delta T^*_{avg,ul} = (7.1 + 0.0099(t/\tau))(1 - e^{-0.22t/\tau}) \qquad \text{(for } \Delta T^*_{ul,avg}\text{)} \quad [5\text{-}10]$$

Note: The x-axis of figures 5.6 and 5.7 should be divided by 2.2.

NIST-GCR-92-613

Characterization of the Confined Ceiling Jet in the Presence of an Upper Layer in Transient and Steady-State Conditions

V. Motevalli and C. Ricciuti

Worcester Polytechnic Institute
Worcester, MA 01609

August 1992

Sponsored by:
U.S. Department of Commerce
Barbara Hackman Franklin, *Secretary*
Technology Administration
Robert M. White, *Under Secretary for Technology*
National Institute of Standards and Technology
John W. Lyons, *Director*

Notice

This report was prepared for the Building and Fire Research Laboratory of the National Institute of Standards and Technology under grant number 60NANBOD1049. The statements and conclusions contained in this report are those of the authors and do not necessarily reflect the views of the National Institute of Standards and Technology or the Building and Fire Research Laboratory.

Characterization of the Confined Ceiling Jet in the Presence of an Upper Layer in Transient and Steady-State Conditions

FINAL REPORT
August 1990 - July 1991

by

Vahid Motevalli and Christina Ricciuti
Center for Firesafety Studies
Worcester Polytechnic Institute
Worcester, Massachusetts 01609

Submitted to:

U.S. Department of Commerce
National Institute for Standards and Technology
Building and Fire Research Laboratory
Gaithersburg, Maryland 20899

Submitted by: 
Vahid Motevalli, Ph.D.
Assistant Professor

PREFACE

This is a final report on the project entitled "Characterization of the Confined Ceiling Jet in the Presence of an Upper Layer in Transient and Steady-State Conditions" which was performed under Grant No. 60NANBOD1049. The total duration of this project was one year. This report essentially and for the most part constitutes the thesis completed by Christina Ricciuti.

Abstract

Although both confined and unconfined smooth ceiling jets have been previously studied, the data from small-scale experiments evaluated in this report provided a unique opportunity to characterize the transience of a ceiling jet in the presence of a developing upper layer.

The development of an upper layer in an enclosure fire has notable effects on the ceiling jet. The presence of this hot gas layer increases the temperature in the ceiling jet and the heat transfer to the ceiling. Accurate prediction of the characteristics of the confined ceiling jet is important in calculating the response time of detection and suppression devices. This report examines data from a study of small-scale fire induced ceiling jet in a confined situation for a smooth horizontal ceiling. These results were obtained from experiments conducted at the National Institute of Standards and Technology, Center for Fire Research using 2.0 and 0.75 kW fires at r/H locations of 0.26 and 0.75. The data gathered from these experiments represents a collection of transient and steady-state temperature and velocity measurements of a confined ceiling jet and upper layer. The results from this data were compared to similar experimental data collected in a previous study for unconfined ceiling jet using the same apparatus. Comparison of the confined and unconfined ceiling jet data, quantification of the developing upper layer and analysis of heat transfer to the ceiling, are presented in this report. Despite the limited data, it is concluded that the unconfined ceiling jet correlations may only be valid at the very early time, prior to development of the upper layer and that steady-state unconfined correlations are certainly invalid for confined conditions. The velocity of the confined ceiling jet within the upper layer is 20-25% less than the unconfined case affecting the heat transfer coefficient. The heat transfer analysis showed that values of 4-5 $W/m^2°C$ can be expected. Comparisons with LAVENT computer program are also presented in this report.

Acknowledgements

The authors would like to acknowledge The National Institute of Standards and Technology, Center for Fire Research for their partial support under Grant No. 60NANBOD1049.

Table of Contents

Page

List of Figures vi
List of Tables ix
Nomenclature x

Chapter 1 - Introduction 1
1.1 Description of Problem 2
1.2 Objectives 3

Chapter 2 - Literature Review 6
2.1 Experimental Work 6
2.2 Theoretical Work 9

Chapter 3 - Apparatus and Data Collection 11
3.1 Collected Data 11
3.2 Experimental Apparatus 13
3.3 Experimental Method and Collection of Data 14

Chapter 4 - Data Analysis 17
4.1 Ceiling Jet Velocity Profile 18
4.2 Ceiling Jet Maximum Velocity 19
4.3 Ceiling Jet Temperature Profile 22
4.4 Ceiling Jet Maximum Temperature 23

Chapter 5 - Development and Characteristics of the Upper Layer 39
5.1 Development of the Upper Layer 40
5.2 Average Upper Layer Temperature 41
5.3 Energy Balance for the Upper Layer 43

Chapter 6 - Predicting Ceiling Jet Behavior 54
6.1 Equations for the Ceiling Jet in the Upper Layer 54
6.2 LAVENT 59

Chapter 7 - Prediction of Heat Transfer to the Ceiling and Maximum Ceiling Jet Temperature 69
7.1 Thermal Boundary Layer 69
7.2 The Heat Transfer Coefficient 71
7.2.1 Numerical Analysis 72
7.2.2 Exact Solution 73
7.2.3 Cooper and Woodhouse 74

Page
7.3 Comparison with the Experimental Data 76

Chapter 8 - Conclusions 82

References 86

Appendices

Appendix A - Temperature and Velocity Data For Ceiling Jet
Appendix B - Temperature Data for Ceiling jet and Upper Layer
Appendix C - Test Conditions and Constants
Appendix D - Heat Conduction Program - ASCL
Appendix E - Ceiling Surface Temperature

List of Figures

		Page
Figure 1.1 -	Confined Ceiling Jet and Developing Upper Layer	2
Figure 3.1 -	Experimental Apparatus for Confined Ceiling	13
Figure 4.1 -	Velocity Profile for 2.0 Kilowatt Fire, r/H of 0.26	29
Figure 4.2 -	Velocity Profile for 2.0 Kilowatt Fire, r/H of 0.75	29
Figure 4.3 -	Velocity Profile, Confined vs. Unconfined for 2.0 Kilowatt Fire, r/H of 0.26, 5 Seconds and Steady State	30
Figure 4.4 -	Velocity Profile, Confined vs. Unconfined for 2.0 Kilowatt Fire, r/H of 0.75, 5 Seconds and Steady State	30
Figure 4.5 -	Ceiling Jet Temperature Profile for 2.0 Kilowatt Fire, r/H of 0.26	31
Figure 4.6 -	Ceiling Jet Temperature Profile for 2.0 Kilowatt Fire, r/H of 0.75	31
Figure 4.7 -	Upper Layer Temperature Profile for 2.0 Kilowatt Fire, r/H of 0.26	32
Figure 4.8 -	Upper Layer Temperature Profile for 2.0 Kilowatt Fire, r/H of 0.75	32
Figure 4.9 -	Upper Layer Temperature Profile for 0.75 Kilowatt Fire, r/H of 0.26	33
Figure 4.10-	Upper Layer Temperature Profile for 0.75 Kilowatt Fire, r/H of 0.75	33
Figure 4.11-	Normalized Temperature Profile, r/H of 0.26	34
Figure 4.12-	Normalized Temperature Profile, r/H of 0.75	34
Figure 4.13 -	Confined Vs. Unconfined Ceiling Jet Temperature, 5 Seconds	35
Figure 4.14 -	Confined Vs. Unconfined Ceiling Jet Temperature, 30 Seconds	35

Page

Figure 4.15 - Confined Vs. Unconfined Ceiling Jet Temperature, 1 Minute 36

Figure 4.16 - Confined Vs. Unconfined Ceiling Jet Temperature, Steady State 36

Figure 4.17 - Maximum Ceiling Jet Temperature Vs. Time 37

Figure 4.18 - Maximum Ceiling Jet Temperature Vs. Time Normalized by Q^* and T_∞ 37

Figure 4.19 - Curve Fit for Maximum Ceiling Jet Temperature 38

Figure 4.20 - Comparison of Maximum Ceiling Jet Temperature in Small-Scale Confined Ceiling Jet Experiments 38

Figure 5.1 - Average Upper Layer Temperature Vs. Time 51

Figure 5.2 - Maximum vs. Average Upper Layer Temperatures, 2.0 Kilowatt Fire 51

Figure 5.3 - Maximum vs. Average Upper Layer Temperatures, 0.75 Kilowatt Fire 52

Figure 5.4 - Curve Fit for Average Upper Layer Temperature 52

Figure 5.5 - Control Volume for Energy Balance of the Upper Layer 44

Figure 5.6 - Average Upper Layer Temperature Using τ from Veldman et al. (1977) 53

Figure 5.7 - Maximum Ceiling Jet Temperature Using τ from Veldman et al. (1977) 53

Figure 6.1 - Comparison of Small-Scale Experimental Data Using Evans Correlations for ΔT_{max} ; Q from 0.63-2.0 kW 64

Figure 6.2 - Comparison of Experimental Temperature Data with LAVENT Results: Confined Ceiling, 2.0 kW, r/H=0.26, 1 Minute 64

		Page
Figure 6.3 -	Comparison of Experimental Temperature Data with LAVENT Results: Confined Ceiling, 2.0 kW, r/H=0.26, 3 Minutes	65
Figure 6.4 -	Comparison of Experimental Temperature Data with LAVENT Results: Confined Ceiling, 2.0 kW, r/H=0.26, Steady State	65
Figure 6.5 -	Comparison of Experimental Velocity Data with LAVENT Results: Confined Ceiling, 2.0 kW, r/H=0.26, Steady State	66
Figure 6.6 -	Comparison of Experimental Temperature Data with LAVENT Results: Confined Ceiling, 2.0 kW, r/H=0.75, Steady State	66
Figure 6.7 -	Comparison of Experimental Temperature Data with LAVENT Results: Confined Ceiling, 0.75 kW, r/H=0.26, Steady State	67
Figure 6.8 -	Comparison of Experimental Temperature Data with LAVENT Results: Confined Ceiling, 0.75 kW, r/H=0.75, Steady State	67
Figure 6.9 -	Comparison of Unconfined Ceiling Jet Temperature Profile with LAVENT Results	68
Figure 6.10-	Comparison of Unconfined Ceiling Jet Velocity Profile with LAVENT Results	68
Figure 7.1 -	Heat Transfer Coefficient	80
Figure 7.2 -	Energy Balance at the Ceiling	80
Figure 7.3 -	Heat Transfer Coefficient to the Ceiling Using the Exact Solution	81
Figure 7.4 -	Comparison of Numerical and Exact Solution for $\dot{q}''_{cond}$	81

List of Tables

		Page
Table 3.1 -	Data Collected for Confined Ceiling	12
Table 4.1 -	Maximum Velocity with Position for the 2.0 Kilowatt Fire	21
Table 4.2 -	Maximum Temperature and Position for the 2.0 Kilowatt Fire	24
Table 5.1 -	Upper Layer Temperature for the 2.0 kW fire at r/H of 0.26	47
Table 5.2 -	Upper Layer Temperature for the 2.0 kW fire at r/H of 0.75	48
Table 5.3 -	Upper Layer Temperature for the 0.75 kW fire at r/H of 0.26	49
Table 5.4 -	Upper Layer Temperature for the 0.75 kW fire at r/H of 0.75	50
Table 7.1 -	Heat Transfer Coefficient	78
Table 7.2 -	Heat Transfer Coefficient calculated Using Cooper and Woodhouse	76

Nomenclature

b_c	Characteristic fire plume radius at the ceiling level, (m)
c_p	Specific heat at constant pressure, (kJ/kg k)
d_c	Ceiling thickness, (m)
d_w	Wall thickness, (m)
g	Gravitational acceleration, (m/s^2)
h	Convective heat transfer coefficient, (W/m^2 k)
H	Height of the burner above the ceiling, (m)
k	Thermal conductivity, (W/m k)
ℓ	Gaussian Thickness, (m)
Nu	Nusselt number
Pr	Prandtl number
Q	Heat source strength, kW
Q^*	Normalized rate of heat release
$\dot{q}''_{cond}$	Conductive heat transfer, (kW/m^2)
$\dot{q}''_{conv}$	Convective heat transfer
$\dot{q}''_{rerad}$	Radiative heat transfer
r	Radial distance from the centerline of the plume, (m)
R	Radius of the confined ceiling, (m)
Re_H	Reynolds number at the plume centerline
Re_x	Local Reynolds number
t	Time, (sec)
T	Absolute temperature, (K)
ΔT	$T-T_\infty$ (°C)
$\Delta T_{ul,avg}$	Average upper layer temperature, (°C)
U_p	Centerline plume velocity, (m/s)
V	Ceiling jet velocity, (m/s)
y	Depth of upper layer, (m)
z	Distance measured down from the ceiling, (m)
z_o	Location of the virtual origin measured up from the burner, (m)
Z	Height of the layer interface measure from the burner, (m)

Greek Symbols

α	Thermal diffusivity, (m^2/s)
δ	Boundary layer characteristic thickness, (m)
δ_{Tmax}	Thermal boundary layer thickness, (m)

$\delta_{V\,max}$	Momentum boundary layer thickness, (m)
δ_c	Ceiling thickness, (m)
ϵ	Emissivity
θ	Non-dimensionalized thermal excess temperature
λ	Fraction of radiative heat loss from the fire
ρ	Density, (kg/m^3)
σ	Stephan-Boltzmann constant, (N/m^2k^4)
τ	Time constant, (s)

Subscripts

c	Ceiling property
g	Fire product property
max	Maximum value for that property
T	Related to temperature
V	Related to velocity
∞	Ambient
1	Relates to the lower layer
2	Relates to the upper layer

Chapter 1: Introduction

One of the important elements to be modeled during a developing enclosure fire is the ceiling jet flow. This jet is formed when the fire plume impinges on the ceiling and expands radially. The velocity and temperature characteristics of this ceiling jet are used to model compartment fire-induced flows, determine the activation time of detection and suppression devices, convective heat transfer to the ceiling and development of the upper layer.

This report is the result of the analysis of data collected by Motevalli for confined smooth ceiling jets in transient and steady-state conditions. Comparison with the unconfined study by Motevalli and Marks (1990) is also made. The data collected for the unconfined case is extensive and detailed. A more limited set of data were collected for the confined case than for the unconfined case, however, a good comparison can be made between the data collected for the two cases. The same apparatus was used to test both cases, but modified for the second case to create a confined ceiling by adding a one-half meter curtain wall to the perimeter of the ceiling. Examination and comparison of the two cases helped to define the confined ceiling jet characteristics and the effect of the developing upper layer. The results can be used to aid in the development and verification of compartment fire models and to improve the design and placement of heat detectors and sprinklers. Results from the steady-state unconfined ceiling jet have been used to predict the ceiling jet characteristics for confined ceiling jets at early times in the fire. The basis for comparison is the fact that the unconfined ceiling jet has been studied

extensively. Using the unconfined ceiling jet permitted the study of the jet characteristics alone without any interference from the developing upper layer. The unconfined ceiling jet simulates a condition where the walls are much further from the plume centerline. It is held that during early stages of a fire where the walls are much further from the plume centerline there is not sufficient time for the build up of an upper layer that will have a significant effect on the ceiling jet.

1.1 Description of the Problem

In an enclosure fire the plume impinges on the ceiling and flows radially outward, parallel to the ceiling, forming a ceiling jet. In the case of the unconfined ceiling (ceiling boundaries much farther than H), the jet flows along the ceiling entraining the enclosure's cooler ambient air and transferring heat to the ceiling. The ceiling jet grows

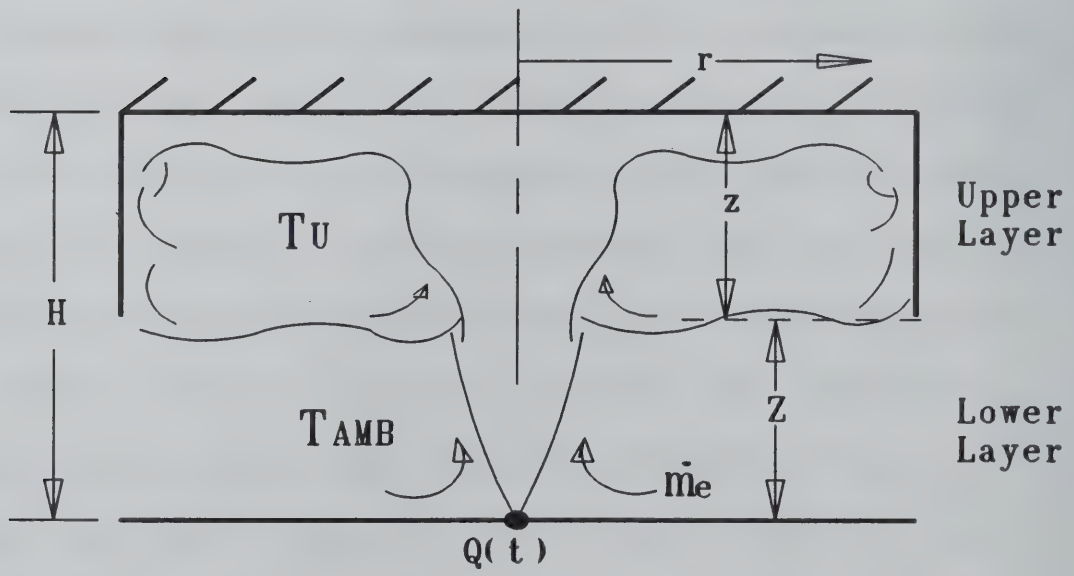

Figure 1.1 - Confined Ceiling Jet and Developing Upper Layer

in thickness as the temperature and velocity decrease. In an enclosure, this jet is forced to turn again when the flow encounters a wall, as shown in figure 1.1. This jet will cause the formation of an upper layer of hot gases and fire products. The ceiling jet is at elevated temperatures and velocities when it encounters the boundaries. As the upper layer forms, it effects the characteristics of the ceiling jet and portion of the plume contained in the upper layer. The plume and ensuing ceiling jet contained in the upper layer have a lower momentum and an increased temperature. These effects on the ceiling jet need to be closely examined and quantified to define the confined ceiling jets characteristics. Characterization of the confined ceiling jet is attempted here through analysis of the confined ceiling jet data and comparison with the unconfined data.

1.2 Objectives

This study is concerned with the characterization of the confined ceiling jet in the presence of an upper layer, the development of the layer and the comparison of these characteristics to the unconfined ceiling jet. Data from the experiments and results will be presented here in a manner that will aid other researchers studying ceiling jets.

The ceiling jet is studied using detailed temperature and velocity measurements. Temperature measurements were also obtained for the upper layer. Three objectives are addressed in this work. The first objective is to compare and analyze the data for the confined ceiling with the correlations obtained from the unconfined ceiling and to determine differences in the characteristics of the ceiling jet due to the effect of the upper

layer development on the ceiling jet. Consideration will be given to examination of both the ceiling transient and steady-state conditions and whether the upper layer temperature can be assumed uniform in the vertical and radial directions.

The second objective is to quantify the transient and steady-state characteristics of the confined ceiling jet and the upper layer. While the fire source is in a steady state condition, the ceiling heating creates a transient condition affecting both the upper layer and the ceiling jet. Changing and developing temperature and velocity profiles of the confined ceiling jet are studied due to their importance in designing and predicting the operation time of detection and suppression devices. These devices are designed to operate early in the event of a fire when the ceiling jet is changing rapidly with time. Velocity measurements will be examined for changing characteristics and trends as the upper layer develops. Since no velocity measurement of the ceiling jet has been obtained in the presence of the upper layer, the analysis of the velocity measurements will be a significant contribution. This data will be used to test existing correlations developed by Cooper (1984) and Evans (1984) for calculating the characteristics of the plume immersed in the upper layer and the enclosure fire model LAVENT developed by Cooper (1990).

The third objective is to analyze the heat transfer from the ceiling jet to the ceiling. It is important to quantify this phenomenon to aid in understanding the energy

transfer in an enclosure fire environment and ceiling jet modelling.

Chapter 2: Previous Work

Early studies of ceiling jets were limited to analog modeling in different media such as salt water simulation. Since that time, ceiling jet studies have mostly used full-scale and laboratory-scale fires in unconfined and confined conditions. Still missing from this growing base of fire studies are measurements in the transient period, essentially ceiling heating effects on the ceiling jet in both steady and growing fires, detailed temperature measurements, measurements for confined ceiling jet velocity and quantification of the effect of the upper layer on the confined ceiling jet. Previous works that are related in developing the history of ceiling jet study will be examined here. In reviewing these previous studies it is convenient to break them into two categories. These categories are experimental and theoretical work.

2.1 Experimental Work

Several investigations of confined ceiling jets, produced from small buoyant sources, have been conducted. These studies include Ellison and Turner (1959) who studied inclined plumes and surface jets using salt water to model entrainment and predict mean velocity and fluid concentration. Baines and Turner (1969) also used salt water modeling to simulate the buoyant plume and ensuing ceiling jet. Prahl and Emmons (1975) studied the resulting flow through enclosure openings using kerosene and water.

The first comprehensive experimental investigation of confined ceiling jets was conducted by Zukoski and Kubota (1977) to examine the effect of an upper layer on the ceiling jet flow field and heat transfer to the walls and ceiling. In their study, two separate small-scale models were used. Flow patterns were examined in a room model with a cut-out door and an enclosure created by a ceiling and curtain wall. A smoke tracer was used to visually observe the flow field in the enclosure. Temperature measurements were obtained in the upper layer at various radial locations. Nine thermocouples were placed on a movable probe with 5 cm spacings between the top six and 2.5 cm spacing between the bottom three. Using these measurements temperature maps of the upper layer were developed. These maps show a uniform "well-mixed" upper layer temperature. They also found the convective heat transfer coefficient (to the ceiling) in a range between 5-40 $W/m^2°C$. They concluded that the level of the gas temperature increases as the walls heat up and the heat transfer to the walls decreases, and the mixing process of the upper layer is independent of the heat transfer to the walls.

You and Faeth (1978) conducted small-scale fire tests to examine the effect of the upper layer and fire impingement on the ceiling. They considered both confined and unconfined cases. During the experiments, measurements were obtained of heat fluxes received at the ceiling, flame heights, flame lengths along the ceiling and mean temperature profiles within the ceiling jet flow. Results from the experiments were compared to available correlations with relatively good agreement.

Small-scale enclosure tests were also conducted by Evans (1983). Data from these experiments were collected during steady-state conditions. In the experiments, the plumes centerline temperature from the ambient lower layer through the interface into the upper layer were measured. The temperature of the layer just outside the plume at steady-state was also measured. The objective of this study was to develop a simple approximation for the plume's new characteristics when contained in the upper layer to be used in models for calculation of ceiling jet characteristics in an enclosure.

Full-scale enclosure fire tests were conducted by Mullholland et al. (1981), Steckler et al. (1982) and Cooper et al. (1982a). Limited upper layer temperature measurements were recorded in all these experiments.

Mullholland et al. (1981) studied smoke movement, heat flux to the ceiling and the filling of an enclosure using smoke generated by a diffusion flame. Steckler et al. (1982) concentrated on examining flows through an opening. Data from transient full-scale fire tests was used to evaluate room fire flow theories dealing with opening and entrainment flows. Cooper et al. (1982) used steady-state and time varying heat release rates in full-scale multi-room fire scenarios to generate an experimental data base to use in verifying mathematical fire simulation models. The testing focussed on smoke filling and selected measurements of the increasing temperatures over time.

Many studies have been conducted to find the heat transfer coefficient and the heat transferred to the ceilings (confined and unconfined) and walls of an enclosure. Veldman et al. (1977), Zukoski and Kubota (1977), You and Faeth (1979), Quintere and McCaffery (1980), Woodhouse and Marks (1985), Alpert (1987) and Motevalli and Marks (1990a&c) conducted experimental work which addressed the heat transferred to the unconfined ceiling. Woodhouse and Marks (1985) studied the transient thermal response of unconfined ceilings above fires. The results of Woodhouse and Marks experiments included a data base of ceiling temperatures as a function of time and position from the plume center line for a range of ceiling material properties. Cooper (1982) and Cooper and Stroup (1987) examined convective heat transfer to the ceiling using data from these experimental studies. In these papers a method was developed for estimating the heat transfer to the unconfined ceiling.

2.2 Theoretical Work

Cooper and Woodhouse (1986) reevaluated the calculations for the heat transfer to an unconfined ceiling developed in previous works. This work also related the heat transferred by the unconfined ceiling jet to the heat transferred by the confined ceiling jet. Their analysis developed an independent estimate for the surface temperature of an adiabatic ceiling and re-radiation from the ceiling was also considered.

In other studies, Morita and Hirota (1989) examined the convective heat flow and turbulent convection and radiation in a fire compartment using numerical analysis.

Cooper (1988, 1989) examined negatively buoyant ceiling jet driven wall flows and the heat transfer to the walls from these flows.

In earlier works, Evans (1984) and Cooper (1984) focussed on plume interaction with a developing upper layer and its behavior in a two layer environment. The primary results were the development of an equivalent point source fire. Relationships were developed which account for the hot gas layer on the fire plume and ceiling jet. These relationships are examined further in Chapter 5.

Chapter 3: Apparatus and Data Collection

3.1 Collected Data

The data presented in this study were collected by Motevalli at the National Institute for Standards and Technology, Center for Fire Research in Gaithersburg, Maryland. The data were collected from small-scale experiments using the methods and apparatus discussed in Sections 3.2, 3.3 and Motevalli and Marks (1990c). Two fire strengths, 2.0 and 0.75 kilowatts, were used in an experimental set-up modeling a confined ceiling. The floor to ceiling height was one meter, resulting in Q^* range of 0.00069-0.00189 (appendix C) which simulates fires of 6.3 to 17.3 kW in a typical 2.4 m high enclosure. These fire strengths were chosen to correspond to the unconfined ceiling experiments previously performed (Motevalli and Marks, 1990c). Ceiling jet, upper layer and ceiling surface temperatures were measured at radial locations of 0.26 and 0.75 meters as a function of time. Velocity measurements of the ceiling jet were recorded for the 2.0 kW fire at both radial locations over a period of 40 minutes. Velocity measurements for the 0.75 kW fire seemed unreliable, probably due to the weakness of the generated plume. A list of the experiments conducted is shown in Table 1.

The upper layer temperature was measured for each of the four cases over a time period of 40 minutes. The data for individual records were collected for a 5 second

period. The time interval between each record was 10 seconds for the first 5 minutes and then the frequency of data collection was changed to 20 second intervals.

Table 3.1
Data Collected for Confined Ceiling

Heat Release Rate	r/H Locations			
	0.26		0.75	
	Temperature	Velocity	Temperature	Velocity
2.0 kW	X	X	X	X
0.75 kW	X		X	

This resulted in 135 data records for the 40 minute test. A different data collection frequency was used to measure temperature and velocity of the ceiling jet during the experiments (see sec. 3.3). Each record was a little more than ten seconds in length. The time interval between each record was 20 seconds. At five minutes, data collection was changed to a cyclic form. Every 260 seconds, four data records, 10 seconds in length, were collected at intervals of 20 seconds to form each cyclic group. This resulted in 43 temperature and velocity data records.

Appendix A contains the values of temperature and velocity in the ceiling jet for a 2.0 kW fire at r/H locations of 0.26 and 0.75. The data is presented in tabular form for times of 5 seconds, 1, 2, 3, 5, 10, 15, 20, 25 minutes and steady state average. Appendix B contains temperature data of the ceiling jet and upper layer for the 0.75 and

2.0 kilowatt fire at r/H locations of 0.26 and 0.75. The data is presented for times of 2.5, 10 and 30 seconds and 1, 2, 3, 4, 5, 6, 7, 8, 9, 10, 15, 20, 22, 25, 28, 32, 35, and 38 minutes. Appendix E contains ceiling surface temperature measurements.

3.2 Experimental Apparatus

The apparatus and instrumentation used for the confined ceiling experiments is shown in Figure 3.1. The apparatus is the same used in the unconfined studies (Motevalli and Marks, 1990c) with one modification. A curtain wall was added to model an enclosure. The depth of the curtain wall, z, was 0.5 meters with a ceiling height, H, of 1.0 meter, (thus, the distance between the floor and the bottom of the curtain wall, Z=0.5). The ceiling was constructed of 1.27 centimeter thick fiberboard with a measured emissivity

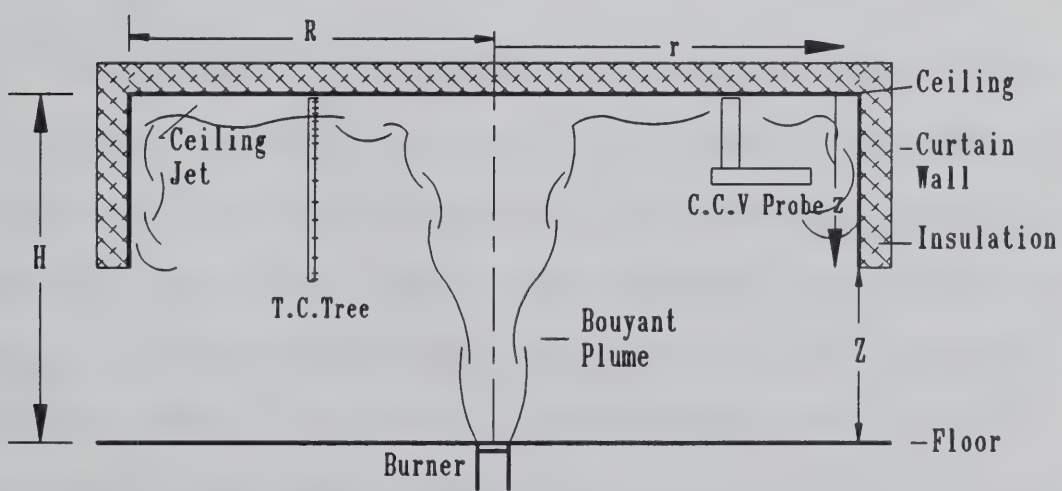

Figure 3.1 - Experimental Apparatus for Confined Ceiling

of 0.9. The ceiling was insulated on the back side with 8.26 centimeter thick layer of standard fiberglass insulation, (R-11). The curtain walls were constructed of corrugated cardboard which was also insulated.

The fire was produced by premixing methane and air at stoichiometric conditions. The burner had a diameter of 2.7 centimeters. Fire strengths were calculated using a heating value for Methane of 49.997 MJ/kg and an air/fuel ratio of 9.52. Steady fire sources with heat release rates of 0.75 and 2.0 kilowatts were used in these experiments. For a detailed account of the apparatus and test method refer to Motevalli and Marks (1990c).

3.3 Experimental Method and Collection of Data

Temperature and velocity of the ceiling jet were measured simultaneously and nearly continuously with an array of sensors using a technique named the Cross Correlation Velocimetry, (CCV). Motevalli et al. (1990a, 1992) used and expanded upon a method to measure velocity developed by Cox (1977,1980). The CCV technique employs the temperature of the fluid as a tracer and obtains the velocity of the fluid particles via cross-correlation of the temperature-time records of a thermocouple pair. Using an array of sensor pairs stacked vertically below the ceiling, flow velocity and temperature can be determined at any distance below the ceiling at a given radial location. The thermocouple pairs are located on the CCV probe at locations; 1.19, 3.175, 6.35, 9.525, 12.7, 19.5, 25.4 and 50.8 millimeters measured from the top of the support. The top of the CCV probe was located at distances of 0.5, 32.5, and 58.5 mm

below the ceiling for the confined ceiling experiments. This gave detailed temperature and velocity profile for the ceiling jet from 0.5 to 10.93 centimeters below the ceiling. The data acquisition system was limited to sixteen single ended channels. The CCV probe requires two data point for each location measured vertically from the ceiling, thus measurements were recorded for eight locations per experiment. Three separate experiments were required to develop a detailed ceiling jet profile. Some scatter was introduced into the profiles using this approach.

To obtain temperature measurements in the upper layer, a second probe was developed. This probe used single thermocouples to measure the temperature at the locations; 0.2, 1, 2, 4, 6, 8, 11, 15, 21, 25, 35, 40, 45, 48, 50 and 52 centimeters below the ceiling. This thermocouple probe allowed temperature to be measured at 16 z-locations during each experiment.

Voltage signals from the thermocouple were amplified using a 16-channel amplifier before being sent to an HP6942A multiprogrammer. The multiprogrammer scanned the amplified voltages and stored these values in its internal memory in digital form before transferring them to the computer intermittently at a rate of 33 kHz. The digitized voltage data were then processed to produce velocity and temperature values.

To measure the temperature of the ceiling, K-type thermocouples were placed flush with the lower surface of the ceiling at the r/H locations where the ceiling jet

temperatures measurements would be made. These thermocouples were connected to a reference junction at room temperature and connected to a chart recorder to provided a continuous temperature time record of the ceiling temperature, ΔT_c, at that location.

Chapter 4: Data Analysis

Data from the confined ceiling jet experiments showed well-defined temperature and velocity profiles in the presence of an upper layer for the range of r/H locations examined in these experiments. The ceiling jet is a boundary-layer type flow and therefore, the velocity and temperature profiles quantify the momentum and energy contents of the ceiling jet and their transport. Motevalli and Marks (1990a) found the unconfined ceiling jet to be a highly turbulent flow with large thermal fluctuations. The structure of a turbulent boundary layer flow is very complex. In order to characterize the ceiling jet and understand the transport of mass, momentum and energy by the jet, key parameters need to be quantified. These parameters establish how the thermal and momentum boundary layers change with time and position. These characteristics formulate the basis needed to predict the magnitude and position of the maximum temperature and velocity and the jet momentum and thermal thicknesses.

The ceiling jet velocity is zero at the ceiling surface. It increases to a maximum velocity, V_{max}, at a distance δ_{Vmax} away from the ceiling. This distance is noted as the ceiling jet momentum boundary layer thickness. The ceiling jet temperature varies from the ceiling temperature to a maximum ceiling jet temperature, ΔT_{max}, where $\Delta T_{max} = T_{max} - T_{\infty}$, in a thermal boundary layer of thickness, δ_{Tmax}. Beyond δ_{Tmax}, the ceiling jet behaves like a free jet at early times, before the formation of an upper layer. Once an upper layer begins to develop the ceiling jets temperature and velocity are affected. The

ceiling jet Gaussian momentum and thermal thicknesses, ℓ_T and ℓ_V, used by Motevalli and Marks (1990c) to define the jet characteristic thickness flow for the unconfined ceiling jet do not hold for the confined ceiling jet due to the presence of an upper layer.

4.1 Ceiling Jet Velocity Profiles

The ceiling jet velocity profiles were formed by combining sets of eight data points from three runs. Data collection during the experiment was limited to eight data points on the thermocouple probe. Consequently the data became somewhat prone to scatter when these sets were combined to form complete temperature and velocity profiles.

Figures 4.1 and 4.2 show the velocity profiles for the 2 kW fire at r/H locations of 0.26 and 0.75, respectively. These graphs demonstrate the effect of the upper layer on the velocity of the ceiling jet. As the upper layer begins to develop, the flow of the ceiling jet at each r/H location is retarded as is evident in reduction of the velocity, especially V_{max}. Figures 4.3 and 4.4 show the confined and unconfined ceiling jet velocity profiles at 5 seconds and steady-state. The confined ceiling jet flow at five seconds closely correlates with the unconfined ceiling jet data for the same case in profile shape and magnitude of the velocity. After one minute into the flow the upper layer has developed sufficiently enough to alter the shape and values of the profile. The velocity profile in the ceiling jet does not change much once the upper layer has become fully formed and has reached an equilibrium. The confined ceiling jet velocity, similar to the unconfined case, seems to be unaffected by the heat transfer to the ceiling, but may be

affected by the upper layer development shown by a 10-20% reduction in velocity. The ceiling jet maintains a nearly steady maximum velocity and velocity profile as shown in figures 4.1 and 4.2 even though the ceiling and ceiling jet temperatures are rising.

Alpert (1971) used the relations for a plume emanating from a point source to normalize the ceiling jet parameters. These relations are assumed to hold true for the confined ceiling jet, but cannot be tested here due to collection of velocity data from only one Q^*. The normalized velocity relation is given as:

$$V^* = \frac{V}{Q^{*\frac{1}{3}} (gH)^{\frac{1}{2}}} = f\,(r/H) \qquad [4\text{-}1]$$

Where Q^*, the normalized heat source strength, from Cooper (1982) is given as:

$$Q^* = \frac{(1-\lambda)\, Q}{\rho_\infty C_p T_\infty g^{\frac{1}{2}} H^{\frac{5}{2}}} \qquad [4\text{-}2]$$

and λ is the fraction of the heat lost due to radiation from the source. The radiative loss is assumed to be negligible for the experiments in this work because the source flame is produced by burning premixed methane and air and is small & almost entirely blue.

4.2 Ceiling Jet Maximum Velocity

The maximum ceiling jet velocity decreases with increasing radial distance, r, measured from the plume centerline impingement point. Due to the turbulent nature of

the flow, there is a considerable net transfer of the component of momentum perpendicular to the ceiling (i.e. in the z direction). This causes a net drop in maximum ceiling jet velocity due to the radial expansion of the flow, as well as viscous losses and buoyancy effects as the radial distance, r, increases. For the 2.0 kilowatt fire the maximum velocity in the ceiling jet is a time averaged velocity of 0.84 and 0.37 m/s for the r/H locations of 0.26 and 0.75, respectively. There is a substantial momentum loss over the short distance between the two measured radial locations.

The momentum boundary layer thickness, δ_{Vmax}, represent the thickness of the viscous flow regime. The viscous effects cause a slowing of the flow velocity from a maximum velocity at δ_{Vmax}, decreasing to a velocity of zero at the ceiling. The thickness of the momentum boundary layer quickly reaches a steady state value as shown by a nearly constant value of δ_{Vmax} over time. This trend is more difficult to observe for r/H of 0.75 due to a flatter velocity profile and radial component of the velocity losing its dominance. (This introduces more errors in the CCV measurements.) The exact location of δ_{Vmax} is hard to define due to the spacing of the thermocouples at this distance below the ceiling. The average δ_{Vmax} for the two kilowatt fires are 2 and 27 mm for the radial locations of 0.26 and 0.75, respectively. This shows the thickness of the boundary layer is growing with an increase in r as expected. Viscous effects cause the flow to be slowed, thus increasing the distance from the ceiling to the point of maximum velocity. The same phenomenon was shown to occur in the unconfined ceiling jet flow, Motevalli and Marks (1990). Table 4.1 lists the maximum velocity, V_{max} and its distance from the

ceiling, δ_{Vmax}, for the two cases. In this table the data point for δ_{Vmax} at two minutes may be unreliable. This was the last measurement recorded by the thermocouple located at 10.03 mm below the ceiling before communication with one of the thermocouples in the pair was lost. No velocity measurements were recorded at 20 minutes for r/H of 0.75.

Table 4.1 - Maximum Velocities with Position for the 2.0 Kilowatt Fire

	r/H Location			
	0.26		0.75	
Time (min)	V_{max} (m/s)	δ_{vmax}* (mm)	V_{max} (m/s)	δ_{vmax} (mm)
0.08	0.920	1.69	0.631	33.69
1.0	0.798	1.69	0.571	20.55
2.0	0.920	10.03	0.324	26.90
3.0	0.798	1.69	0.308	33.69
5.0	0.798	1.69	0.267	26.90
10.0	0.798	3.68	0.273	20.55
15.0	0.855	1.69	0.308	33.69
20.0	0.855	1.69	----	--
26.0	0.829	1.69	0.363	26.90
S.S.	0.841	1.69	0.353	20.55

* The velocity profile characteristically had a flat peak for the maximum velocity value over a range of between 1-10 mm. The values in the table are the first point from the ceiling that recorded maximum velocity.

4.3 Ceiling Jet Temperature Profile

Two sets of temperature profiles were collected during these experiments. Temperature profiles of the ceiling jet between 0.05 and 10 cm below the ceiling were collected simultaneously with the velocity profiles using the CCV probe for the 2.0 kilowatt fire. Temperature profiles for the upper layer were collected separately using the thermocouple tree for the 2.0 and 0.75 kilowatt fires. These upper layer temperature profiles also include measurements within the ceiling jet but with much less detail than the measurements obtained using the CCV probe. The growth of the ceiling jet thermal boundary layer and jet development over time for the 2.0 kilowatt fire at r/H of 0.26 and 0.75 is demonstrated in figures 4.5 and 4.6. At r/H of 0.75, it is clear that the ceiling jet loses most of its distinction and is much less defined compared to r/H=0.26 location. Figures 4.7 and 4.8 help to develop the full picture of the ceiling jet for the confined ceiling jet by including the upper layer. These figures demonstrate the increase in the ceiling jet temperature over time. The ceiling jet temperature reaches 80-90% of the steady state condition in about 4-5 minutes into the fire. The temperature in the jet decreases near the ceiling due to the heat transfer from the gas to the ceiling. The temperature is transient during this period due to this heat transfer and the entrainment of increasingly warmer gases from the upper layer. The heat transfer to the ceiling is examined further in Chapter 7. Similar behavior is observed in plots of the temperature distribution within the upper layer for the 0.75 kW fire, shown in figures 4.9 and 4.10. The time scale development of the upper layer is discussed in chapter 5.

The temperature profiles were non-dimensionalized by ΔT_{max} at different times. These plots, at r/H of 0.26 and 0.75 are presented in figures 4.11 and 4.12. The plots show the profiles at 1, 5, 10, and 40 minutes into the fire for each fire size at that radial location. Each graph exhibits good correlation between the ceiling jet thermal boundary layer thickness for all time periods. The non-dimensionalized temperature does not correlate as well for the upper layer between different times. This demonstrates the upper layer temperature is developing at slightly slower rate than the ceiling jet and indicates that ΔT_{max} is not the right correlation parameter for the upper layer temperature.

4.4 Ceiling Jet Maximum Temperature

Figures 4.13-4.16 show the comparison of the confined and unconfined ceiling jet temperature profiles as a function of time. At five seconds (temperature averaged from 0-10 seconds), the profile of the confined ceiling jet matches that of the unconfined ceiling jet in profile shape and thickness. The magnitude of the temperatures of the two cases are not the same. It was expected that for this time period the confined and unconfined ceiling jet temperatures would be closer in magnitude. The time averaging (10 seconds) for the confined temperature profiles, may be contributing since the upper layer formation (at the later time, e.g. 5-10 seconds) would definitely cause the jet temperature to be higher. The different lengths of the sampling period, seven seconds for the unconfined and ten seconds for the confined, can be another cause for the larger difference seen in figure 4.13. Differences may have also occurred due to the time the clock was started. Time zero was set when the first temperature increase was registered

at the top thermocouple. For the second and third runs (combined with the data from the first run to form a complete profile), the top thermocouple was much further below the ceiling, 32.5 and 58.5 mm, respectively.

At thirty seconds, the shape of the temperature profile for the confined ceiling jet is changing significantly (Figure 4.14). The position of the maximum temperature δ_{Tmax} has shifted farther away from the ceiling. In the unconfined ceiling jet study by

Table 4.2 - Maximum Temperature and Position for the 2.0 Kilowatt Fire

	r/H Location			
	0.26		0.75	
Time (min)	ΔT_{max} (C)	δ_{Tmax} (mm)	ΔT_{max} (C)	δ_{Tmax} (mm)
0.08	35.48	6.85	16.46	26.9
1.0	49.21	10.03	35.40	33.7
2.0	54.69	10.03	39.27	35.7
3.0	56.84	6.85	41.14	35.7
5.0	58.50	6.85	43.64	35.7
10.0	59.70	6.85	47.89	26.9
15.0	58.33	13.20	48.67	35.7
20.0	60.19	6.85	49.26	33.7
26.0	59.81	10.03	51.02	26.9
S.S.	61.42	10.03	50.86	26.9

Motevalli and Marks (1990a), it was found that δ_{Tmax} decreased as the ceiling approached steady state. This was expected because as the ceiling is heated, the convective heat transfer from the ceiling jet is reduced. Therefore, the maximum ceiling jet temperature occurs closer to the ceiling. The data for the confined ceiling jet δ_{Tmax} and ΔT_{max} are presented in Table 4.2. In this table, the position, δ_{Tmax}, shows no pattern of approaching the ceiling with time. However, in the measurements recorded using the thermocouple tree, a movement of δ_{Tmax} away from the ceiling is apparent especially at r/H of 0.75. The results for ΔT_{max} and δ_{Tmax} from the thermocouple probe are contained in chapter 5, Tables 5.1-5.4. This phenomenon could be due to the entrainment of the warmer gases from the upper layer. Also the development of a flatter profile over time may have confused the process of locating the real maximum temperature.

At one minute after the fire was ignited, the temperature at any given location in the confined ceiling jet is 20- 75% greater than that in the unconfined ceiling jet. This presents an argument against using equations for the unconfined ceiling jet to predict the conditions in a ceiling jet confined by an enclosure, even at early times in the fire.

At steady state, the ceiling jet profile is not as steep as the earlier profiles due to the development of the upper layer. However the ceiling jet still maintains a temperature that is $\sim$50% greater than the unconfined ceiling jet for the 2.0 kilowatt fire and $\sim$25% greater for the 0.75 kilowatt fire.

The increase in the maximum temperature for the four cases of the confined ceiling jet with respect to time is shown in figure 4.17. It is important to be able to characterize the maximum ceiling jet temperature with respect to time in calculating the reaction time of heat detection and suppression systems. After 4- 5 minutes into the experiment, the temperatures have reached 80-90% of their steady state values. The temperature variation at r/H of 0.75 shows a slower approach to steady state. Figure 4.18 shows ΔT^*_{max}, where;

$$\Delta T^*max = \frac{\Delta T_{max}}{Q^{*\frac{2}{3}} T_\infty} \qquad [4\text{-}3]$$

There seems to be a good correlation between both fires for each radial location but data from different r/H locations do not correlate. Figure 4.19 shows ΔT^*_{max} normalized by an r/H function as an attempt to collapse all the data. The equation for the r/H function for the unconfined ceiling experimental data developed by Motevalli and Marks (1990a) did not correlate the confined ceiling jet data. A function for r/H was developed by correlating the results of the four experimental cases.

$$f\,(r/H) = -5.02\,(r/H) + 13.95 \qquad [4\text{-}4]$$

This function is linear because the four data points for the experiments fall on the two r/H locations examined in these experiments. More experiments are needed to obtain a more comprehensive empirical relation for the steady state confined ceiling jet maximum temperature. Figure 4.19 shows an exponential behavior of ΔT_{max} as a function of time normalized by the time constant, τ. A fit to the data provides a prediction of the

maximum temperature in the ceiling jet as a function of time when the fire size and radial location is known and the time constant can be calculated. The equation for the curve is given as:

$$\frac{\Delta T^{*}_{max}}{f\,(r/H)} = 1 - \exp\left(\frac{-0.5\,t}{\tau}\right) \qquad [4.5]$$

where the time constant was experimentally defined as the time when 63% of the steady state value was reached.

The maximum confined ceiling jet temperature obtained in these experiments was compared to confined ceiling jet data measured in the experiments of You and Faeth (1978) and Zukoski and Kubota (1977). The data of You and Faeth (1978) are from a detailed study of a steady state ceiling jet induced by burning methanol through a wick with a heat release rate of 242-254 Watts. The ceiling was constructed of a copper plate. The curtain walls were made from 244 mm deep aluminum sheets. Zukoski and Kubota's (1977) data is for fire from a propane-air burner with strengths of 1.17 and 1.53 kW. The ceiling was constructed from a cold-rolled steel plate. The curtain walls were made from 30 cm deep corrugated paper. Figure 4.20 shows the comparison of data using equation 4-3. Using this correlation does not provide a good agreement between the experiments. This was also true of the correlation Motevalli and Marks (1990c) used to correlate the small-scale unconfined experiments, $\Delta T/(Q^{2/3}\ H^{-5/3})$. The upper layer temperature effects the maximum ceiling jet temperature. This difference

in upper layer temperature is due to the amount of heat lost to the ceiling and ceiling height. A new correlation for confined ceiling jet maximum temperature is needed.

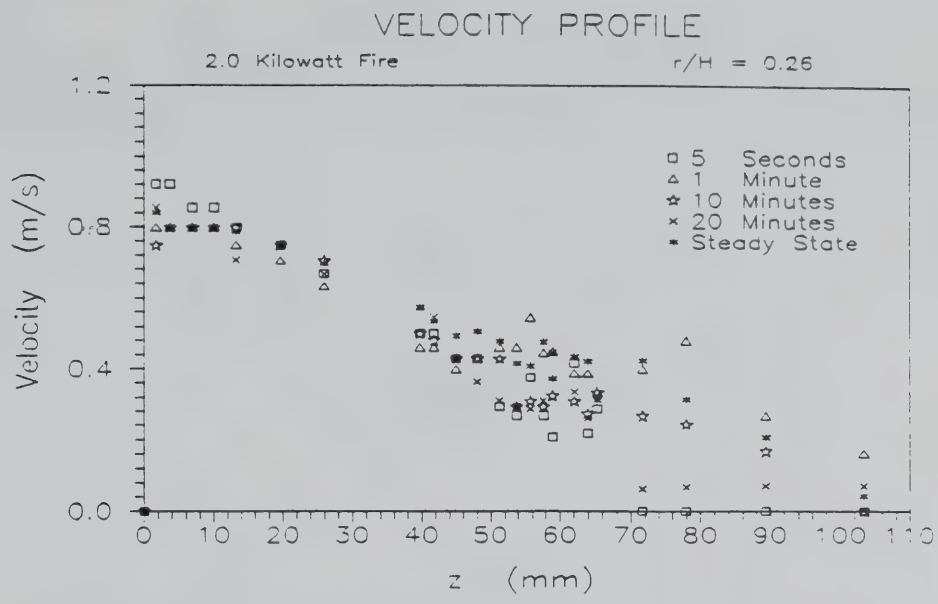

Figure 4.1 - Velocity Profiles for 2.0 Kilowatt Fire, r/H of 0.26

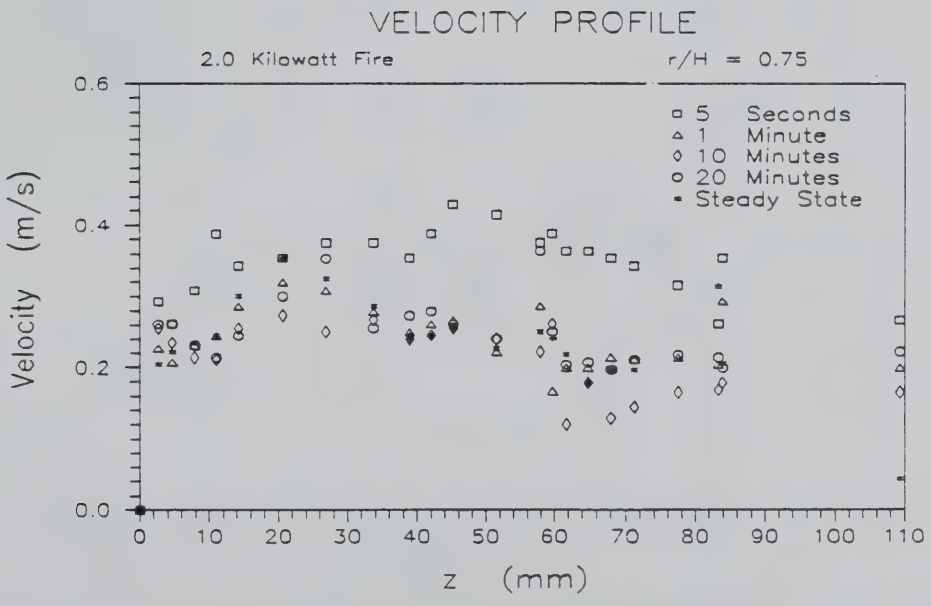

Figure 4.2 - Velocity Profile for 2.0 Kilowatt Fire, r/H of 0.75

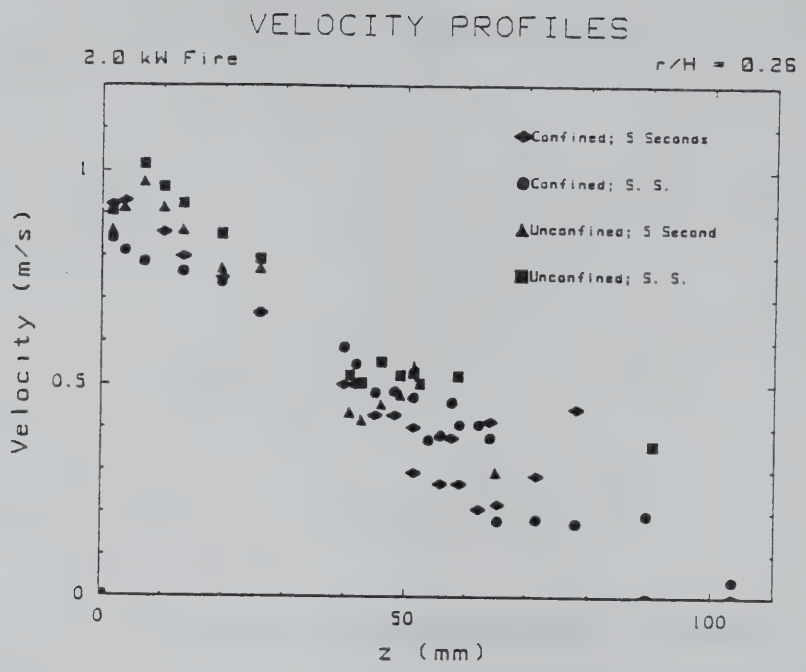

Figure 4.3 - Velocity Profile, Confined vs .Unconfined for 2.0 Kilowatt Fire, r/H of 0.26, 5 Seconds and Steady State

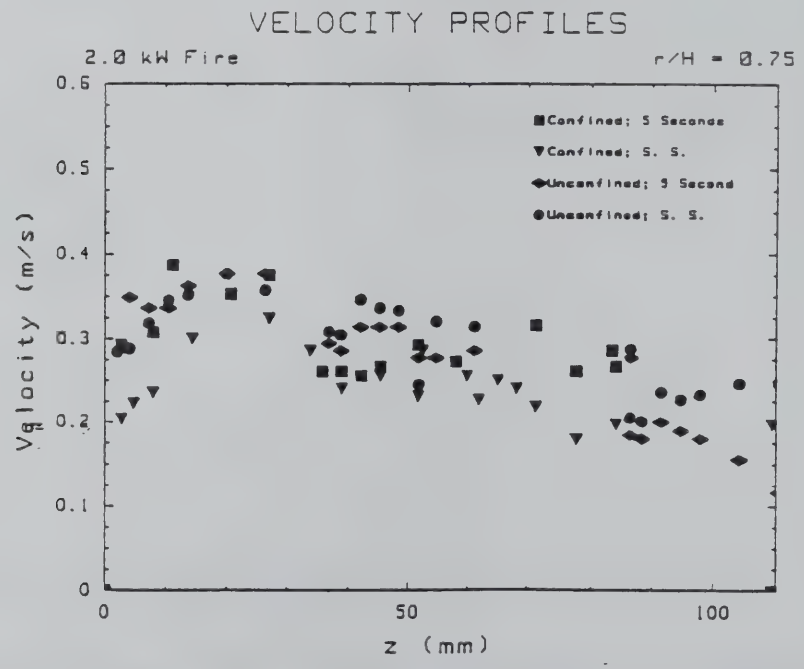

Figure 4.4 - Velocity Profile, Confined vs. Unconfined for 2.0 Kilowatt Fire, r/H of 0.75, 5 Seconds and Steady State

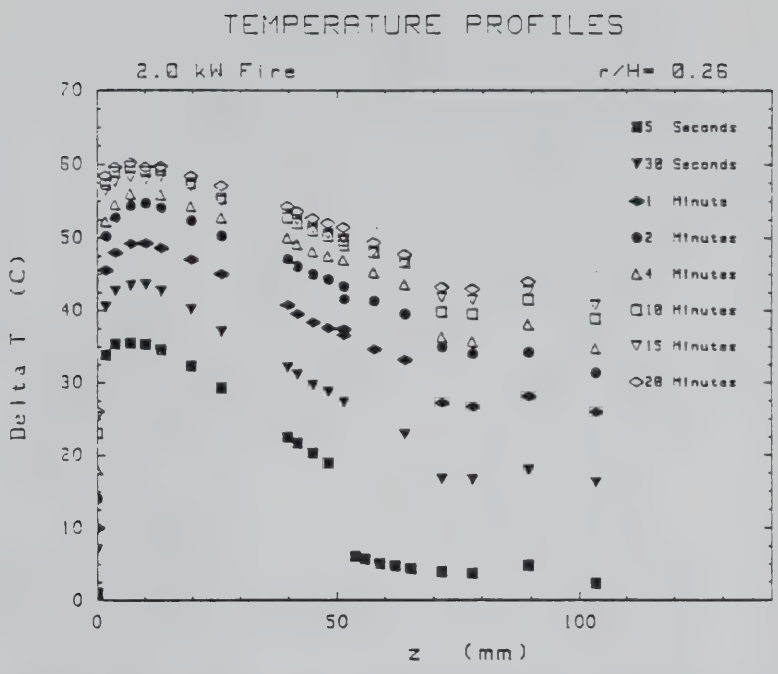

Figure 4.5 - Ceiling Jet Temperature Profile for 2.0 Kilowatt Fire, r/H of 0.26

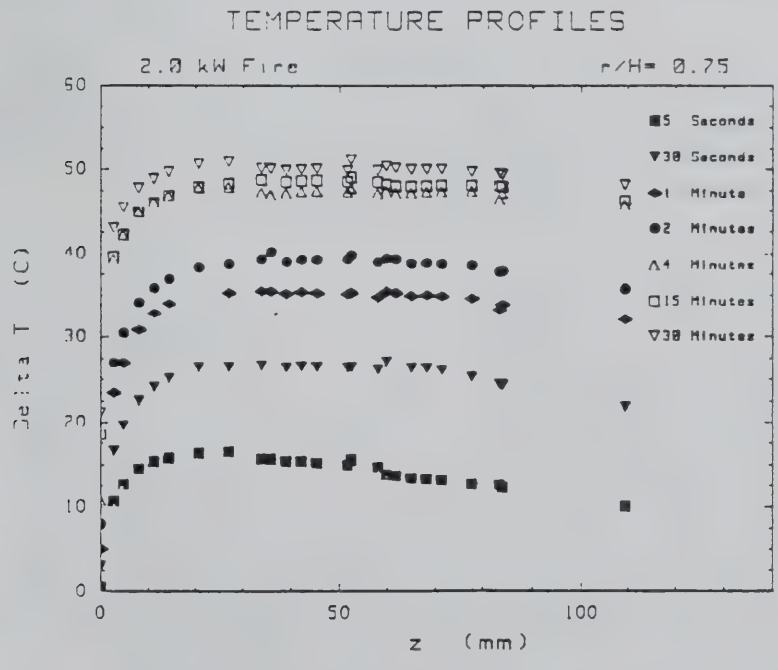

Figure 4.6 - Ceiling Jet Temperature Profile for 2.0 Kilowatt Fire, r/H of 0.75

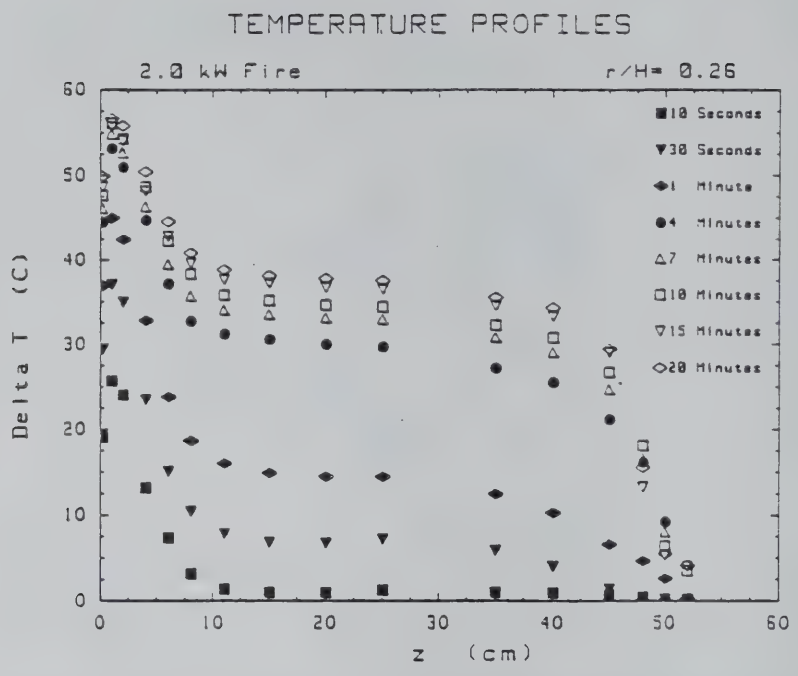

Figure 4.7 - Upper Layer Temperature Profile for 2.0 Kilowatt Fire, r/H of 0.26

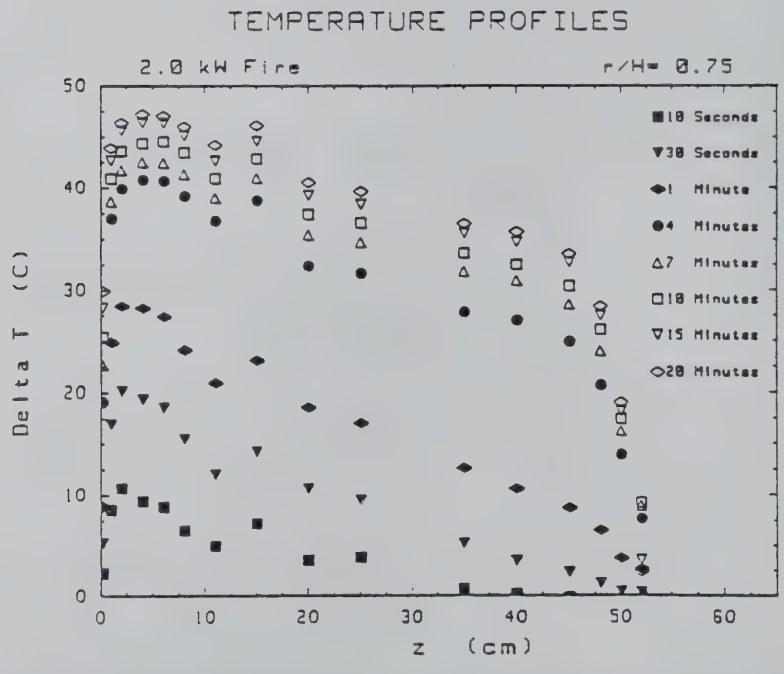

Figure 4.8 - Upper Layer Temperature Profile for 2.0 Kilowatt Fire, r/H of 0.75

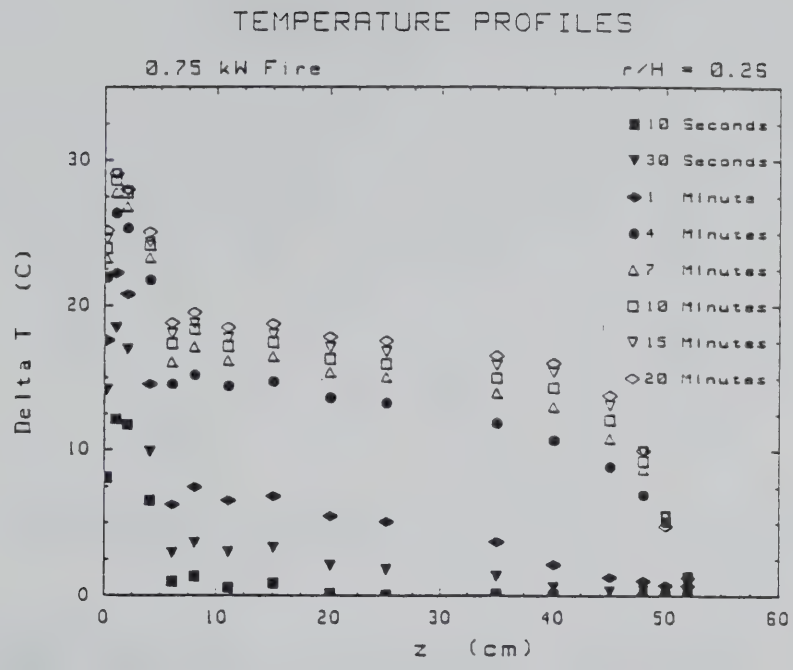

Figure 4.9- Upper Layer Temperature Profile for 0.75 Kilowatt Fire, r/H of 0.26

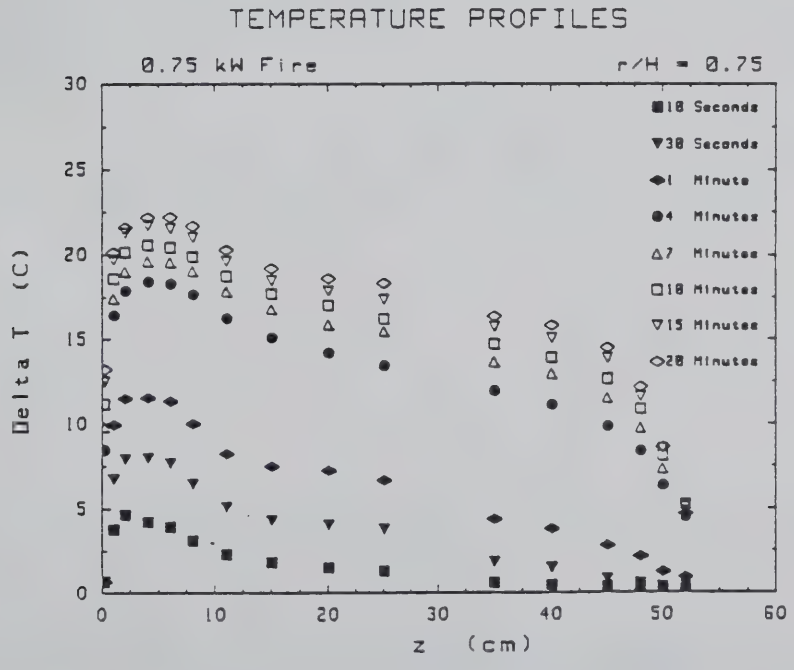

Figure 4.10- Upper Layer Temperature Profile for 0.75 Kilowatt Fire, r/H of 0.75

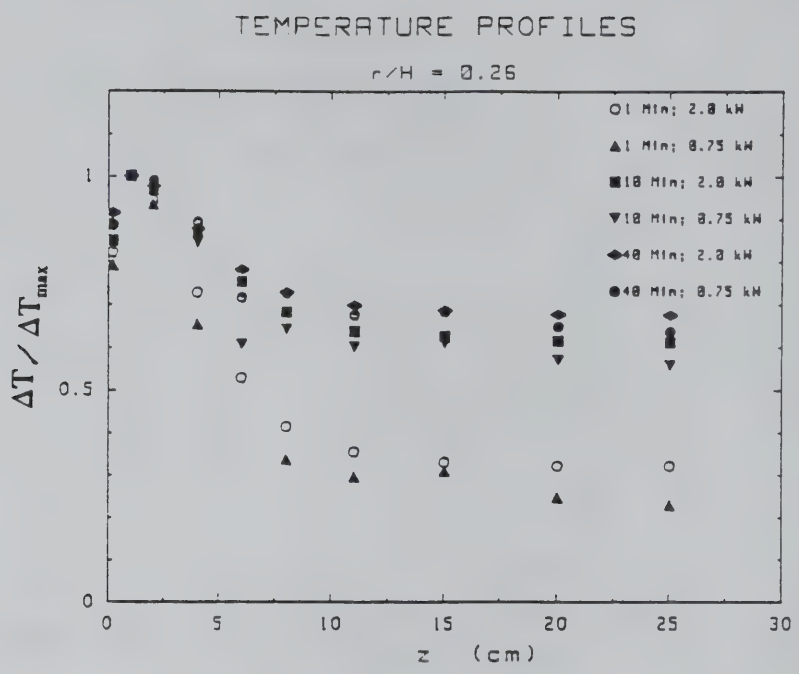

Figure 4.11 - Normalized Temperature Profile, r/H of 0.26

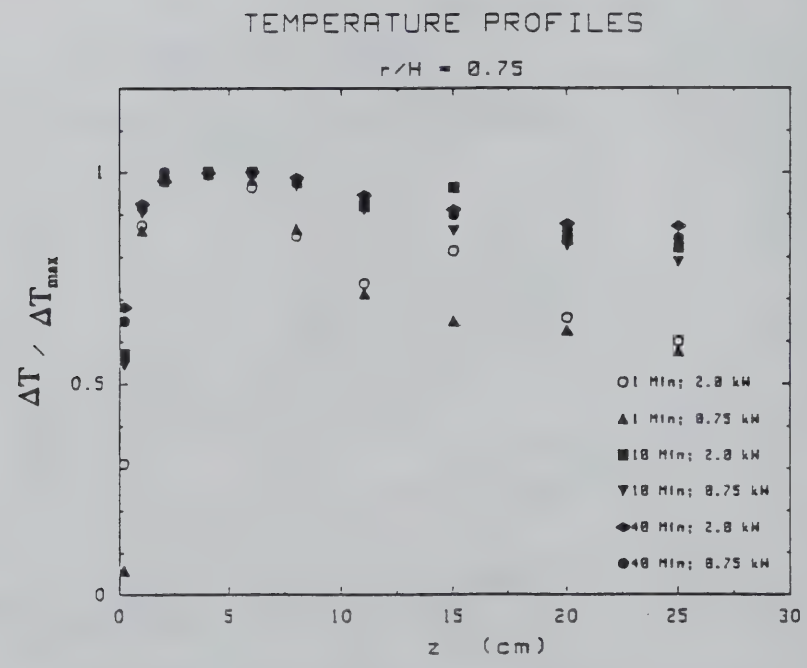

Figure 4.12 - Normalized Temperature Profile, r/H of 0.75

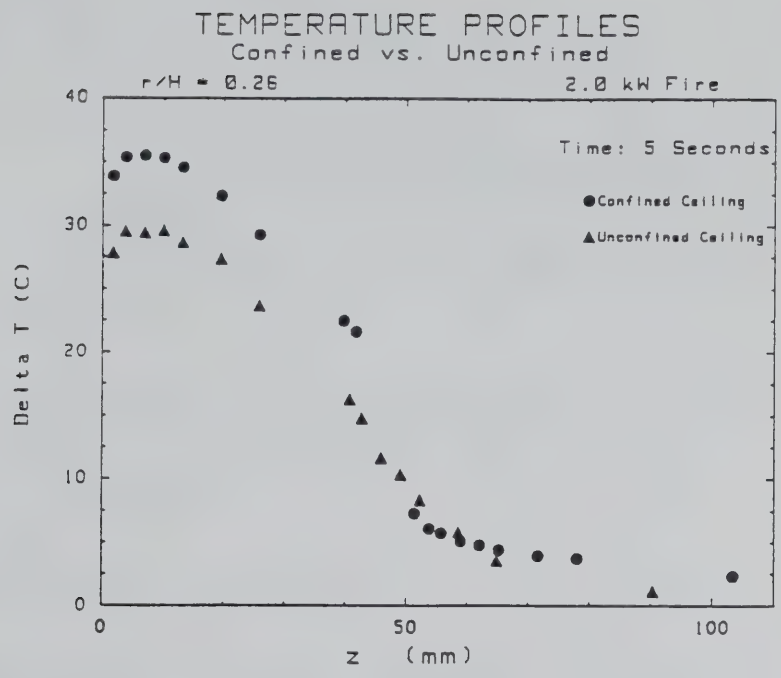

Figure 4.13 - Confined Vs. Unconfined Ceiling Jet Temperature, 5 Seconds

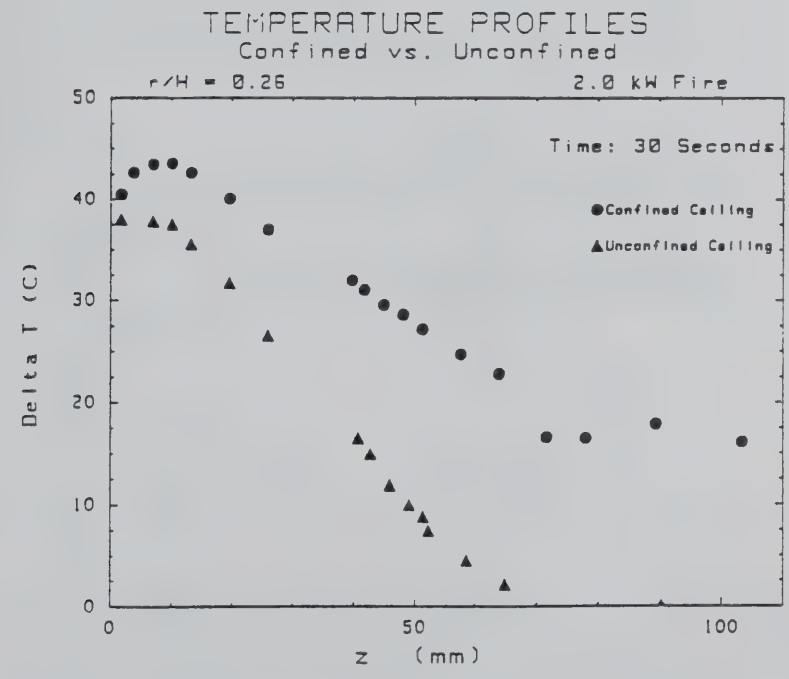

Figure 4.14 - Confined Vs. Unconfined Ceiling Jet Temperature, 30 Seconds

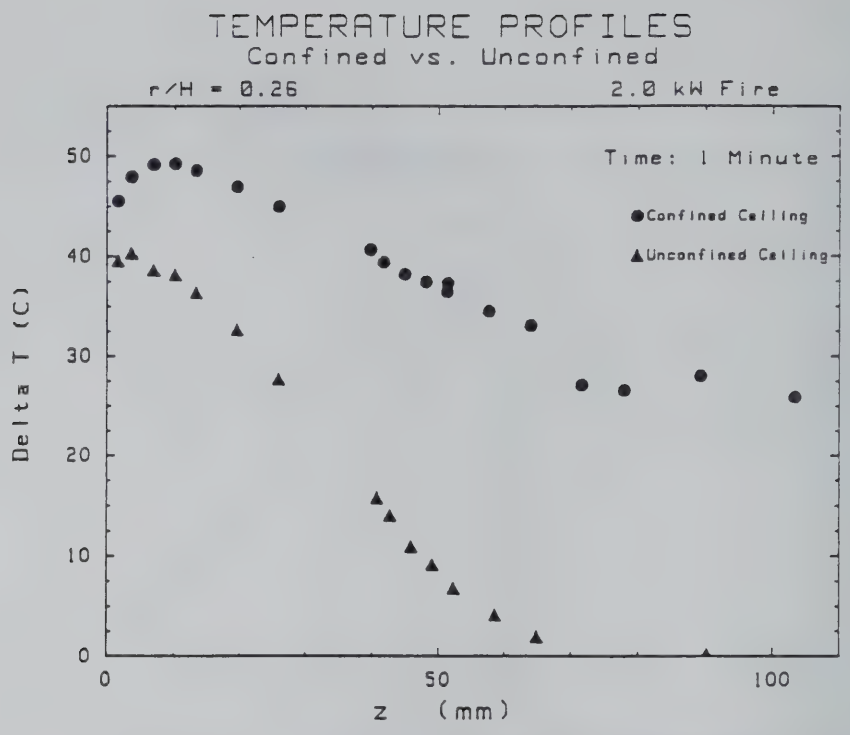

Figure 4.15 - Confined Vs. Unconfined Ceiling Jet Temperature, 1 Minute

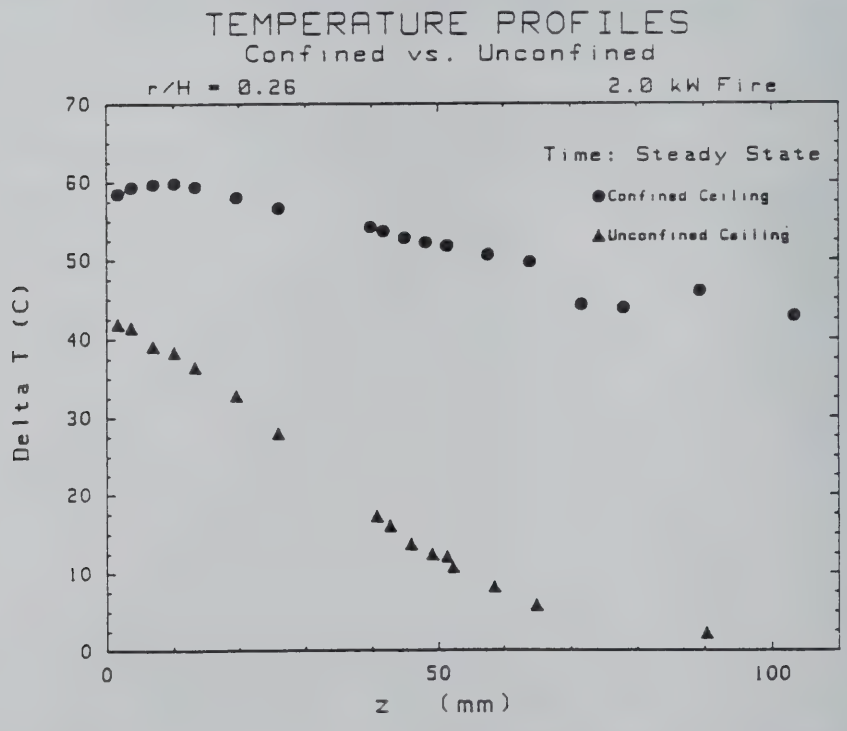

Figure 4.16 - Confined Vs. Unconfined Ceiling Jet Temperature, Steady State

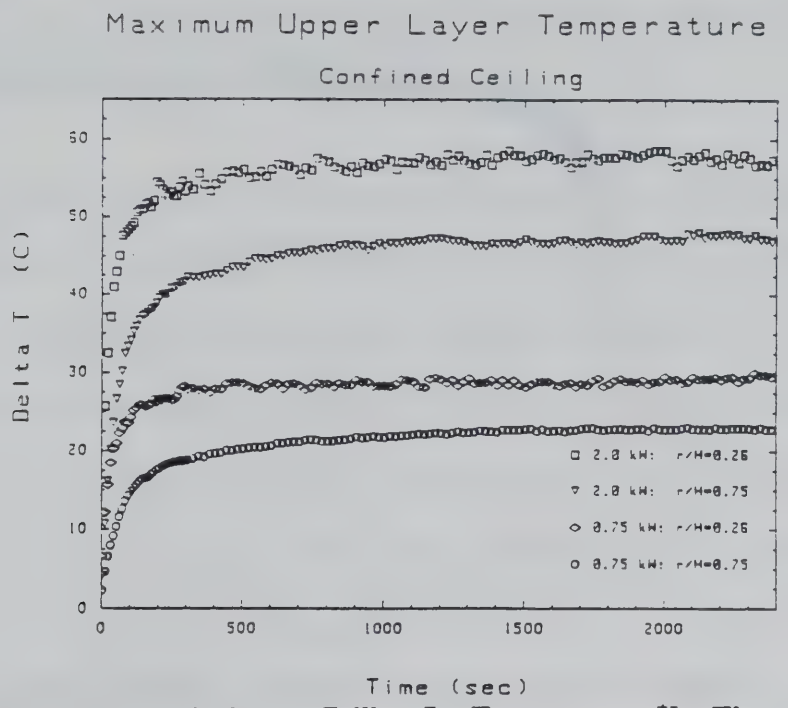

Figure 4.17 - Maximum Ceiling Jet Temperature Vs. Time

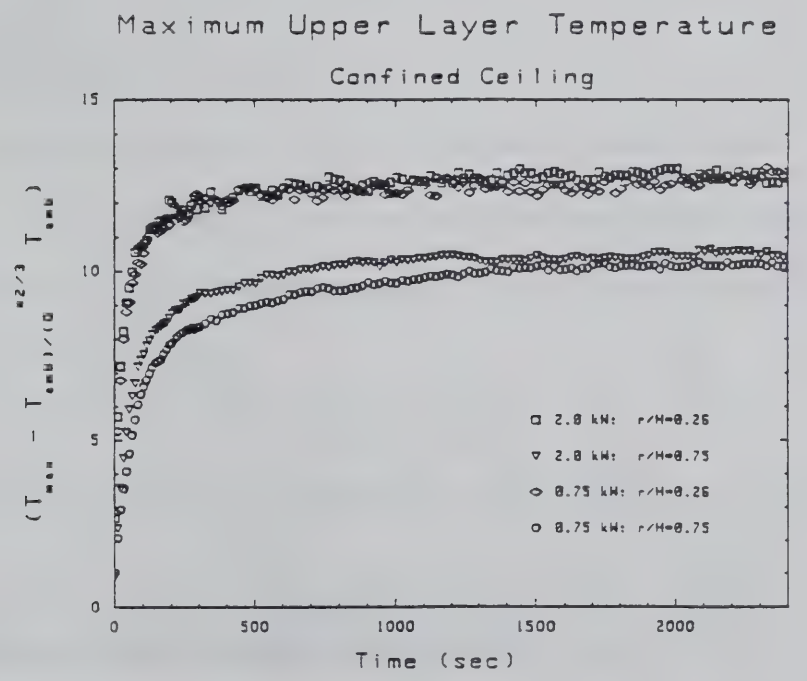

Figure 4.18 - Maximum Ceiling Jet Temperature Vs. Time Normalized by Q^* and T_∞

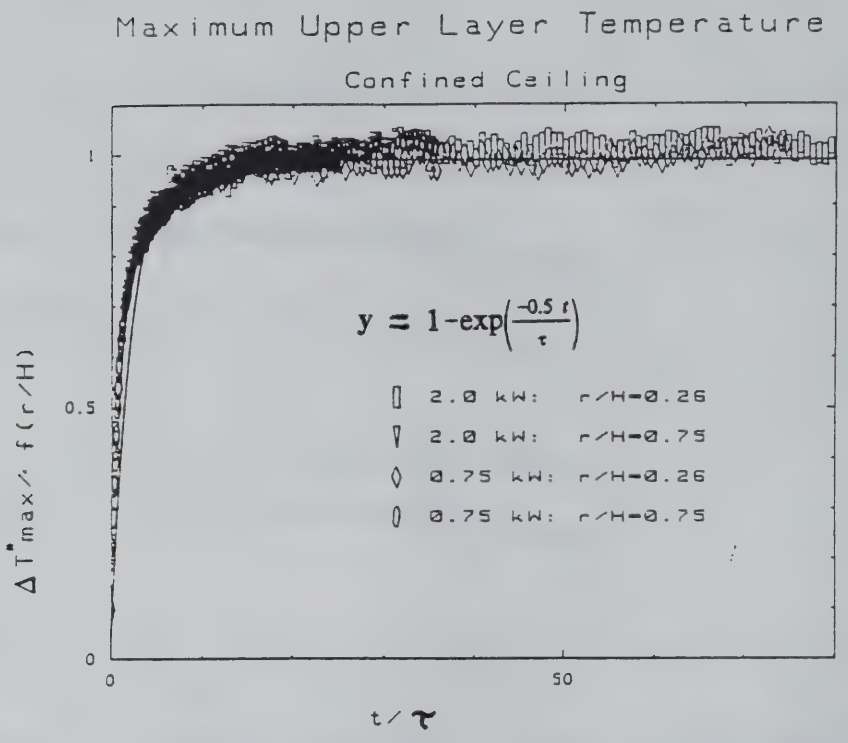

Figure 4.19 - Curve Fit for Maximum Ceiling Jet Temperature

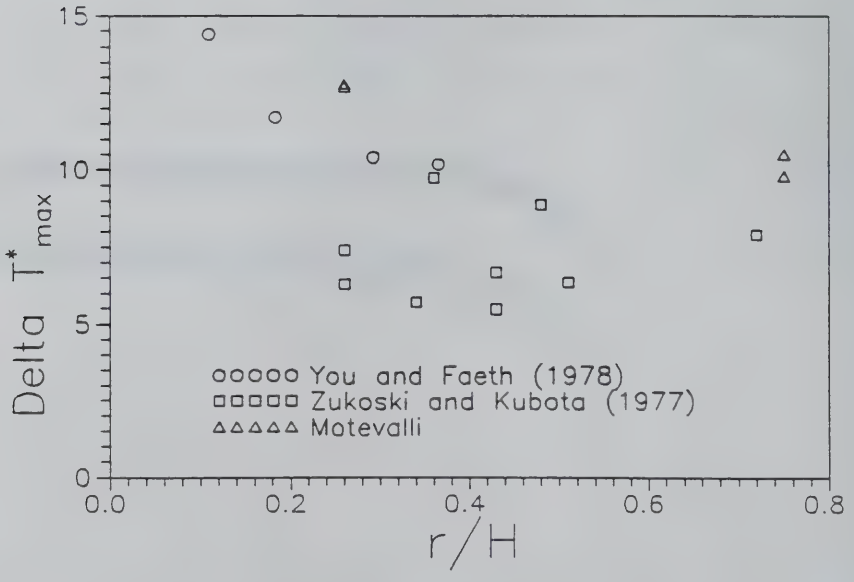

Figure 4.20 - Comparison of maximum Ceiling Jet Temperature in Small-Scale Confined Ceiling Jet Experiments

Chapter 5: Development and Characteristics of the Upper Layer

Most computer fire models use a two-zone approach to simulate an enclosure fire. The lower of the two zones is assumed to remain at or near ambient conditions. The upper layer is described in terms of averaged properties. By definition all products of combustion are contained in the upper layer. This layer has a changing thickness, z_i, and a corresponding descending interface between the two layers, parallel to the floor. The upper layer is assumed to have a uniform upper layer temperature, T_{ave}, and uniform concentration of combustion products. This assumption allows a compromise between accuracy in simulation and practicality of implementation. Full-scale testing at NBS (Cooper et al., 1982) and small-scale testing by You and Faeth (1978) have shown this approach to be reasonable for general modeling of fire growth and conditions in enclosure fires and propagation of combustion products to other rooms. In these experiments a distinct ceiling jet is found to exist within the upper layer throughout the duration of the test. Currently, most compartment fire models use the two zone method to describe the fire environment.

For calculations of activation times for sprinklers and heat detectors a more detailed description of the upper layer, specifically the ceiling jet contained in the upper layer is necessary. Chapter six examines some of the methods and models available for these calculations. The development of the upper layer and calculation of an accurate

upper layer temperature is examined for fires and conditions of these experiments in this chapter. The calculations and equations are based on a limited amount of experimental data. Broader testing would be needed to develop equations for general use.

5.1 Development of the Upper Layer

In these experiments the upper layer develops quickly but takes 20-30 minutes to reach a thermal steady state. The ceiling jet maintains a distinct profile throughout the development of the upper layer. The temperature versus time profiles for the ceiling jet and upper layer have already been shown for the four confined ceiling experiments in figures 4.8-4.11. These graphs showed that the upper layer develops almost immediately, however, in the first few seconds of the fire the layer temperature is much lower than the steady state value. These figures show an interface that is located at the bottom of the curtain wall from the onset of fire. The values for the temperature at the interface fluctuate due to interface instabilities.

The upper layer at r/H of 0.26 contains a ceiling jet with a thickness of 0-10 cm. From 10 to 35 cm the temperature in the z direction is nearly constant. At 35 cm the temperature tapers off toward ambient temperature. At r/H of 0.75, the ceiling jet thickness increases to 12 cm. From this point the ceiling jet slowly tapers off to ambient temperature at $\sim$53 cm below the ceiling.

5.2 Average Upper Layer Temperature

An average temperature for the upper layer was calculated based on the approximate relation shown below. Simpson's rule was used to calculate the integral

$$T_{avg,ul} = \frac{1}{z_i} \int_0^{z_i} T dz \qquad [5\text{-}1]$$

where z_i is equal to 50 cm.. The average temperature, $T_{avg,ul}$, is shown in tables 5.1-5.4 for the 2.0 and 0.75 kilowatt fires at r/H of 0.26 and 0.75. The maximum temperature and its position in the ceiling jet for these fires are also listed in tables 5.1-5.4. Figure 5.1 shows a graph of the average upper layer temperatures verses time. This figure shows the $T_{avg,ul}$ is nearly constant at both r/H locations for the 0.75 kilowatt fire. The average upper layer temperature at both r/H locations for the 2.0 kilowatt fire is not as similar as for the weaker 0.75 kilowatt fire. The slight differences between the average upper layer temperatures for the 2.0 kW fire are thought to be due to the effect of the plume on the lower portion of the upper layer. The air entrainment causes a lower temperature in the region for the stronger fire at r/H of 0.26 only. These differences could also be due to the differences between the experiments caused by slight timing discrepancies and ambient conditions. The curves show very little convergence or divergence based on which two z-locations are chosen as the limits of the integral in equation 5-1. The upper layer depth was chosen to be the same as the depth of the curtain wall, 50 cm. If the ceiling jet portion is removed from the upper layer temperature profile, there is not much change in value of the average upper layer temperature. If the interface region between the upper and lower layers, 50-52 cm, is

included in the averaging, again little difference occurs in the average upper layer temperature.

Tables 5.1-5.4 along with figures 5.2 and 5.3 show a large difference between the maximum ceiling jet temperature and the calculated average upper layer temperature. This difference is greater during the early transient times. As the ceiling jet reaches steady-state the difference between the maximum and average upper layer temperature is still large, on the order of 25-50%. This illustrates the importance of using the ceiling jet temperatures as opposed to an average temperature to calculate a more accurate time to detector operation and amount of heat transferred to the ceiling.

To predict the average upper layer temperature as a function of time, a correlation relating the temperature to the fire heat release rate and characteristic thermal response time was developed. The average upper layer temperatures were normalized with respect to Q and T_∞ using equation.

$$\Delta T^*_{avg,ul} = \frac{\Delta T_{avg,ul}}{Q^{*\frac{2}{3}} T_\infty} \qquad [5\text{-}2]$$

Time was normalized using the time constant, τ. The experimental time constant is equal to the time the temperature is 63% of the maximum temperature. The time constant for the developing average upper layer temperature was derived from the experimental data and is 115 for the 2.0 kW fire and 167 for the 0.75 kW fire. This lead to the plot

presented in figure 5.4. A curve was fit to this graph using the linear least squares fit in DATA-TAP plotting program (Timlin and Mihalisin, 1987) also shown in figure 5.4. This curve provides an empirical relation for the average upper layer temperature with respect to time. This relation is given as:

$$\Delta T^{*}_{avg,ul} = (7.1+.045(t/\tau))\ (1-e^{-t/\tau}) \qquad [5\text{-}3]$$

5.3 Energy Balance for the Upper Layer

The time-scale of formation of the maximum ceiling jet and upper layer temperature was examined in section 5.2. An empirical equation was developed to calculate the average upper layer temperature as a function of time. The characteristic thermal response time, τ, needs to be quantified for equation [5-3] to be useful. For the general case, a correlation must be developed to calculate the time constant using known parameters. A correlation to solve for τ is developed by non-dimensionalizing the unsteady energy balance equation of the upper layer. Using a control volume approach the conservation of energy is represented by:

$$\Delta E = Q_{in} - Q_{out} \qquad [6\text{-}11]$$

where;

$$\Delta E = \rho_u\ C_v\ V_c\ \frac{d\Delta T_{ul,avg}}{dt}$$

$$\dot{Q}_{in} = \dot{m}_{in} c_p \Delta T_p$$

$$Q_{out} = (\dot{m}_{out} c_p \Delta T_p) + h_c A_c (T_g - T_c) \qquad [5\text{-}5]$$

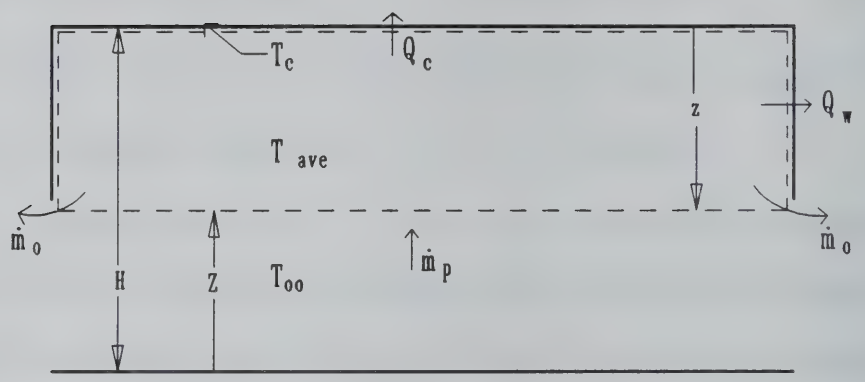

Figure 5.5 - Control Volume for Energy Balance of the Upper Layer

In this model gas radiation is neglected. Figure 5.5 shows the control volume for the upper layer. The results of this process yield τ as a function of the dimensionless groups

$$\frac{(H - z_i)}{\tau U_p \gamma} = f\left(\frac{h_c}{\rho C_p U_p}\right) \qquad [5\text{-}6]$$

However, there is not enough data available to determine the function.

Veldman et al. (1977) derived a similar functional relation for the time constant for an unconfined ceiling using a ceiling element as the control volume. This correlation was used to solve for a time constant to use in equation 5-3. The time constant as developed by Veldman et al. (1977) is given here in a modified form for ΔT_{max} and essentially in the original form for the average upper layer temperature in equation 5-8.

$$\tau = \left(\frac{\rho_\infty c_{p_\infty}}{\rho_c c_{p_c}}\right) \frac{\sqrt{gH}}{\delta} Q^{*-1/3} f(r/H)^{-1} \qquad \text{(for } \Delta T^*_{max}\text{)} \quad [5\text{-}7]$$

$$\tau = \left(\frac{\rho_\infty c_{p_\infty}}{\rho_c c_{p_c}}\right) \frac{\sqrt{gH}}{\delta} Q^{*-1/3} \qquad \text{(for } \Delta T^*_{ul,avg}\text{)} \quad [5\text{-}8]$$

Equation 5-7 shows that τ is a function of the ceiling properties. This is implied in equation 5-6 as well where h_c has to be determined from an energy balance at the ceiling, which includes conduction heat transfer and reradiation from the ceiling surface (see chapter 7 for details).

Since the average upper layer temperature is not a function of radial location, f(r/H) was dropped from equation 5-7. As shown in equation 5-8 this relation provides a time constant proportional to the experimentally determined time constants for the average upper layer temperature. Figure 5.6 shows the use of Veldman's time constant to correlate the average upper layer temperatures. The result is the same as shown in figure 5.4. Equation 5-7 was used to calculate the value for the time constant for the

maximum ceiling jet temperature where f(r/H) is found in equation 4-4. The substitution of τ developed by Veldman et al. (1977) is shown in figure 5.7. The correlation using the experimentally determined τ is shown in figure 4.19. Figure 4.19 shows a better correlation of the data during the first 10 minutes. Thus, equations 5-9 and 5-10 can be readily used to compute the average upper layer temperature and the maximum ceiling jet temperature (for the confined condition) in conjunction with a value for τ calculated using either equation 5-7 or 5-8, as appropriate.

$$\frac{\Delta T^*_{max}}{f(r/H)} = 1 - e^{(-.01t/\tau)} \qquad \text{(for } \Delta T^*_{max}\text{)} \quad [5\text{-}9]$$

$$\Delta T^*_{avg,ul} = (7.1 + 0.0045(t/\tau))(1 - e^{-0.1t/\tau}) \qquad \text{(for } \Delta T^*_{ul,avg}\text{)} \quad [5\text{-}10]$$

Table 5.1 - Upper Layer Temperature

2.0 Kilowatt Fire - r/H= 0.26

Time (m)	ΔT_{max} (C)	δ_{Tmax} (cm)	$\Delta T_{ave,ul}$ (C)
0.042	12.08	2.0	0.73
0.16	25.68	1.0	2.98
0.50	37.06	1.0	8.01
1.0	45.00	1.0	14.85
2.0	50.59	1.0	23.42
3.0	52.09	1.0	26.97
4.0	53.13	1.0	28.56
5.0	53.94	1.0	29.66
6.0	54.09	1.0	30.63
7.0	54.81	1.0	31.27
8.0	55.57	1.0	31.90
10.0	56.09	1.0	32.87
15.0	55.67	1.0	34.21
20.0	56.63	1.0	35.30
22.0	56.65	1.0	35.37
28.0	57.1	1.0	35.64
32.0	58.08	1.0	36.09
35.0	57.45	1.0	36.14
38.0	58.07	1.0	36.14

Table 5.2 - Upper Layer Temperature

2.0 Kilowatt Fire - r/H= 0.75

Time (m)	ΔT_{max} (C)	δ_{Tmax} (cm)	$\Delta T_{ave,ul}$ (C)
0.042	6.57	2.0	0.99
0.16	10.65	2.0	3.42
0.50	20.11	2.0	8.89
1.0	28.41	2.0	16.33
2.0	35.83	4.0	24.71
3.0	38.25	4.0	28.41
4.0	40.74	4.0	30.72
5.0	42.17	4.0	32.06
6.0	42.29	4.0	32.72
7.0	42.51	4.0	33.70
8.0	43.51	4.0	34.46
10.0	44.52	6.0	35.53
15.0	46.36	4.0	37.21
20.0	47.22	4.0	38.29
22.0	46.20	4.0	37.91
28.0	46.48	6.0	38.35
32.0	47.56	4.0	38.79
35.0	47.62	4.0	38.85
38.0	47.24	4.0	38.58

Table 5.3 - Upper Layer Temperature

0.75 Kilowatt Fire - r/H= 0.26

Time (m)	ΔT_{max} (C)	δ_{Tmax} (cm)	$\Delta T_{ave,ul}$ (C)
0.042	6.57	2.0	.55
0.16	12.11	1.0	1.14
0.50	18.43	1.0	2.85
1.0	22.24	1.0	5.52
2.0	25.47	1.0	9.51
3.0	26.55	1.0	11.81
4.0	26.37	1.0	12.98
5.0	27.77	1.0	13.75
6.0	27.83	1.0	14.29
7.0	27.78	1.0	14.76
8.0	28.67	1.0	15.18
10.0	28.62	1.0	15.71
15.0	29.03	1.0	16.39
20.0	29.07	1.0	16.97
22.0	28.55	1.0	17.20
25.0	28.10	1.0	16.93
28.0	28.19	1.0	17.25
32.0	29.06	1.0	17.60
35.0	29.47	1.0	17.60
38.0	29.24	1.0	17.81

Table 5.4 - Upper Layer Temperature

0.75 Kilowatt Fire - r/H= 0.75

Time (m)	ΔT_{max} (C)	δ_{Tmax} (cm)	$\Delta T_{ave,ul}$ (C)
0.042	2.27	2.0	0.73
0.16	4.67	2.0	1.48
0.50	7.96	4.0	3.42
1.0	11.53	4.0	6.10
2.0	15.65	4.0	9.83
3.0	17.26	4.0	11.82
4.0	18.39	4.0	13.13
5.0	18.70	4.0	13.82
6.0	19.26	4.0	14.37
7.0	19.62	4.0	14.75
8.0	19.98	4.0	15.15
10.0	20.59	4.0	15.71
15.0	21.71	4.0	16.68
20.0	22.18	6.0	17.33
22.0	22.36	6.0	17.54
25.0	22.77	4.0	17.73
28.0	22.63	6.0	17.93
32.0	22.82	6.0	18.09
35.0	22.79	6.0	18.21
38.0	22.94	6.0	18.23

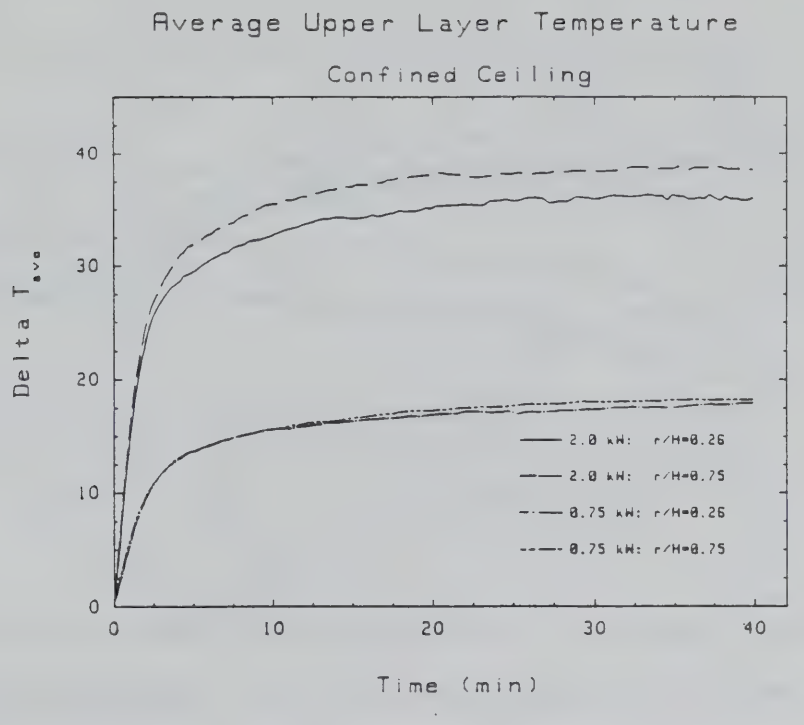

Figure 5.1 - Average Upper Layer Temperature vs. Time

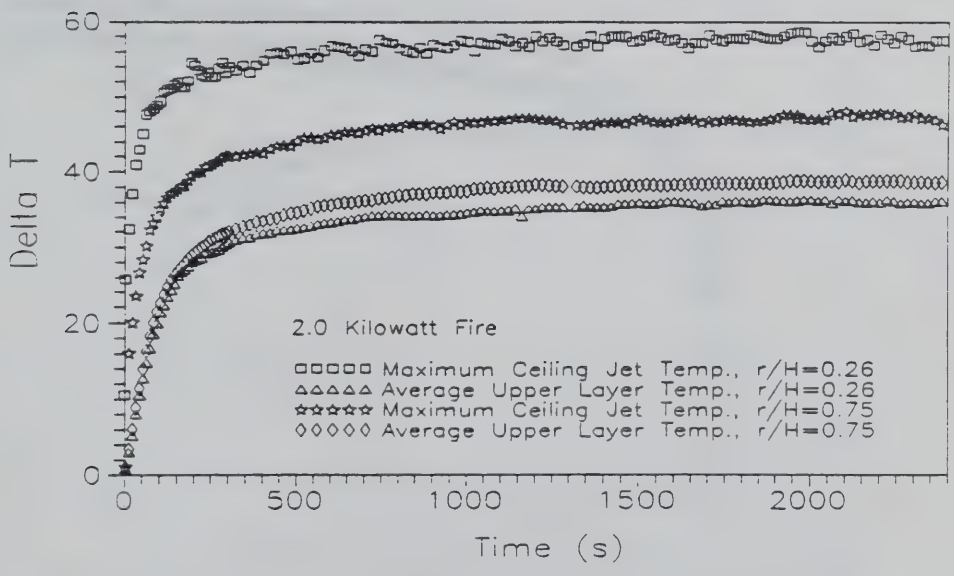

Figure 5.2 - Maximum vs. Average Upper Layer Temperature, 2.0 kW Fire

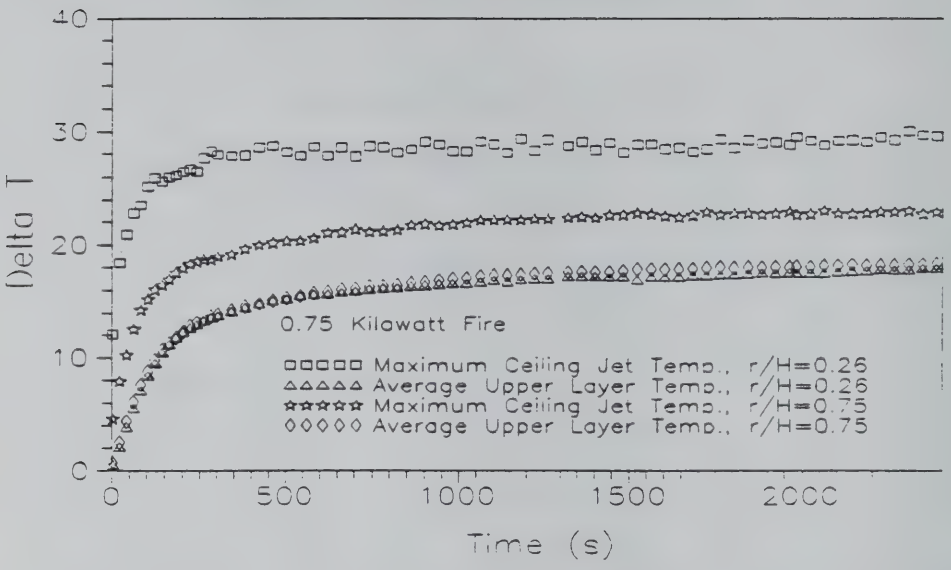

Figure 5.3 - Maximum vs. Average Upper Layer Temperature, 0.75 kW Fire

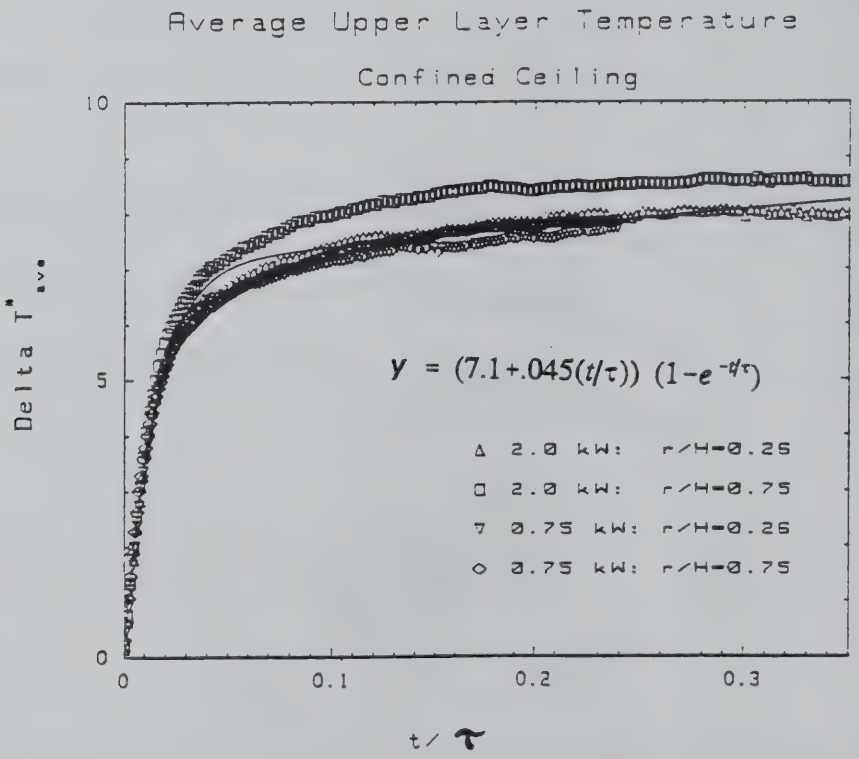

Figure 5.4 - Curve Fit for Average Upper Layer Temperature

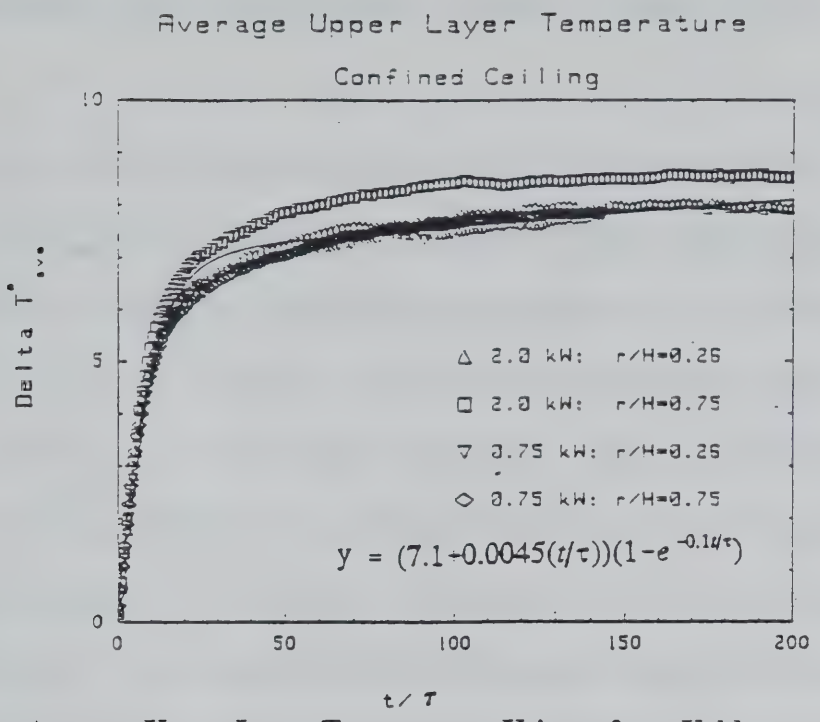

Figure 5.6 - Average Upper Layer Temperature Using τ from Veldman et. al. (1977)

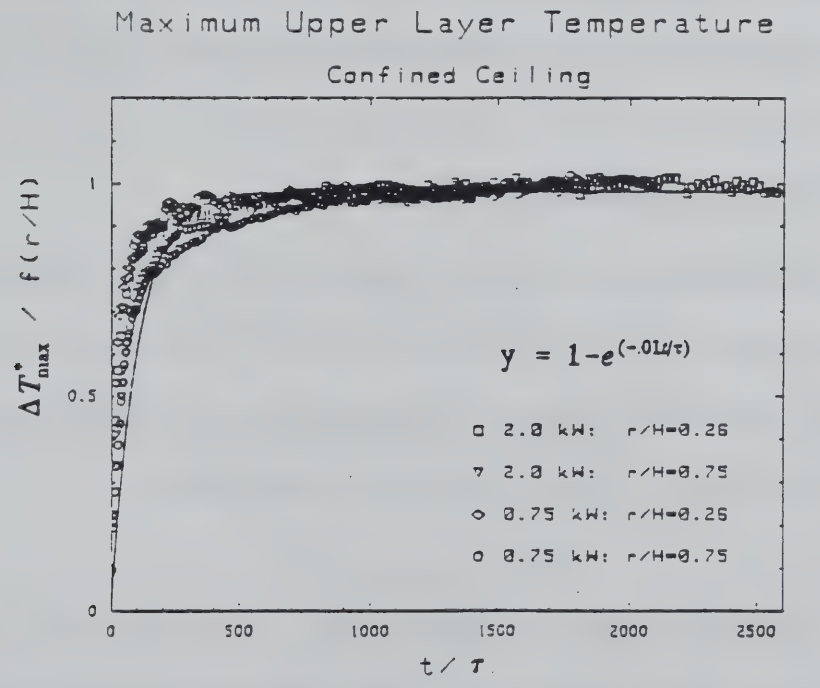

Figure 5.7- Maximum Ceiling Jet Temperature Using τ from Veldman et. al.(1977)

Chapter 6: Predicting Ceiling Jet Behavior

Fire models are used as tools to predict characteristics and development of a fire and to aid in system design or failure analysis. Friedman (1990) identified 36 computer models currently in use to predict the developing fire and surrounding environment. These models are used to predict detector and sprinkler activation times, smoke movement, fire products concentration, temperatures, fire growth rate and occupant evacuation times. Most of these models were developed through analysis of full and small-scale test data. The experimental data collected by Motevalli for confined and unconfined ceiling jets is analyzed and used to examine some of the equations relevant to this work that make up the basis of the fire models. LAVENT (Cooper, 1990) is studied for its prediction of ceiling jet temperatures and the developing upper layer. This code uses correlated to defined ceiling jet velocity and temperature in the upper layer.

6.1 Equations for the Ceiling jet in the Upper Layer

Correlations for the maximum temperature and velocity of the unconfined ceiling jet on a smooth ceiling were developed by Alpert (1972), Heskasted and Delichatsios (1978), Cooper (1982) (based on the experimental data of Heskasted and Delichatsios (1978) and Alpert (1972)) and Motevalli and Marks (1990a).

When these equations are used to model a confined ceiling with a diameter in the order of only a few floor to ceiling heights, the temperature of the ceiling jet will be

under-predicted while the ceiling jet velocity will be over predicted. This occurs because the effects of the developing upper layer are not accounted for. These effects result in a higher temperature and reduced ceiling jet velocity. Ignoring the effects of the upper layer on the ceiling jet by using these unconfined ceiling jet equations is probably conservative (increased temperature, but reduced velocity, i.e. competing mechanisms) for predicting detector operation. However, using the correlations for the unconfined ceiling jet presents a less accurate measure of the ceiling jet characteristics and will under-predicts thermal damage. Evans (1984) and Cooper (1984) have developed methods to account for the upper layer's effect on the ceiling jet characteristics. These methods use an equivalent point source fire which is substituted for the actual fire. This new source is calculated to account for the developing upper layer's effects in the enclosure and on the ceiling jet. It assumes the ceiling jet results from a plume that is fully contained in the upper layer. New values are then calculated for the fire source strength, Q_2, and location beneath the ceiling, H_2. The equations by Evans (1984) are given as:

$$Q_2^* = \left[(1 + C_T Q^{*2/3})/\xi C_T - 1/C_T\right]^3/2 \qquad [6\text{-}1]$$

where the new fire source strength can be calculated using;

$$Q_2 = Q_2^* \rho_\infty c_{P,\infty} T_\infty \sqrt{g Z^5} \qquad [6\text{-}2]$$

and the new height can be calculated using;

$$Z_2 = \left[\frac{\xi Q^* C_T}{Q_2^{*1/3}\left[(\xi-1)(\beta^2+1) + \xi C_T Q_2^{*2/3}\right]} \right]^{2/5} Z \qquad [6\text{-}3]$$

$$H_2 = H - Z + Z_2 \qquad [6\text{-}4]$$

The temperature ratio, ξ, is defined as:

$$\xi = \frac{T_{ul,avg}}{T_\infty} \qquad [6\text{-}5]$$

The values of constants C_T and β are 9.115 and 0.913 respectively from Zukoski et al. (1980).

After a substitute source in the warm upper layer has been calculated, any correlation developed for the unconfined ceiling can be used to calculate maximum temperature and velocity. Upper layer conditions replace the ambient conditions in these equations. To test this approach, ΔT^*_{max} was calculated using correlations Heskestad and Delichatsios (1978):

$$\Delta T^*_{max} = [0.188 + 0.313 r/H]^{-4/3} \qquad [6\text{-}6]$$

and Motevalli and Marks (1990c):

$$\Delta T^*_{max} = 0.166(r/H)^{-2} + 1.2(r/H)^{-1} + 2.0 \qquad [6\text{-}7]$$

Negligible difference in the calculations for ΔT^*_{max}, using Evans approach, were found when applying these two correlations. The maximum temperature in the ceiling jet was then calculated using the relation:

$$T_{max} = Q_2^{*2/3}\, T_{ul,avg}\, \Delta T^*_{max} + T_{ul,avg} \qquad [6\text{-}8]$$

The resulting maximum ceiling jet temperatures using this approach were much lower than expected. This approach did not predict any significant increase in ceiling jet maximum temperature over the average upper layer temperature. Evans (1984) compares this method to other laboratory scale experiments and experiences the same results. It appears that Evans' method even employing Motevalli's correlations under predicts the actual maximum ceiling jet temperature data. Figure 6.1 shows ΔT^*_{max} of the small scale experimental data of Motevalli and Zukoski and Kubota (1977) and the ΔT^*_{max} predicted by Evans' correlations using Motevalli's and Mark's unconfined ceiling jet correlation. The temperature of the ceiling jet for the experiments is consistently higher than predicted by Evans' method.

This method was found to be accurate for full-scale fires by Evans. Evans (1984) indicates the difference in the maximum ceiling jet temperature between the full-scale and small-scale fires could be the result of weaker turbulent mixing in the small-scale fires.

Because full-scale tests were used to develop the empirical correlations of Alpert (1972) and Heskestad and Delichatios (1978) for ΔT_{max}, Evans (1984) recommends that the existing correlations for ΔT^*_{max} be used in application to fires that are larger than the laboratory experiments used to test his correlations. However, the correlation for ΔT^*_{max} by Motevalli and Marks (eqn. 6-7) used here to test Evans upper layer correlations agreed very well with the empirical relations by Heskestad and Delichatsios (equation [6-6]) which is from large scale experiments. It follows that some other factor is creating the error in prediction of small-scale experimental data.

Cooper (1984) has also developed a method to estimate the plume properties and resulting ceiling jet characteristics. Cooper's equations account for the situation where only part of the plume is flowing into the upper layer and impinging on the ceiling. In his procedure the first step is to calculate the mass flow in the plume which enters the upper layer, $\dot{m}_2^*$:

$$\dot{m}_2^* = \frac{1.04599\sigma + 0.360391\sigma^2}{1 + 1.37748\sigma + 0.360391\sigma^2} \qquad [6\text{-}9]$$

where;

$$\sigma = [\xi/(\xi - 1)]\left[(1 + C_T(Q_2^*)^{2/3})/\xi) - 1\right] \qquad [6\text{-}10]$$

and ξ can be calculated from equation 6.5. Then the new interface height, source strength and equivalent source to ceiling height can be calculated by:

$$Z_2 = Z\ \xi^{3/5}\ (m_2^*)^{2/5}\ [(1+\sigma)/\sigma]^{1/3} \qquad [6\text{-}11]$$

$$Q_2 = Q\left[\sigma m_2^*/(1+\sigma)\right] \qquad [6\text{-}12]$$

$$H_2 = H - Z + Z_2 \qquad [6\text{-}13]$$

The value for ΔT_{max} from Cooper's equations was slightly higher than calculated using Evans' equations. However, the predicted value was still significantly lower than the experimental data of this work. These same equations are used in the computer code LAVENT. The results are shown in section 6.2.

6.2 LAVENT (Link-Actuated ceiling VENTs)

The computer code LAVENT was developed by Cooper (1988b) and Davis and Cooper (1989, 1991) to estimate the fire generated environment and the response of heat actuated detectors and ceiling vents in well ventilated compartments fires with draft curtains. The model assumes the upper layer is of a uniform temperature and density. An axi-symmetric ceiling jet flow is modeled using calculated temperature and velocity distributions. This allows the model to calculate the heat transfer to the fusible links more accurately since both radial and vertical location of the link within the jet are important when using velocity and temperature distributions. The program requires the user to input fire size, room geometry and fusible link properties as well as output and solver parameters. The program's output can be examined in tabular or graphical

format. In the graphical format the x and y axes can be chosen from ten parameters to create a graph. These parameters are

- Layer temperature,
- Jet velocity at the link,
- Jet temperature at the link,
- Link temperature,
- Fire output,
- Layer height,
- Plume flow,
- Layer mass,
- Ceiling vent area, and
- Time.

This program was used to model the experiments for confined ceiling jets described in this report. The apparatus was modeled using a square ceiling of the same area and a curtain wall containing the same upper layer volume. (Values used for these parameters are contained in Appendix C.) Temperature and velocity profiles were developed by specifying sprinkler heads at various vertical locations in the ceiling jet. These profiles were compared with the experimental data for a 2.0 kW fire (following discussion first addresses this fire size) and are presented in figures 6.2-6.8. Figures 6.2-6.4 compare the temperature profiles measured in the experiments versus the temperature developed using LAVENT at the radial location of 0.26 meters. Figure 6.2 shows the two profiles at one minute. Here the average upper layer temperatures and profile shapes are similar, however, the experimental ceiling jet temperatures are 25% greater than those calculated by LAVENT. Figure 6.3 shows the same comparison at 3 minutes into the fire. The difference between the two profiles has increased. The average upper layer temperature from the experimental data is greater than the average upper layer temperature predicted by LAVENT as is the overall temperature profile. At

steady state, the two temperature profiles are separated by 20-30% as shown in figure 6.4. This Figure also includes Motevalli and Marks prediction for the unconfined ceiling jet temperature profile for this experimental set-up. Little difference exists between the predictions of the ceiling jet temperatures by LAVENT (2.0 kW fire size) and the measured unconfined ceiling jet temperature experimental conditions. Figure 6.5 shows the comparison for the steady state velocity profiles. Both the shape and the magnitude predicted by LAVENT are different than the experimental measurements. LAVENT's profile resembles the unconfined ceiling jet profile but greatly overpredicts the confined ceiling jet velocity 20-30% and under predicts the ceiling jet momentum boundary layer thickness. This may be due to the fact that Cooper (1988a) bases the ceiling jet velocity on momentum driven wall jets. Figures 6.6, 6.7, and 6.8 present the temperature profiles for the other three cases and show that LAVENT consistently under-predicts the temperature.

LAVENT was also used to model the unconfined experiments of Motevalli and Marks (1990c). The unconfined ceiling jet case in Motevalli and Marks experiments was simulated by specifying the height to the bottom of the curtains wall equal to the ceiling height. Using this approach, the program will model an extensive unconfined ceiling. In this case, the ceiling jet will not be affected by the build up of an upper layer. The program still over predicted the velocity and under-predicted the temperature. This is shown in figures 6.9 and 6.10.

The LAVENT results consistently gave an over-prediction of velocities and an under prediction of ceiling jet and upper layer temperatures obtained experimentally. The results were closer at early times in the fire but quickly diverged. Very few limitations are listed for the use of the program. The limitations listed for the model by Davis and Cooper (1991) for the plume model are satisfied. The plume model requires the ratio of $Q^{2/5}/D$ to fall between approximately 7-700$kW^{2/5}/m$ to be valid. The values for this ratio for the experiments are 33 and 49 $kW^{2/5}/m$. The entrainment model is only valid for cases as present in the experiments where there is no substantial in-depth combustion.

A few assumption are inherent in the model that do not represent conditions in the experiment. These assumptions may be fully responsible for the difference in results. The substantially lower ceiling jet and upper layer temperatures could be caused by the method used to describe heat transfer in the compartment. The thermal response of the ceiling in LAVENT is calculated assuming convective heating from the ceiling jet, radiative heating from the fire, convective cooling from the backside of the ceiling and re-radiation from both sides of the ceiling to ambient. The values of emissivity of the ceiling is assumed to be a black-body with a value of one. The ceiling used in the experiments has a calculated emissivity of 0.91. The fraction of the fires energy radiated to the ceiling and surroundings is assumed to be 0.35. In the experiments a methane flame was used as the fire source. It can be reasonably assumed that little energy was lost by radiation from the flame to the surroundings. The ceiling used in the experiments

was insulated and much less heat was transmitted through the insulation then was calculated through the thin fiberboard ceiling modeled by the program.

LAVENT was run again to model the 2.0 kW fire using a modified value for the heat release rate, Q. A new heat release of 3.077 kW was chosen assuming that 35% of this energy was lost to radiation and a full 2.0 kW of convective energy entered the plume. The predicted temperature profiles were higher than the measured values for the early transitional times, (figures 6.2 and 6.3). As the fire approached steady state, LAVENT produced a close approximation of the ceiling jet profile and a very good prediction of the upper layer temperature. The velocity profile still overpredicted the experimental values by more than 50%. These results show the routines contained in LAVENT may be able to predict the temperature profile for the small-scale experiments if some of the values assumed by LAVENT could be user input based on the case modeled. The velocity profile predictions do not seem to be effective in predicting the experimental velocities. The velocity in the jet does not seem to account for the effect of the upper layer in reducing momentum as seen in the comparison between the confined and the unconfined experiments. Many of the shortcomings in LAVENT seem to be due to the use of wall-jet theory in developing the ceiling jet model. This is especially true for the ceiling jet velocity predictions.

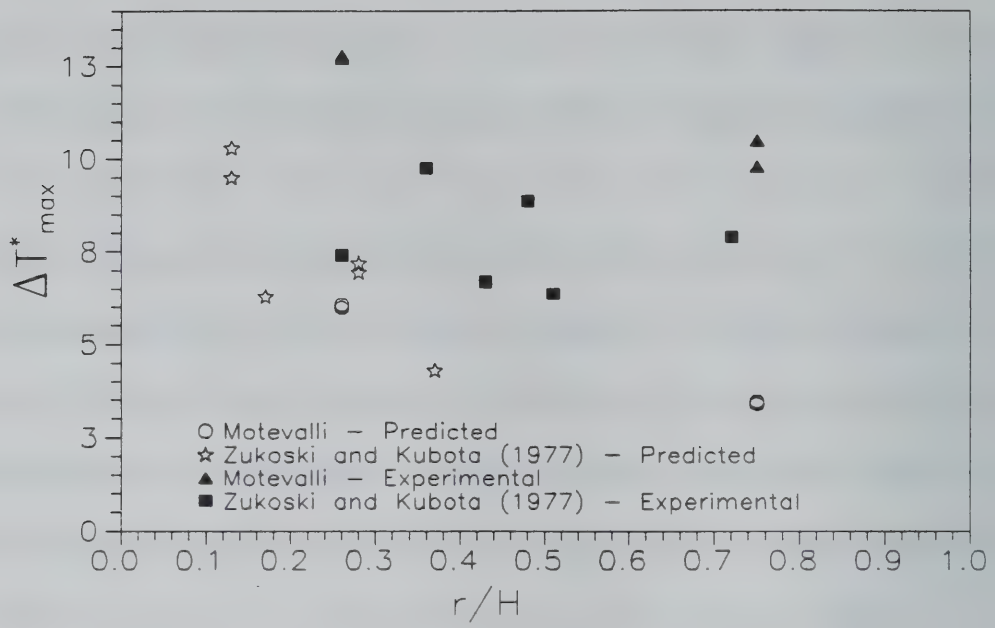

Figure 6.1 - Comparison of Small Scale Experimental Data Using Evans Correlations for ΔT^*_{max}; Q from 0.63-2.0 kW

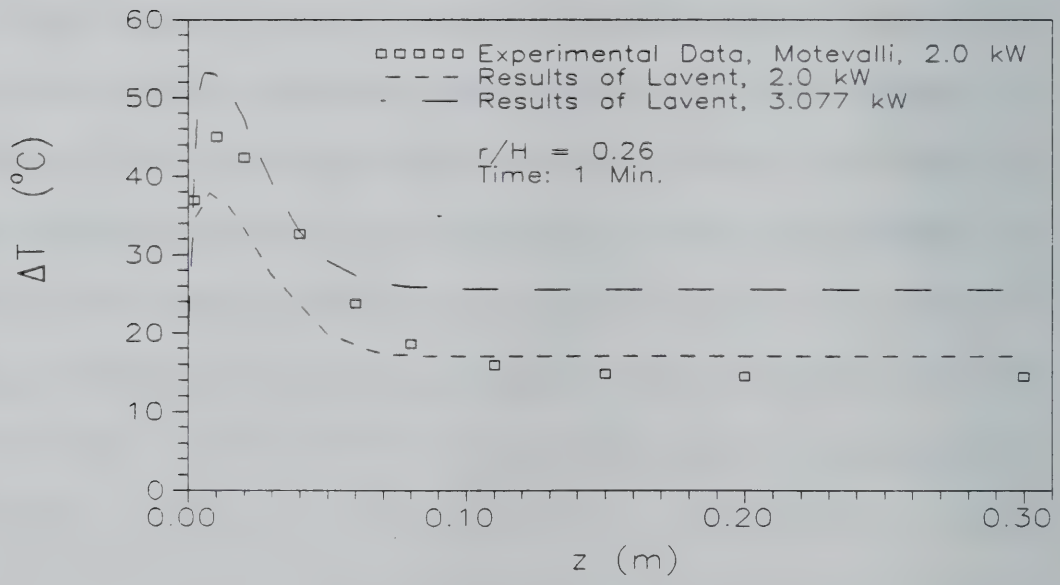

Figure 6.2 - Comparison of experimental Temperature Data with LAVENT Results: Confined Ceiling, 2.0 kW, r/H = 0.26, 1 Minute

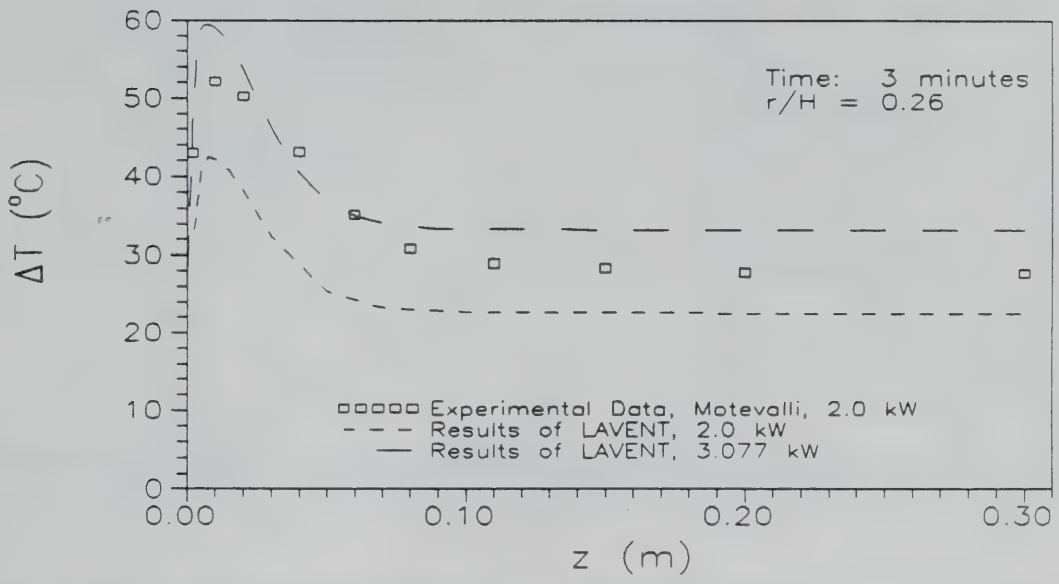

Figure 6.3 - Comparison of Experimental Temperature Data with LAVENT Results: Confined Ceiling, 2.0 kW, r/H = 0.26, 3 Minutes

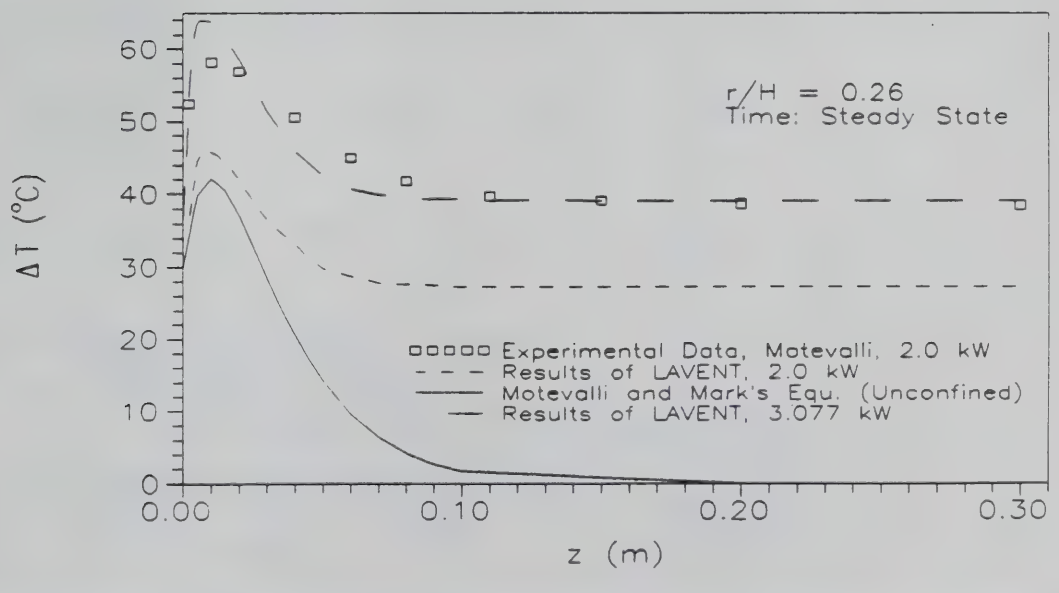

Figure 6.4 - Comparison of Experimental Temperature Data with LAVENT Results: Confined Ceiling, 2.0 kW, r/H= 0.26, Steady State

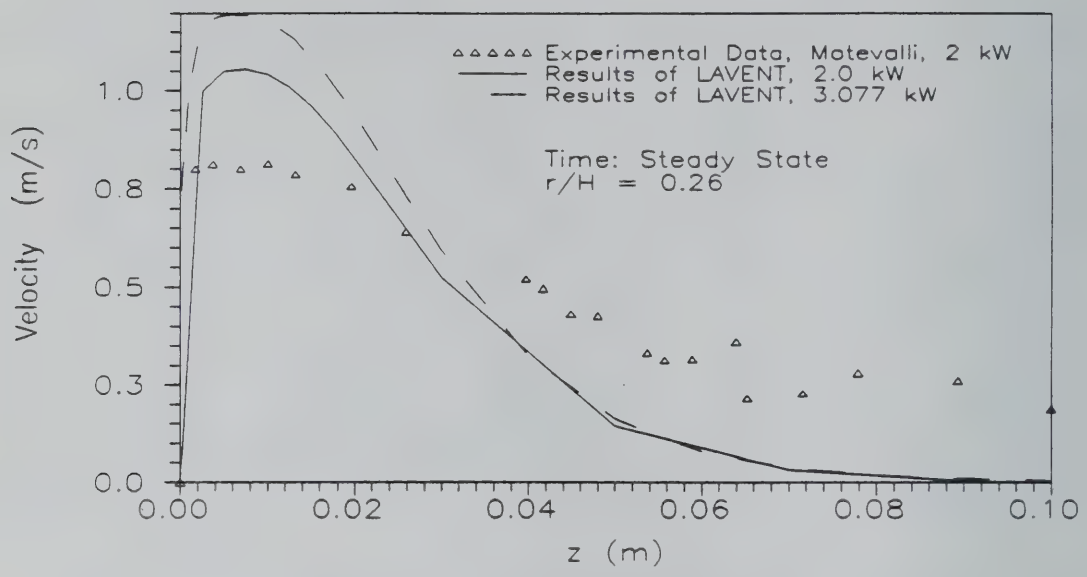

Figure 6.5 - Comparison of Experimental Velocity Data with LAVENT Results: Confined Ceiling, 2.0 kW, r/H= 0.26, Steady State

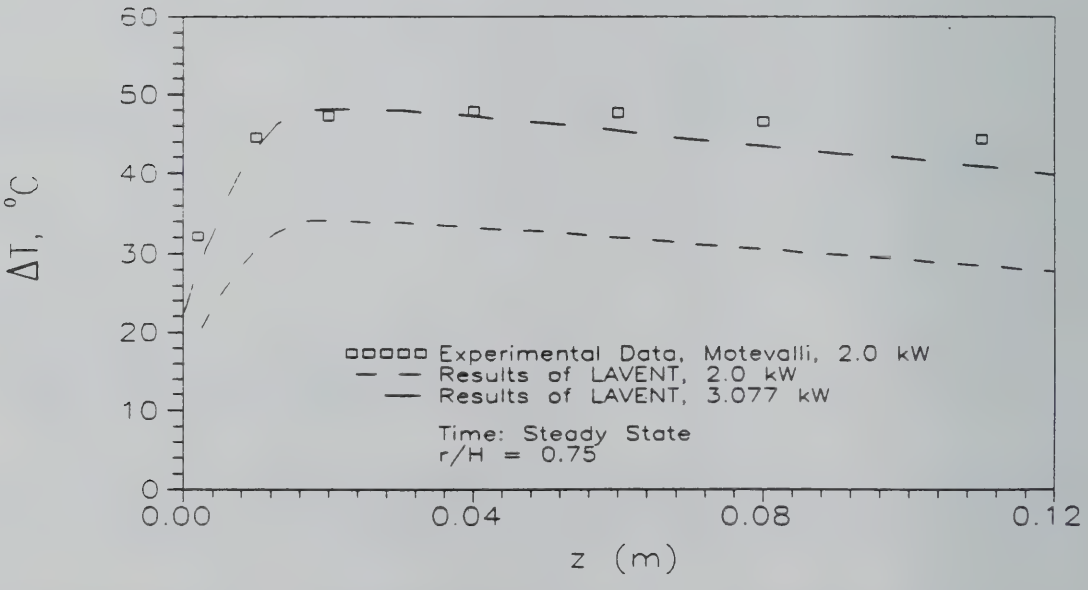

Figure 6.6 - Comparison of Experimental Temperature Data with LAVENT Results: Confined Ceiling, 2.0 kW, r/H= 0.75, Stesdy State

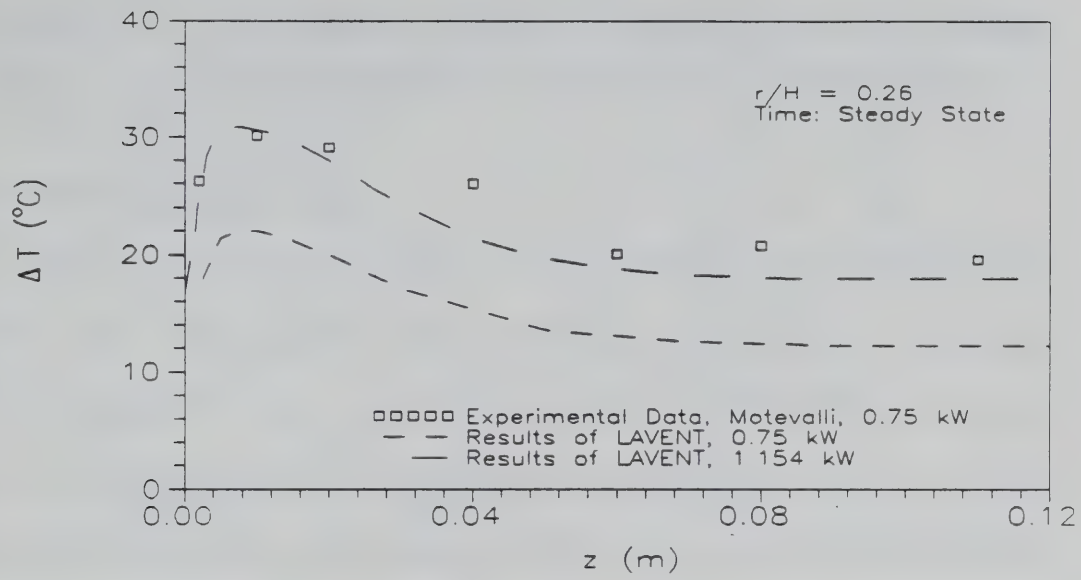

Figure 6.7 - Comparison of Experimental Temperature Data with LAVENT Results: Confined Ceiling, 0.75 kW, r/H= 0.26, Steady State

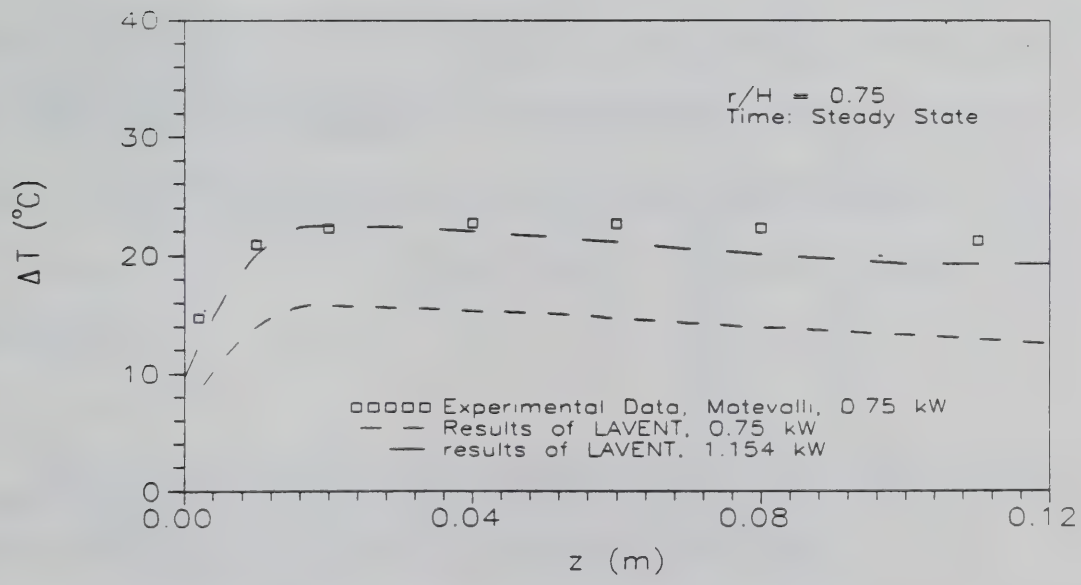

Figure 6.8 - Comparison of Experimental Temperature Data with LAVENT Results: Confined Ceiling, 0.75 kW, r/H= 0.75, Steady State

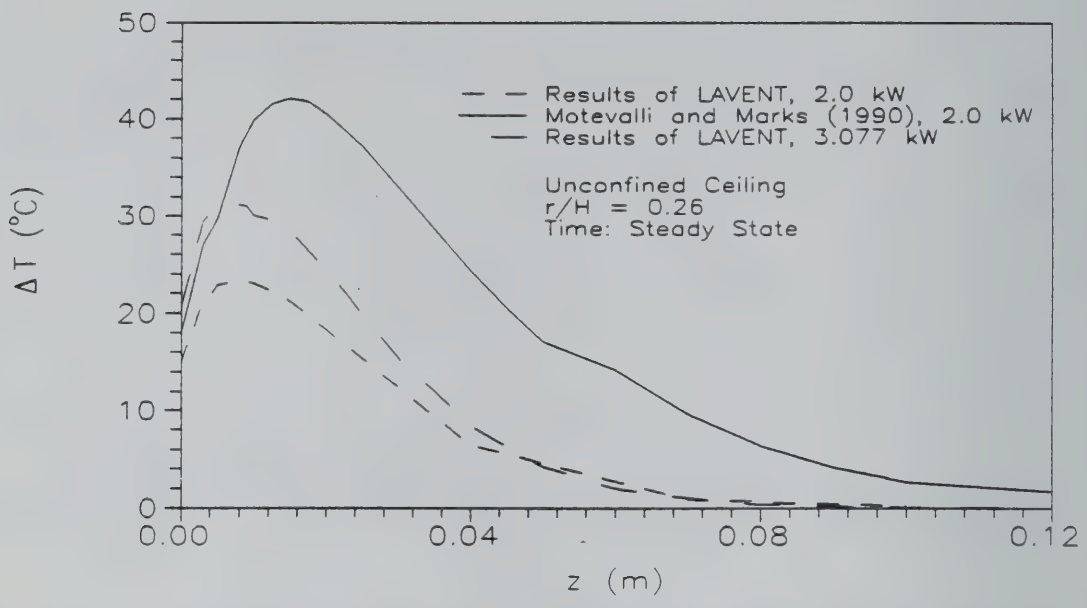

Figure 6.9 - Comparison of Unconfined Ceiling Jet Temperature Profile With LAVENT Results

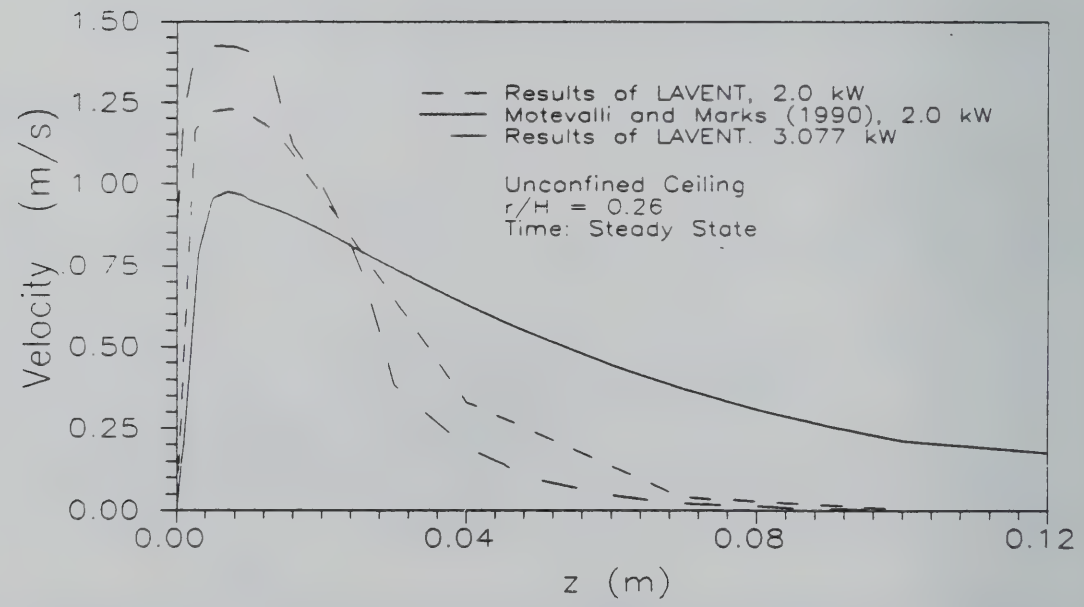

Figure 6.10 - Comparison of Unconfined Ceiling Jet Velocity Data with LAVENT Results

Chapter 7: Prediction of Heat Transfer to the Ceiling and Maximum Ceiling Jet Temperature

7.1 Thermal Boundary Layer

When the ceiling jet flows under the ceiling, which is at a lower temperature, heat transfer occurs between the two mediums. The gas temperature, T_g varies from a maximum temperature, T_{max}, to the ceiling temperature, T_c. The variation takes place in a region defined as the thermal boundary layer. Heat is transferred to the ceiling within the thermal boundary layer primarily by convection. Convective heat transfer to the ceiling can be defined by:

$$\dot{q}''_{conv} = h(T_g - T_c) \qquad [7\text{-}1]$$

where h, the convective heat transfer coefficient, has the dimensions of W/m^2K. The heat transfer coefficient is dependent on the fluid properties and flow characteristics. The heat transfer coefficient can be approximated for most cases with a Prandtl number in the range of 0.6-1.5. The Prandtl number for this case is assumed to be approximately 0.7.

Many empirical relations have been reported for the Nusselt number such as the one shown below for turbulent flow over a flat plate (Drysdale 1985):

$$\overline{Nu} = 0.037\ Re^{4/5}\ Pr^{1/3} \qquad [7\text{-}2]$$

The ceiling jet flow is an unsteady, low Reynolds number flow with large eddy structures and no relation for Nu is truly valid for this case. The Reynolds number for flow over a flat plate, Re_{crit}, must be $\geq 3 \times 10^5$ for equation 7-2 to be valid. The Reynolds numbers for the 2.0 kW fire range from 9645-30162. The Reynold's numbers are in the laminar range, however, the flow has been characterized as turbulent containing large eddy structures by Alpert (1971) and Motevalli et al. (1992).

The convective heat transfer to the ceiling is calculated using three approaches. In the first approach, an energy balance at the ceiling surface is used to account for conduction to the solid, convective heating of the ceiling and re-radiation from the surface. A finite difference model is used to solve for the conduction into the ceiling from the experimentally measured ceiling surface temperature. In the second approach, a classical exact solution for transient heat conduction in a semi-infinite solid is used with a convective boundary condition at the ceiling surface. This solution does not account for re-radiation from the ceiling surface. In the third approach, Cooper and Woodhouse's (1986) empirical relation was used to solve for the convective heat transfer coefficient, h.

7.2 The Heat Transfer Coefficient

The heat transferred to the ceiling by convection, $\dot{q}''_{conv}$, is equal to the amount of the heat conducted into the ceiling and reradiated from the ceiling surface. The ceiling was assumed to be perfectly insulated and is modeled as a semi-infinite solid. This is represented by the equation:

$$\dot{q}''_{conv} = \dot{q}''_{cond} + \dot{q}''_{r} \qquad [7\text{-}3]$$

Heat is conducted at the ceiling surface according to Fourier's heat conduction equation

$$\dot{q}''_{cond} = -k \left.\frac{\partial T}{\partial z}\right|_{z=0} \qquad [7\text{-}4]$$

where k is the thermal conductivity of the ceiling. Heat is also transmitted from the ceiling to the ambient surroundings by radiation from the ceiling surface and is quantified by the expression:

$$\dot{q}''_{r} = \epsilon_c \sigma (T_c^4 - T_\infty^4) \qquad [7\text{-}5]$$

where ϵ_c is the emissivity of the ceiling and σ is the Stephan-Boltzman constant. This results in an equation for the heat transfer coefficient as follows:

$$h = \frac{\epsilon_c \sigma \left(T_g^4 - T_\infty^4 \right) - k \left(\frac{\partial T}{\partial z} \right)_{z=0}}{T_g - T_c} \qquad [7\text{-}6]$$

This h can be used to solve for other parameters that characterize the energy lost to the ceiling and the time scale of formation of the upper layer and maximum ceiling jet temperature.

7.2.1 Numerical Analysis

A finite difference model was used to solve for the one-dimensional transient heat conduction, $\dot{q}''_{cond}$, into the ceiling. Radial conduction within the ceiling is assumed to be negligible relative to the vertical conduction into the ceiling. The equations were solved using the program contained in Appendix D. The initial condition was prescribed by:

$$at\ t=0; \quad T_c = T_\infty$$

for

$$\frac{\partial^2 T}{\partial z^2} = \frac{1}{\alpha} \frac{\partial T}{\partial t} \qquad [7\text{-}7]$$

and the boundary conditions were given by:

$$at\ z=0;\quad T_C=T_{g,c}$$

$$at\ z=\delta_c;\quad \frac{\partial T}{\partial z}=0$$

The values obtained for $\dot{q}''_{cond}$ are shown in table 7.1.

Once the values for $\dot{q}''_{cond}$ were known, the heat transfer coefficient, h, could be solved for using equation 7-5. The ceiling surface and gas temperatures were obtained during the experiments. The emissivity of the ceiling was experimentally determined by Woodhouse and Marks (1985). The values calculated for h are plotted in figure 7.1 and listed in table 7.1 for selected times of 1, 2, 3, 5, 7, 10, 12, 15, 20, 25, 30, and 35 minutes. Figure 7.2 shows the energy balance at the ceiling surface with respect to time. The lower limit for h can be the laminar flow over the flat plate. The values of local h calculated for laminar flow was in the range of 3.39-3.68 W/m^2K for $x=0.26$ and 1.16-1.78 W/m^2K for $x=0.75$ for a 2.0 Kilowatt fire.

7.2.2 Exact Solution

The solution for a semi-infinite solid where there is a sudden change in environment causing a convection exchange with the ceiling was solved by Gebhart (1971). The Fourier equation for one-dimensional transient heat conduction for regions of uniform thermal conductivity is:

$$\frac{\partial^2 T}{\partial z^2} = \frac{1}{\alpha}\frac{\partial T}{\partial t} \qquad [7\text{-}8]$$

Using the method of Laplace transforms and the boundary conditions;

$$at\ z=\delta;\quad \frac{\partial \Theta}{\partial x}=0$$

$$at\ z=0;\quad q''=-k\frac{\partial \Theta}{\partial x}=h\left(\Theta-\Theta_{x=0}\right)$$

The exact solution as presented in Gebhart (1971) becomes:

$$\Theta = 1-erf\,\eta-\left[\exp\left(\frac{hx}{k}+\frac{h^2\alpha\tau}{k^2}\right)\right]\left[1-erf\left(\eta+\frac{h\sqrt{\alpha t}}{k}\right)\right] \qquad [7\text{-}9]$$

This solution does not account for re-radiation from the ceiling. The results for h calculated by iteratively solving the exact solution are presented in figure 7.3. Figure 7.4 shows a comparison between the exact and numerical solution of the $\dot{q}''_{conv}$. Since the exact solution does not account for the re-radiation, it was expected that the value of $\dot{q}''_{conv}$ would compare to the numerical value of $\dot{q}''_{cond}$. Figure 7.4 shows $\dot{q}''_{cond}$ from the numerical solution and $\dot{q}''_{conv}$ from the exact solution are similar in characteristic shape and magnitude.

7.2.3 Cooper and Woodhouse

Cooper (1982, 1984) and Cooper and Woodhouse (1986) have developed a method to estimate the convective heat transfer to the unconfined ceiling. This method

can be adjusted for use with enclosure fires by using Cooper's (1984) method for substitute fire size and height discussed in chapter 6. This heat transfer method accounts for re-radiation from the ceiling surface and variations in the characteristic Reynold's number in the plume. This method is valid for a range of r/H from 0-2.2. The correlations were generated using transient data from the experiments of Veldman et al. (1977). These equations must be modified for use with the confined ceiling case. The equations 6-9 through 6-13 must be used to calculate a new source strength and height Q_2 and H_2.

Cooper and Woodhouse (1986) proposed an equation for h for $r/H > 0.2$

$$\frac{h}{h'} = 0.283\ Re_H^{-0.3}\ Pr^{-2/3}\ (r/H)^{-1/2}\ \frac{(r/H-0.0771)}{(r/H+0.279)} \qquad [7\text{-}10]$$

where

$$h' = \rho_\infty C_p \sqrt{g H_2} Q_2^{*1/3} \qquad [7\text{-}11]$$

$$Re_H = g^{1/2} H_2^{3/2} Q_2^{*1/3} / \nu$$

These equations predict a value for the heat transfer coefficient twice that calculated numerically from the experimental data (see section 7.2.1). The values for h in W/m^2K for the four experimental cases are shown in table 7.2.

Table 7.2

Heat Transfer Coefficient Calculated from Cooper and Woodhouse (1986)

	h (W/m^2)	
	r/H Location	
Q	0.26	0.75
2.0 kW	13.5	7.26
0.75 kW	10.8	5.68

The second part of this method calculates an adiabatic temperature to be used to calculate the heat convected to the ceiling using the equation

$$\dot{q}''_{conv} = h(T_{ad}-T_c)$$

Again the equation for T_{ad} does not predict values in agreement with the maximum temperature obtained experimentally.

7.3 Comparison with Experimental Data

Zukoski and Kubota (1977) and You and Faeth (1978) conducted small-scale experiments which measured heat transfer to the ceiling. You and Faeth (1978) measured wall heat fluxes during the transient period, 0-7 minutes. The corresponding jet temperature was measured only at steady state, the period when a constant ceiling temperature was obtained. An equation was developed to estimate the heat flux to the unconfined ceiling as a function of radial distance.

$$\frac{\dot{q}''}{\dot{Q}H^2} = 0.353Pr^{-2/3}\left[1+18.87\left[(r/H)^2 - 0.0287\right]\right]^{-(1+0.059Pr^{-2/3})} \qquad [7\text{-}12]$$

All the relevant factors are not considered by this equation. This function over predicts the values of $\dot{q}''_{conv}$ obtained in this work. The values for heat flux to the ceiling in You and Faeth's experiments are much larger than the values calculated here. This is due to the different factors in the experiments, such as ceiling height, layer depth, and ceiling material.

Zukoski and Kubota (1977) measured the transient wall temperature, the steady state gas temperature close to the ceiling and the increase in internal energy of the ceiling. The heat transfer to the ceiling was calculated from these values. Again the differences between the heat transfer coefficient and heat flux to the ceiling was twice the values reported here. The heat transfer coefficients were normalized for all the experiments using h′ from equation [7-11]. The data for the three experiments did not correlate. Other factors that differ between the experiments must be considered for proper comparison.

Table 7.1 - Heat Transfer Coefficient[1]

Fire Size:		2.0 kW		0.75 kW	
r/H Location:		0.26	0.75	0.26	0.75
1 Minute	$\dot{q}''_{cond}$	131.4	71.3	63.3	31.1
	T_c	305.8	300.8	300.4	294.8
	T_g	341.0	324.4	318.2	304.5
	h	5.28	4.14	4.9	4.16
2 Minutes	$\dot{q}''_{cond}$	126.1	79.2	64.7	34.3
	T_c	309.9	303.9	302.5	296.3
	T_g	346.6	331.8	321.5	308.7
	h	5.60	4.41	5.31	4.15
3 Minutes	$\dot{q}''_{cond}$	119.3	68.8	56.7	30.62
	T_c	312.4	305.4	303.8	297.0
	T_g	347.2	334.2	321.6	310.3
	h	6.16	4.23	5.61	3.89
5 Minutes	$\dot{q}''_{cond}$	105.6	73.5	51.4	28.2
	T_c	315.5	308.3	305.4	298.0
	T_g	349.2	338.2	323.8	311.8
	h	6.55	4.82	5.65	3.97
7 Minutes	$\dot{q}''_{cond}$	83.3	62.1	41.62	26.15
	T_c	317.1	310.0	306.2	298.7
	T_g	350.8	338.5	323.8	312.7
	h	6.18	4.97	5.64	4.07
10 Minute	$\dot{q}''_{cond}$	65.71	55.23	30.64	23.02
	T_c	318.9	312.7	306.9	299.7
	T_g	352.1	340.5	324.6	313.6
	h	6.15	5.26	5.26	4.24

[1] $\dot{q}''_{cond}$, T and h have units of W/m^2, K and W/m^2K, respectively.

Table 7.1 - Heat Transfer Coefficient (Cont.)[2]

Fire Size:		2.0 kW		0.75 kW	
r/H Location:		0.26	0.75	0.26	0.75
12 Minutes	$\dot{q}''_{cond}$	55.41	45.84	27.08	20.84
	T_c	319.9	313.1	307.5	300.2
	T_g	352.3	341.5	323.8	314.4
	h	6.18	5.12	5.68	4.21
15 Minutes	$\dot{q}''_{cond}$	45.88	38.84	23.00	18.98
	T_c	321.4	314.4	308.3	300.9
	T_g	351.7	342.4	324.4	314.6
	h	6.61	5.25	5.78	4.58
20 Minutes	$\dot{q}''_{cond}$	23.93	25.13	14.81	11.44
	T_c	322.0	315.6	308.9	301.5
	T_g	352.6	343.2	325.3	315.2
	h	5.95	5.10	5.45	4.20
25 Minutes	$\dot{q}''_{cond}$	11.74	15.26	10.64	7.74
	T_c	322.1	316.2	309.6	301.9
	T_g	353.5	343.2	324.5	315.8
	h	5.46	5.01	5.92	4.03
30 Minutes	$\dot{q}''_{cond}$	6.39	11.12	8.76	6.10
	T_c	322.3	316.8	310.2	302.3
	T_g	353.7	342.7	324.6	315.8
	h	5.30	5.18	6.26	4.17
35 Minutes	$\dot{q}''_{cond}$	3.85	9.15	7.87	5.31
	T_c	322.4	317.4	310.8	302.6
	T_g	353.7	343.6	325.5	315.8
	h	5.31	5.26	6.31	4.40

[2] $\dot{q}''_{cond}$, T and h have units of W/m^2, K and W/m^2K, respectively.

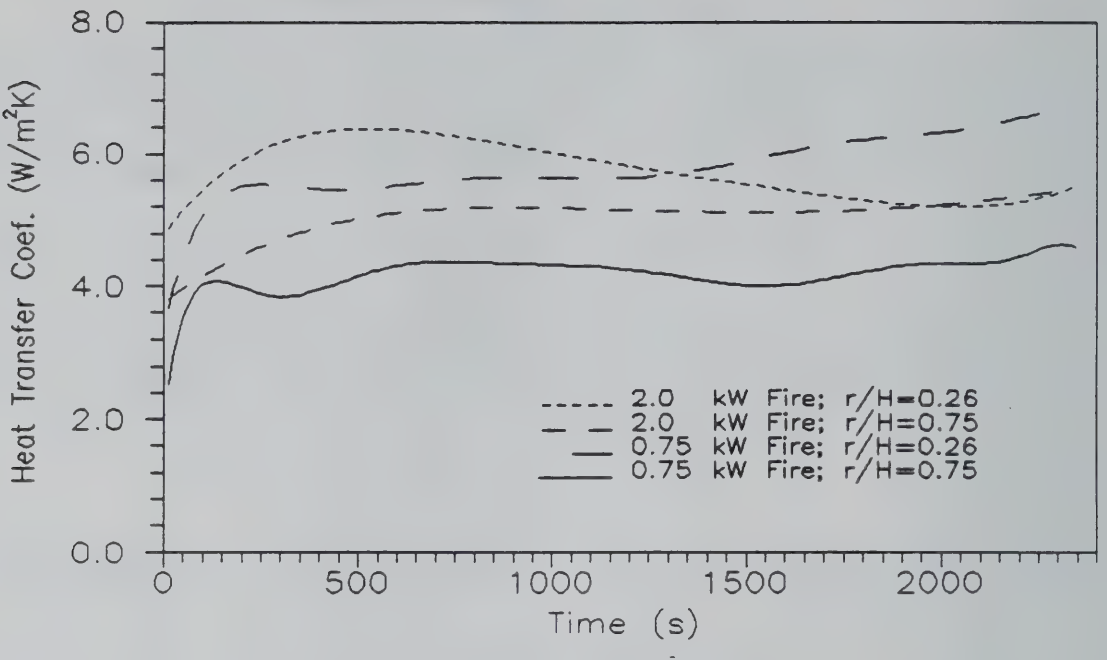

Figure 7.1 - Heat Transfer Coefficient

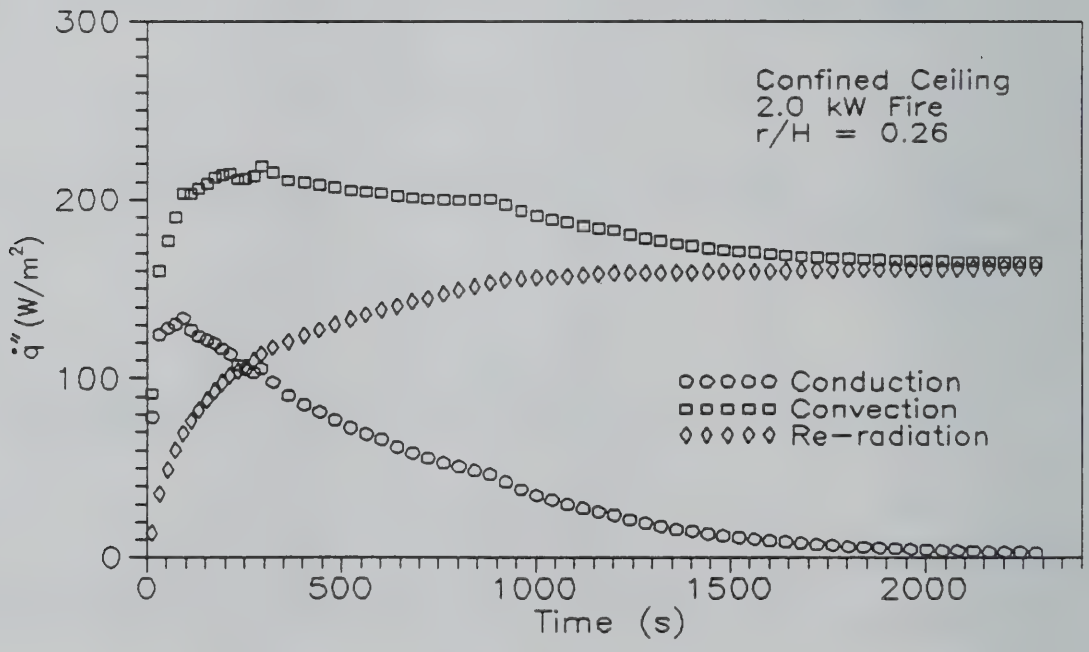

Figure 7.2 - Energy Balance at the Ceiling

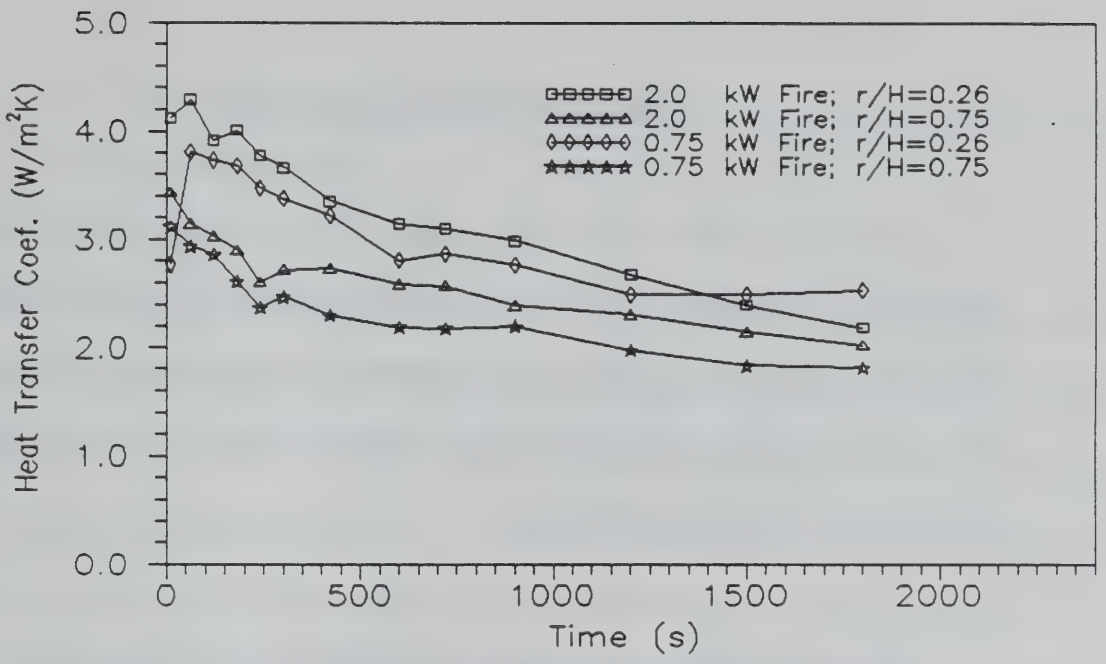

Figure 7.3 - Heat Transfer Coefficient Calculated Using Exact Solution

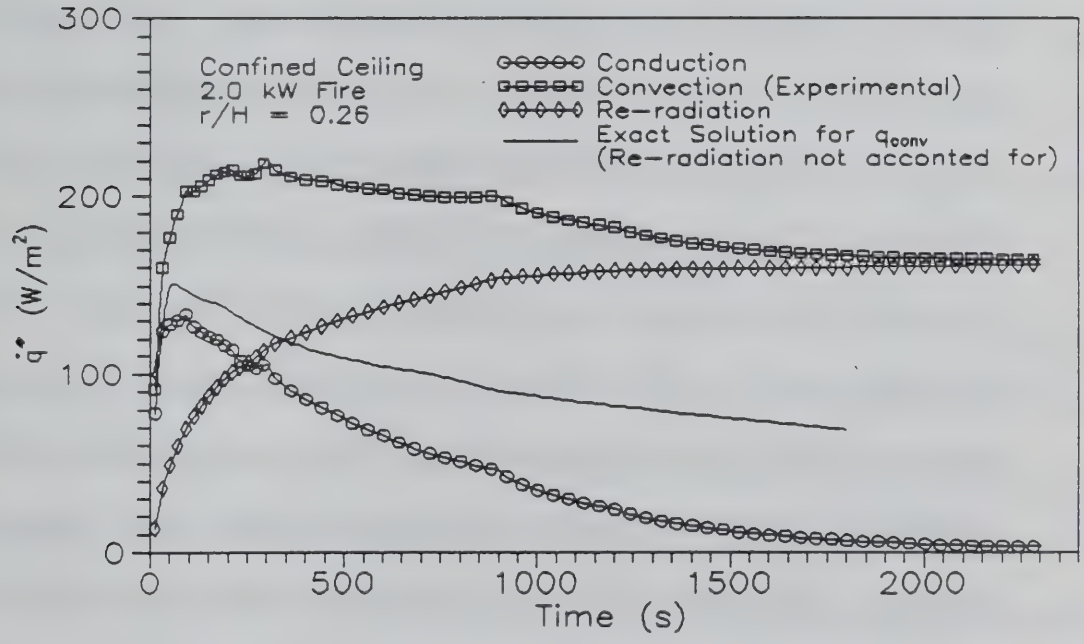

Figure 7.4 - Comparison of Numerical and Exact Solution for q_{conv}

Chapter 8: Conclusions

It has been shown here that the ceiling jet in an enclosure has characteristics significantly different than those of an unconfined ceiling jet due to the presence of the upper layer. These effects become apparent almost immediately after the start of a fire. This report examined these differences by comparing the two cases and attempted to quantify these different characteristics.

The first objective was to examine the differences in temperature and velocity profiles between the confined and unconfined ceiling jets. Data was collected from the two sets of experiments using essentially the same apparatus. Significant differences between the two cases were expected and found. Although the ceiling jet thermal and momentum boundary layer thicknesses were similar, the magnitude of the maximum temperature and velocity and overall profile values were much different. The maximum ceiling jet temperature for the confined ceiling was 25-50% higher than for the unconfined ceiling jet. The ceiling jet maximum velocity was 10-20% lower than the maximum velocity of the unconfined ceiling jet. The temperature of the confined ceiling jet profile was found to be transient due to the heat transfer to the ceiling and walls. Transience in the ceiling jet was also due to the developing upper layer. This upper layer was at a temperature above ambient and caused the temperature of the ceiling jet to be elevated due to the entrainment of the increasingly warmer gases in the layer. The

velocity in the confined ceiling jet was lower probably due to increased momentum loses induced by the upper layer.

The second objective was the quantification of the characteristics of the confined ceiling jet and upper layer. The maximum ceiling jet temperature was found to be a function of fire size and radial location. The non-dimensionalized maximum ceiling jet temperature correlated quite well with respect to fire size and r/H location. A correlation was developed for the maximum ceiling jet temperature as a function of a time and a characteristic time constant. An average upper layer temperature was also calculated from the experimental data. It was found that there was no significant difference in the average upper layer temperature with respect to the radial locations examined in these experiments, however, a distinct ceiling jet still existed at both r/H locations. The temperature in the ceiling jet ranged from 30 to 300% above the average upper layer temperatures. The difference in the temperature being greater, up to 300%, during the earlier transient times. A correlation was also developed to calculate the average upper layer as a function of time. Thus, two empirical relations now exists for the maximum ceiling jet temperature and the average upper layer temperature as a function of Q^*, r/H location (for maximum temperature only), ambient conditions and time. The characteristic time for the transience of the upper layer and the ceiling jet temperature was adopted from Veldman et al. (1977). This characteristic time, τ, is a function of the fire size, ceiling height and material properties.

The third objective was to analyze the heat transfer from the ceiling jet to the ceiling. Values for the heat convection to the ceiling and re-radiation from the ceiling surface were found numerically. The values for the local heat transfer coefficient were in the range of 3-6 W/m^2K. These values were verified using an exact solution to the Fourier heat conduction equation using a convection boundary condition. The results using both methods showed good agreement. These values were compared to data from other small-scale confined ceiling jet experiments. The values for the heat transfer coefficients and heat flux to the ceiling could not be correlated between experiments due to dependency of the correlation to ceiling material and conduction heat transfer through the ceiling.

Several methods available to solve for conditions in the confined ceiling jet, heat transfer to the ceiling and the computer model LAVENT were examined for their ability to predict values obtained in these experiments. None of the methods examined were adequate in predicting the experimental results. With some modifications in input LAVENT predicted the temperature profile in the upper layer, however, the calculations for velocity were 50% higher than the experimental data. This would not allow for accurate prediction of link actuation time, a main feature of the model. The results of this study show significant differences exist between the two cases. To fully understand and predict the fire environment in an enclosure, the confined ceiling jet and upper layer

must be more accurately characterized. Some characteristics in this experiment have been quantified but large-scale experiments are necessary to verify and expand these correlations.

References

Alpert, R. L., "Calculations of Response Times of Ceiling Mounted Fire Detectors", *Fire Technology*, Vol. 8, pp 181-189, (1972).

Alpert, R. L., "Convective Heat Transfer in the Impingement Region of a Buoyant Plume", *Journal of Heat Transfer*, Vol. 109, pp. 120-124, (1987).

Baines, W. D. and Turner, J. S., "Turbulent Buoyant Convection from a Source in a Confined Region", *Journal of Fluid Mechanics*, Vol. 37, pp 51-62, (1969).

Bangaro, M., Laouisset, M. and Lockwood, F.C., "Field Model Prediction of Some Room Fires", *Fire Dynamics and Heat Transfer*, HTD-Vol. 25, ASME, New York, NY, pp. 107-114. (1983).

Beyler, C. L., "Fire Plumes and Ceiling Jets", *Fire Safety Journal*, Vol 11, pp.53-75, (1986).

Cooper, L. Y., Harkleroad, M., Quintere, J., and Rinkinen, W., "An Experimental Study of Upper Hot Layer Stratification in Full-Scale Multiroom Fire Scenarios", *Journal of Heat Transfer*, Vol. 104, pp. 741-749, (1982).

Cooper, L. Y., "Heat Transfer From a Buoyant Plume to an Unconfined Ceiling", *Journal of Heat Transfer*, Vol. 104, pp. 446-451, (1982).

Cooper, L. Y., "A Buoyant Source in the Lower of Two, Homogeneous Stably Stratified Layers," *Twentieth Symposium (International) on Combustion*, The Combustion Institute, pp. 1567-1573, (1984).

Cooper, L. Y. and Woodhouse, A, "A Buoyant Plume-Driven Adiabatic Ceiling Temperature Revisited", *Journal of Heat Transfer*, Vol. 108, pp. 822-826, (1986).

Cooper, L. Y. and Stroup, D. W., "Test Results and Predictions for the Response of Near-Ceiling Sprinkler Links in a Full Scale Compartment Fire", National Bureau of Standards, Report No. NBSIR 87-3633, (1987).

Cooper, L. Y., "Ceiling Jet-Driven Wall Flows in Compartment Fires", *Combustion, Science and Technology*, Vol. 62, pp. 285-296, (1988).

Cooper, L. Y., "Estimating the Environment and the Response of Sprinkler Links in Compartment Fires with Draft Curtains and Fusible Link-Actuated Ceiling Vents - Part I: Theory", National Bureau of Standards, Report No. NBSIR 88-3734, (1988).

Cooper, L. Y., "Heat Transfer in Compartment Fires Near Regions of Ceiling Jet Impingement", *Journal of Heat Transfer*, Vol. 11, pp 455-460, (1989).

Cooper, L.Y., "Estimating the Environment and the Response of Sprinkler Links in Compartment Fires with Draft Curtains and Fusible Link-Actuated Ceiling Vents-Theory", Fire Safety J., Vol. 16, p. 137-163, (1990).

Cox, G., "Gas Velocity Measurements in Fire by the Cross-Correlation of Random Thermal Fluctuations- A Comparison of Conventional Techniques", *Combustion and Flame*, Vol. 28, pp. 155-163, (1977).

Cox, G. and Chitty, R., "A Study of the Deterministic Properties of Unbounded Fire Plumes", *Combustion and Flame*, Vol. 39, pp. 191-209, (1980).

Davis, W. D. and Cooper, L. Y., "Estimating the Environment and the Response of Sprinkler Links in Compartment Fires with Draft Curtains and Fusible-Link-Actuated Ceiling Vents - Part II: User Guide for the Computer Code LAVENT", National Institute of Standards and Technology, Report no. NISTIR 89-4122, (1989).

Davis, W. D. and Cooper, L. Y., "Estimating the Environment and the Response of Sprinkler Links in Compartment Fires with Draft Curtains and Fusible-Link-Actuated Ceiling Vents", *Fire Technology*, pp 113-127, May (1991).

Drysdale, D, "An Introduction to Fire Dynamics", John Wiley and Sons, (1985).

Ellison, T. H and Turner, J. S., "Turbulent Entrainment in Stratified Flows", *Journal of Fluid Mechanics*, Vol. 6, pp. 424, (1959).

Evans, D. D., *Fire Technology*, Vol. 20, p.39, (1984).

Evans, D. D., "Plume Flow in a Two-Layer Environment", *Fire Dynamics and Heat Transfer*, HTD-Vol. 25, Asme, New York, NY, pp. 89-95, (1983).

Evans, D. D. and Morehart, J., "Investigation of the Effects of a Stratified Two Layer Environment on Fire Plume Temperatures", ASME-JSME Thermal Engineering Joint Conference, Vol. 1, March 22-27, Honolulu, HI, (1987).

Friedman, R.,"Survey of Computer Models For Fire and Smoke", Factory Mutual Technical Report, Factory Mutual Research Corporation, Norwood, MA, March (1990).

Gebhart, B., "Heat Transfer", McGraw-Hill Book Co., NY, (1971).

Heskestad, G., and Delchatsios, M. A., "The Initial Convective Flow in Fires", Seventeenth Symposium (International) on Combustion, pp. 1113-1123, (1978).

Markatos, N. C., and Pericleous, K. A., "An Investigation of Steady, Three Dimensional Fires in Enclosures", *Fire Dynamics and Heat Transfer*, HTD-Vol. 25, Asme, New York, NY, pp. 115-124. (1983).

Morita, M. and Hirota, M., "Numerical Analysis and Experiments of Convective Heat Flow in Fire Compartments", *Fire Science and Technology*, Vol. 9 No. 1, pp. 11-24, (1989).

Motevalli, V. and Marks, C.H., "Transient and steady State Study of Small-Scale, Fire-Induced Unconfined Ceiling Jets", *Heat and Mass Transfer in Fires*, ASME, HTD-Vol.141, pp. 49-63, (1990).

Motevalli, V, "Numerical Prediction of Unconfined Ceiling Jet Transient Temperature Profiles Using Two-Dimensional Turbulent Continuity and Energy Equations with Empirical Velocity Profiles", *Heat and Mass Transfer in Fires*, ASME, HTD-Vol.141, pp. 85-93, (1990).

Motevalli, V and Marks, C. H., "Transient Characteristics of Unconfined Fire-Plume-Driven Ceiling Jets", National Institute of Standards and Technology, Rpt. No. NIST/GCR-90/574, (1990).

Motevalli, V., Marks, C.H., and McCaffrey, B. J., "Measurements of Velocity and Temperature Profiles in Low-Speed, Turbulent, Non-Isothermal Flows", J. of Heat Transfer, Vol. 114, N0. 2, (1992).

Mulholland, G., Handa, T., Sugawa, O. and Yamamoto, H., "Smoke Filling an Enclosure", *Fire Science and Technology*, Vol. 1, pp. 1-31, (1981).

Prahl, J. and Emmons, H. W., "Fire induced Flows through an Opening", *Combustion and Flame*, Vol. 25, pp. 369-385, (1975).

Quintiere, J. G. and McCaffrey, B. J., "The Burning of Wood and Plastic Cribs in an Enclosure", National Bureau of Standards, Report No. NBSIR 80-2054, (1980).

Quintiere, J. G.,80- Steckler, K. and Corley, D., *Fire Science and Technology*, Vol 4, pp.1 -14, (1984).

Steckler, K. D., Quintiere, J. D. and Rinkinen, W. J., "Flow Induced by Fire in a Compartment", *Nineteenth Symposium (International) on Combustion*, The Combustion Institute, pp. 913-920, (1982).

Timlin, J. and Mihalisin, T., "TEMPLE DATATAP Analysis", Rev. 3.0, Data Analysis and Plotting Prog., Temple University, (1987).

Veldman, C. C., Zukoski, E. E. and Kubota, T., "An Experimental Investigation of The Heat Transfer From a Buoyant Plume to a Horizontal Ceiling- Part I. Unobstructed Ceiling" National Bureau of Standards, Report No. NBS-GCR 77-97, (1977).

Woodhouse, A. and Marks, C. H., "A Study of the Transient Thermal Response of Unconfined Ceiling above Small Fire Plumes", Final Report to the National Bureau of Standards, Center for Fire Research, (1985).

You, H. Z. and Faeth, G.M., "An Investigation of Fire Impingement on a Horizontal Ceiling", National Bureau of Standards, Rpt. No. NBS-GCR-79-188, (1978).

You, H. Z. and Faeth, G.M., "Ceiling Heat Transfer during Fire Plume and Fire Impingement", *Fire and Materials*, Vol. 3, pp. 140-147, (1979).

Zukoski, E. E. and Kubota, T., "An Experimental Investigation of the Heat Transfer from Buoyant Plume to a Horizontal Ceiling- Part 2, Effects of Ceiling Layers", National Bureau of Standards, Rpt. No. NBS-GCR-77-98, (1977).

Zukoski, E. E., Kubota, T. and Cetegen, B. "Entrainment of Fire Plumes", Fire Safety J., 3, p. 107-21, (1980).

Appendix A
Temperature and Velocity Data for Ceiling Jet

Ceiling Type Fiberboard
Fire Strength= 2.0 KW
Ceiling to Floor Height, H: 1.0 m
Probe Location (r/H): 0.26

Time= 5 Seconds

z (mm)	Velocity (m/s)	Delta T (C)	z (mm)	Velocity (m/s)	Delta T (C)
1.7	.920	33.84	3.7	.920	35.34
6.9	.855	35.48	10.0	.855	35.28
13.2	.798	34.53	19.6	.748	32.28
25.9	.665	29.18	39.7	.499	22.37
41.7	.499	21.53	44.9	.428	20.17
48.0	.428	18.81	51.2	.400	16.80
51.3	.293	7.24	53.7	-	6.03
55.7	.267	5.64	57.6	.375	-
58.9	.267	5.04	62.0	.207	4.72
63.9	.414	-	65.2	.218	4.34
71.6	.286	3.89	77.9	.444	3.69
89.3	0.000	4.78	103.3	-	2.30

MAXIMUM VELOCITY (m/s)= .920 Position of maximum (mm)= 3.68
MAXIMUM DELTA T (C)= 35.48 Position of maximum (mm)= 6.85
Data Set I.D.: CF5VCN1

Time= 1 Minute

z (mm)	Velocity (m/s)	Delta T (C)	z (mm)	Velocity (m/s)	Delta T (C)
1.7	.798	45.53	3.7	.798	47.92
6.9	.798	49.13	10.0	.798	49.21
13.2	.748	48.52	19.6	.704	46.90
25.9	.631	44.90	39.7	.461	40.58
41.7	.461	39.37	44.9	.400	38.18
48.0	.428	37.40	51.2	.461	36.45
51.3	-	37.28	53.7	.461	30.08
55.7	.545	29.49	57.6	.444	34.49
58.9	.748	28.87	62.0	-	28.29
63.9	.387	33.04	65.2	.798	27.84
71.6	.599	27.12	77.9	.480	26.57
89.3	.267	28.03	103.3	.162	25.89

MAXIMUM VELOCITY (m/s)= .798 Position of maximum (mm)= 1.69
MAXIMUM DELTA T (C)= 49.21 Position of maximum (mm)=10.03
Data Set I.D.: CF5VCN4 CF5TCN4

Time= 2 Minutes

z (mm)	Velocity (m/s)	Delta T (C)	z (mm)	Velocity (m/s)	Delta T (C)
1.7	.798	50.18	3.7	.798	52.75
6.9	.855	54.36	10.0	.920	54.69
13.2	.855	54.04	19.6	.748	52.29
25.9	.665	50.15	39.7	.521	46.91
41.7	.521	45.91	44.9	.461	44.83
48.0	.461	44.12	51.2	.461	43.16
51.3	-	41.44	53.7	.480	37.26
55.7	.599	36.51	57.6	.414	41.17
58.9	.480	35.93	62.0	.521	35.55
63.9	.461	39.37	65.2	.400	35.42
71.6	-	34.78	77.9	-	33.90
89.3	.461	34.12	103.3	-	31.27

MAXIMUM VELOCITY (m/s)= .920 Position of maximum (mm)=10.03
MAXIMUM DELTA T (C)= 54.69 Position of maximum (mm)=10.03
Data Set I.D.: CF5VCN7 CF5TCN7

Time= 3 Minutes

z (mm)	Velocity (m/s)	Delta T (C)	z (mm)	Velocity (m/s)	Delta T (C)
1.7	.798	52.32	3.7	.798	55.06
6.9	.798	56.85	10.0	-	57.64
13.2	.748	56.44	19.6	.704	54.44
25.9	.665	52.21	39.7	.545	50.39
41.7	.521	49.32	44.9	.480	47.87
48.0	.521	46.78	51.2	.571	45.40
51.3	-	45.04	53.7	.631	38.28
55.7	.665	37.61	57.6	.414	42.50
58.9	.798	36.97	62.0	.748	36.37
63.9	.363	40.07	65.2	.920	35.86
71.6	.148	35.05	77.9	.167	34.64
89.3	.308	35.33	103.3	.058	33.68

MAXIMUM VELOCITY (m/s)= .798 Position of maximum (mm)= 1.69
MAXIMUM DELTA T (C)= 57.64 Position of maximum (mm)=10.03
Data Set I.D.: CF5VCN10 CF5TCN10

Time= 5 Minutes

z (mm)	Velocity (m/s)	Delta T (C)	z (mm)	Velocity (m/s)	Delta T (C)
1.7	.798	56.88	3.7	.798	58.12
6.9	.798	58.50	10.0	–	57.55
13.2	.748	57.36	19.6	.704	55.50
25.9	.665	53.14	39.7	.461	51.41
41.7	.414	50.78	44.9	.363	50.15
48.0	.400	49.66	51.2	.387	49.22
51.3	–	46.92	53.7	.353	41.88
55.7	.316	41.33	57.6	.353	47.77
58.9	.363	40.89	62.0	.499	40.46
63.9	.279	46.53	65.2	–	40.08
71.6	.545	39.45	77.9	.375	39.13
89.3	.194	41.13	103.3	–	38.40

MAXIMUM VELOCITY (m/s)= .798 Position of maximum (mm)= 1.69
MAXIMUM DELTA T (C)= 58.50 Position of maximum (mm)= 6.85
Data Set I.D.: CF5VCN16 CF5TCN16

Time= 10 Minutes

z (mm)	Velocity (m/s)	Delta T (C)	z (mm)	Velocity (m/s)	Delta T (C)
1.7	.748	57.32	3.7	.798	58.93
6.9	.798	59.70	10.0	–	58.99
13.2	.798	59.21	19.6	.748	57.43
25.9	.704	55.34	39.7	.499	52.67
41.7	.480	51.90	44.9	.428	50.90
48.0	.428	50.15	51.2	.428	49.50
51.3	–	48.88	53.7	.300	42.96
55.7	.293	42.36	57.6	.308	47.89
58.9	.293	41.66	62.0	.324	40.99
63.9	.308	46.54	65.2	.273	40.45
71.6	.333	39.66	77.9	.267	39.37
89.3	.245	41.44	103.3	–	38.79

MAXIMUM VELOCITY (m/s)= .798 Position of maximum (mm)= 3.68
MAXIMUM DELTA T (C)= 59.70 Position of maximum (mm)= 6.85
Data Set I.D.: CF5VCN19 CF5TCN19

Time= 15 Minutes

z (mm)	Velocity (m/s)	Delta T (C)	z (mm)	Velocity (m/s)	Delta T (C)
1.7	.855	56.42	3.7	.798	57.65
6.9	.798	58.21	10.0	-	57.90
13.2	.704	58.33	19.6	.748	56.97
25.9	.665	54.98	39.7	.571	53.17
41.7	.545	52.40	44.9	.428	51.24
48.0	.363	50.43	51.2	.308	49.76
51.3	-	49.76	53.7	.293	43.85
55.7	.286	43.34	57.6	.308	48.08
58.9	.444	42.78	62.0	.333	42.37
63.9	.261	46.42	65.2	.324	42.18
71.6	.062	41.66	77.9	.067	41.33
89.3	-	42.63	103.3	.072	40.oo

MAXIMUM VELOCITY (m/s)= .855 Position of maximum (mm)= 1.69
MAXIMUM DELTA T (C)= 58.33 Position of maximum (mm)=13.20
Data Set I.D.: CF5VCN22 CF5TCN22

Time= 20 Minutes

z (mm)	Velocity (m/s)	Delta T (C)	z (mm)	Velocity (m/s)	Delta T (C)
1.7	.855	58.42	3.7	.798	59.58
6.9	.798	60.19	10.0	-	59.60
13.2	.798	59.68	19.6	.798	58.37
25.9	.665	57.04	39.7	.545	54.23
41.7	.461	53.53	44.9	.428	52.57
48.0	.400	51.93	51.2	.375	51.37
51.3	-	54.12	53.7	.363	46.27
55.7	.375	45.76	57.6	.428	49.30
58.9	.400	45.04	62.0	.414	44.44
63.9	.333	47.65	65.2	.333	43.96
71.6	.188	43.13	77.9	.222	42.89
89.3	.060	43.95	103.3	-	42.32

MAXIMUM VELOCITY (m/s)= .855 Position of maximum (mm)= 1.69
MAXIMUM DELTA T (C)= 60.19 Position of maximum (mm)= 6.85
Data Set I.D.: CF5VCN25 CF5TCN25

Time= 26 Minutes

z (mm)	Velocity (m/s)	Delta T (C)	z (mm)	Velocity (m/s)	Delta T (C)
1.7	.829	58.47	3.7	.812	59.31
6.9	.750	59.68	10.0	.773	59.81
13.2	.773	59.35	19.6	.726	57.99
25.9	.649	56.64	39.7	.502	54.23
41.7	.496	53.67	44.9	.431	52.81
48.0	.427	52.23	51.2	.414	51.81
51.3	_	51.78	53.7	.332	46.79
55.7	.313	46.34	57.6	.373	50.62
58.9	.316	45.71	62.0	.415	45.20
63.9	.361	49.70	65.2	.215	44.93
71.6	.227	44.25	77.9	.280	43.84
89.3	.263	46.00	103.3	.187	42.83

MAXIMUM VELOCITY (m/s)= .829 Position of maximum (mm)= 1.69
MAXIMUM DELTA T (C)= 59.81 Position of maximum (mm)=10.03
Data Set I.D.: CF5VC

Time= Steady State (Ave)

z (mm)	Velocity (m/s)	Delta T (C)	z (mm)	Velocity (m/s)	Delta T (C)
1.7	.841	54.62	3.7	.800	55.16
6.9	.761	55.29	10.0	.800	55.40
13.2	.786	55.09	19.6	.744	54.02
25.9	.694	52.76	39.7	.573	55.15
41.7	.534	54.53	44.9	.492	53.47
48.0	.505	52.66	51.2	.477	52.08
51.3	-	50.08	53.7	.414	47.14
55.7	.406	46.80	57.6	.475	50.39
58.9	.371	46.17	62.0	.434	45.70
63.9	.419	49.02	65.2	.311	45.42
71.6	.422	44.69	77.9	.314	44.32
89.3	.206	44.97	103.3	.043	43.49

MAXIMUM VELOCITY (m/s)= .841 Position of maximum (mm)= 1.69
MAXIMUM DELTA T (C)= 55.40 Position of maximum (mm)=10.03
Data Set I.D.: CF5VE CF5TE

Ceiling Type Fiberboard
Fire Strength= 2.0 KW
Ceiling to Floor Height, H: 1.0 m
Probe Location (r/H): 0.75

Time= 5 Seconds

z (mm)	Velocity (m/s)	Delta T (C)	z (mm)	Velocity (m/s)	Delta T (C)
2.7	.293	10.63	4.7	.261	12.63
7.9	.308	14.49	11.0	.387	15.36
14.2	.343	15.77	20.6	.353	16.31
26.9	.375	16.46	33.7	.631	15.63
35.7	.363	15.61	38.9	.353	15.35
42.0	.387	15.36	45.2	.428	15.13
51.5	.414	14.95	52.3	.375	15.58
57.9	.387	14.68	59.7	.363	13.76
61.7	.363	13.61	64.8	.353	13.33
68.0	.343	13.23	71.2	.316	13.09
77.5	.261	12.61	83.3	.353	12.50
83.9	.267	12.18	109.3	-	10.01

MAXIMUM VELOCITY (m/s)= .631   Position of maximum (mm)=33.69
MAXIMUM DELTA T (C)= 16.46   Position of maximum (mm)=26.90
Data Set I.D.: CF6V1A CF6T1A

Time= 1 Minute

z (mm)	Velocity (m/s)	Delta T (C)	z (mm)	Velocity (m/s)	Delta T (C)
2.7	.227	23.37	4.7	.207	26.97
7.9	.231	30.81	11.0	.245	32.84
14.2	.286	33.97	20.6	.571	31.46
26.9	.308	35.21	33.7	.279	35.40
35.7	-	35.39	38.9	.250	35.12
42.0	.261	35.34	45.2	.267	35.21
51.5	.222	35.10	52.3	.286	35.25
57.9	.167	34.75	59.7	.200	35.42
61.7	.200	35.22	64.8	.182	34.87
68.0	.211	34.98	71.2	.214	34.84
77.5	.204	34.58	83.3	.293	33.20
83.9	.200	33.87	109.3	.072	32.02

MAXIMUM VELOCITY (m/s)= .571   Position of maximum (mm)=20.55
MAXIMUM DELTA T (C)= 35.40   Position of maximum (mm)=33.69
Data Set I.D.: CF6V4 CF6T4

Time= 2 Minutes

z (mm)	Velocity (m/s)	Delta T (C)	z (mm)	Velocity (m/s)	Delta T (C)
2.7	.245	26.95	4.7	.218	30.42
7.9	.207	34.11	11.0	.218	35.76
14.2	.250	36.83	20.6	.293	38.27
26.9	.324	38.70	33.7	.308	39.26
35.7	-	40.14	38.9	.279	38.96
42.0	.286	39.24	45.2	.286	39.21
51.5	.293	39.29	52.3	.255	39.76
57.9	.261	38.94	59.7	.200	39.40
61.7	.200	39.25	64.8	.200	38.73
68.0	.132	38.82	71.2	.131	38.68
77.5	.124	38.52	83.3	.255	37.73
83.9	.087	37.82	109.3	.095	35.65

MAXIMUM VELOCITY (m/s)= .324 Position of maximum (mm)=26.90
MAXIMUM DELTA T (C)= 40.14 Position of maximum (mm)=35.67
Data Set I.D.: CF6V7 CF6T7

Time= 3 Minutes

z (mm)	Velocity (m/s)	Delta T (C)	z (mm)	Velocity (m/s)	Delta T (C)
2.7	.231	29.02	4.7	.240	32.60
7.9	.231	36.51	11.0	.218	38.29
14.2	.267	39.31	20.6	.286	40.64
26.9	.279	41.11	33.7	.308	41.14
35.7	-	42.20	38.9	.267	40.89
42.0	.273	41.18	45.2	.293	41.16
51.5	.267	41.18	52.3	.293	42.00
57.9	.222	40.90	59.7	.300	41.72
61.7	-	41.54	64.8	.293	41.18
68.0	.286	41.26	71.2	.182	41.14
77.5	.222	41.11	83.3	.165	40.26
83.9	.076	40.55	109.3	.300	39.05

MAXIMUM VELOCITY (m/s)= .308 Position of maximum (mm)=33.69
MAXIMUM DELTA T (C)= 42.20 Position of maximum (mm)=35.67
Data Set I.D.: CF6V10 CF6T10

Time= 5 Minutes

z (mm)	Velocity (m/s)	Delta T (C)	z (mm)	Velocity (m/s)	Delta T (C)
2.7	.185	30.31	4.7	.188	33.46
7.9	.182	36.54	11.0	.172	38.25
14.2	.191	39.46	20.6	.245	40.91
26.9	.267	41.35	33.7	.261	43.64
35.7	-	44.54	38.9	.245	43.50
42.0	.235	43.77	45.2	.267	43.78
51.5	.255	43.92	52.3	.300	42.41
57.9	.261	43.78	59.7	.300	42.77
61.7	-	42.50	64.8	.261	42.34
68.0	.273	42.41	71.2	.235	42.26
77.5	.179	42.13	83.3	.197	42.73
83.9	.107	41.88	109.3	.255	40.45

MAXIMUM VELOCITY (m/s)= .267 Position of maximum (mm)=26.90
MAXIMUM DELTA T (C)= 44.54 Position of maximum (mm)=35.67
Data Set I.D.: CF6V16 CF6T16

Time= 10 Minutes

z (mm)	Velocity (m/s)	Delta T (C)	z (mm)	Velocity (m/s)	Delta T (C)
2.7	.255	39.33	4.7	.235	42.16
7.9	.214	44.92	11.0	.211	46.11
14.2	.255	46.87	20.6	.273	47.79
26.9	.250	47.89	33.7	.267	47.25
35.7	-	47.00	38.9	.240	47.18
42.0	.245	47.38	45.2	.255	47.42
51.5	.240	47.33	52.3	.222	47.79
57.9	.261	47.13	59.7	.120	47.46
61.7	.179	47.17	64.8	.129	47.21
68.0	.145	47.34	71.2	.165	47.36
77.5	.169	47.40	83.3	.179	46.39
83.9	.162	47.18	109.3	-	45.73

MAXIMUM VELOCITY (m/s)= .273 Position of maximum (mm)=20.55
MAXIMUM DELTA T (C)= 47.99 Position of maximum (mm)=26.90
Data Set I.D.: CF6V23 CF6T23

Time= 15 Minutes

z (mm)	Velocity (m/s)	Delta T (C)	z (mm)	Velocity (m/s)	Delta T (C)
2.7	.165	39.66	4.7	.156	42.23
7.9	.162	44.91	11.0	.174	46.07
14.2	.207	46.91	20.6	.235	47.92
26.9	-	48.31	33.7	.308	48.74
35.7	.286	50.10	38.9	.250	48.52
42.0	.240	48.64	45.2	.245	48.69
51.5	.255	48.54	52.3	.255	49.07
57.9	.300	48.51	59.7	.300	48.21
61.7	.300	48.03	64.8	.255	47.99
68.0	.235	48.05	71.2	.214	48.10
77.5	.214	48.08	83.3	.300	48.03
83.9	.211	47.93	109.3	.082	46.27

MAXIMUM VELOCITY (m/s)= .308 Position of maximum (mm)=33.69
MAXIMUM DELTA T (C)= 50.10 Position of maximum (mm)=35.67
Data Set I.D.: CF6V26 CF6T26

Time= 25 Minutes

z (mm)	Velocity (m/s)	Delta T (C)	z (mm)	Velocity (m/s)	Delta T (C)
2.7	.261	41.04	4.7	.261	43.70
7.9	.231	46.56	11.0	.214	47.98
14.2	.245	49.00	20.6	.300	50.27
26.9	.353	50.65	33.7	.255	47.76
35.7	-	24.39	38.9	.273	47.66
42.0	.279	47.77	45.2	.261	47.86
51.5	.240	47.87	52.3	.363	51.02
57.9	.250	47.97	59.7	.204	49.25
61.7	.207	49.02	64.8	.197	48.84
68.0	.211	48.74	71.2	.218	48.65
77.5	.214	48.39	83.3	-	25.30
83.9	.222	47.88	109.3	-	47.06

MAXIMUM VELOCITY (m/s)= .353 Position of maximum (mm)=26.90
MAXIMUM DELTA T (C)= 50.65 Position of maximum (mm)=26.90
Data Set I.D.: CF6V30 CF6T30

Time= Steady State (Ave)

z (mm)	Velocity (m/s)	Delta T (C)	z (mm)	Velocity (m/s)	Delta T (C)
2.7	.204	42.98	4.7	.222	45.45
7.9	.235	47.77	11.0	.245	48.83
14.2	.300	49.66	20.6	.353	50.58
26.9	.324	50.86	33.7	.286	50.06
35.7	–	50.00	38.9	.240	49.82
42.0	–	49.93	45.2	.255	50.01
51.5	.231	49.77	52.3	.286	51.11
57.9	.182	49.83	59.7	.255	50.32
61.7	.227	50.10	64.8	.250	49.91
68.0	.240	49.91	71.2	.218	49.92
77.5	.179	49.65	83.3	–	49.42
83.9	.197	49.33	109.3	.197	48.11

MAXIMUM VELOCITY (m/s)= .353 Position of maximum (mm)=20.55
MAXIMUM DELTA T (C)= 50.86 Position of maximum (mm)=26.90
Data Set I.D.: CF6VE CF6TE

Appendix B
Temperature Data for Ceiling Jet and Upper Layer

Ceiling Type Fiberboard
Fire Strength= 2.0 kW
Ceiling to Floor Height, H: 1.0 m
Probe Location (r/H): 0.26

Time= 2.5 Seconds

z (cm)	Delta T (C)	z (cm)	Delta T (C)	z (cm)	Delta T (C)
.2	6.70	1.0	11.05	2.0	12.08
4.0	5.19	6.0	1.67	8.0	.39
11.0	.16	15.0	.08	20.0	-.05
25.0	-.01	35.0	-.07	40.0	-.26
45.0	-.44	48.0	-.47	50.0	-.52
52.0	-.32				

Maximum Delta T (C)= 12.08 Position of maximum (cm)= 2.0
Data Set I.D.: Q2H1R26T2S

Time= 10 Seconds

z (cm)	Delta T (C)	z (cm)	Delta T (C)	z (cm)	Delta T (C)
.2	19.07	1.0	25.68	2.0	24.03
4.0	13.13	6.0	7.30	8.0	3.12
11.0	1.36	15.0	.96	20.0	.97
25.0	1.27	35.0	.97	40.0	.96
45.0	.71	48.0	.36	50.0	-.23
52.0	.02				

Maximum Delta T (C)= 25.68 Position of maximum (cm)= 1.0
Data Set I.D.: Q2H1R26T10S

Time= 30 Seconds

z (cm)	Delta T (C)	z (cm)	Delta T (C)	z (cm)	Delta T (C)
.2	29.41	1.0	37.06	2.0	34.91
4.0	23.41	6.0	15.00	8.0	10.33
11.0	7.70	15.0	6.73	20.0	6.68
25.0	7.16	35.0	5.82	40.0	3.97
45.0	1.37	48.0	.45	50.0	.19
52.0	.20				

Maximum Delta T (C)= 37.06 Position of maximum (cm)= 1.0
Data Set I.D.: Q2H1R26T30S

Time= 1 Minute

z (cm)	Delta T (C)	z (cm)	Delta T (C)	z (cm)	Delta T (C)
.2	36.94	1.0	45.00	2.0	42.42
4.0	32.71	6.0	23.74	8.0	18.59
11.0	15.92	15.0	14.83	20.0	14.44
25.0	14.43	35.0	12.44	40.0	10.27
45.0	6.57	48.0	4.64	50.0	2.60
52.0	.29				

Maximum Delta T (C)= 45.00 Position of maximum (cm)= 1.0
Data Set I.D.: Q2H1R26T1M

Time= 2 Minutes

z (cm)	Delta T (C)	z (cm)	Delta T (C)	z (cm)	Delta T (C)
.2	41.32	1.0	50.59	2.0	49.05
4.0	41.30	6.0	32.89	8.0	27.74
11.0	25.47	15.0	24.47	20.0	23.96
25.0	23.74	35.0	21.38	40.0	19.52
45.0	14.96	48.0	11.80	50.0	7.58
52.0	.28				

Maximum Delta T (C)= 50.59 Position of maximum (cm)= 1.0
Data Set I.D.: Q2H1R26T2M

Time= 3 Minute

z (cm)	Delta T (C)	z (cm)	Delta T (C)	z (cm)	Delta T (C)
.2	42.94	1.0	52.09	2.0	50.22
4.0	43.14	6.0	35.16	8.0	30.84
11.0	29.05	15.0	28.35	20.0	27.90
25.0	27.74	35.0	25.71	40.0	23.89
45.0	19.31	48.0	14.97	50.0	9.86
52.0	.27				

Maximum Delta T (C)= 52.09 Position of maximum (cm)= 1.0
Data Set I.D.: 92H1R26T3M

Time= 4 Minutes

z (cm)	Delta T (C)	z (cm)	Delta T (C)	z (cm)	Delta T (C)
.2	44.52	1.0	53.13	2.0	50.91
4.0	44.69	6.0	37.03	8.0	32.59
11.0	31.07	15.0	30.44	20.0	29.89
25.0	29.60	35.0	27.13	40.0	25.53
45.0	21.20	48.0	16.18	50.0	9.22
52.0	.28				

Maximum Delta T (C)= 53.13 Position of maximum (cm)= 1.0
Data Set I.D.: 92H1R26T4M

Time= 5 Minutes

z (cm)	Delta T (C)	z (cm)	Delta T (C)	z (cm)	Delta T (C)
.2	44.61	1.0	53.94	2.0	52.18
4.0	45.34	6.0	38.53	8.0	34.33
11.0	32.38	15.0	31.68	20.0	31.23
25.0	30.94	35.0	28.39	40.0	26.89
45.0	22.48	48.0	16.52	50.0	7.66
52.0	.28				

Maximum Delta T (C)= 53.94 Position of maximum (cm)= 1.0
Data Set I.D.: 92H1R26T5M

Time= 6 Minutes

z (cm)	Delta T (C)	z (cm)	Delta T (C)	z (cm)	Delta T (C)
.2	45.85	1.0	54.09	2.0	51.64
4.0	45.62	6.0	39.34	8.0	35.39
11.0	33.38	15.0	32.76	20.0	32.33
25.0	32.09	35.0	29.90	40.0	28.27
45.0	23.53	48.0	17.25	50.0	7.15
52.0	.28				

Maximum Delta T (C)= 54.09 Position of maximum (cm)= 1.0
Data Set I.D.: 02H1R26T6M

Time= 7 Minutes

z (cm)	Delta T (C)	z (cm)	Delta T (C)	z (cm)	Delta T (C)
.2	46.14	1.0	54.81	2.0	52.63
4.0	46.27	6.0	39.37	8.0	35.57
11.0	33.91	15.0	33.39	20.0	33.00
25.0	32.84	35.0	30.75	40.0	29.03
45.0	24.73	48.0	16.70	50.0	8.02
52.0	.28				

Maximum Delta T (C)= 54.81 Position of maximum (cm)= 1.0
Data Set I.D.: 02H1R26T7M

Time= 8 Minutes

z (cm)	Delta T (C)	z (cm)	Delta T (C)	z (cm)	Delta T (C)
.2	47.23	1.0	55.57	2.0	53.44
4.0	46.98	6.0	40.34	8.0	36.46
11.0	34.73	15.0	34.15	20.0	33.63
25.0	33.34	35.0	31.08	40.0	29.12
45.0	25.48	48.0	18.83	50.0	8.16
52.0	.28				

Maximum Delta T (C)= 55.57 Position of maximum (cm)= 1.0
Data Set I.D.: 02H1R26T8M

Time= 10 Minutes

z (cm)	Delta T (C)	z (cm)	Delta T (C)	z (cm)	Delta T (C)
.2	47.63	1.0	56.09	2.0	54.27
4.0	48.58	6.0	42.17	8.0	38.16
11.0	35.65	15.0	34.99	20.0	34.48
25.0	34.29	35.0	32.15	40.0	30.74
45.0	26.73	48.0	18.14	50.0	6.34
52.0	3.50				

Maximum Delta T (C)= 56.09 Position of maximum (cm)= 1.0
Data Set I.D.: 02H1R26T10M

Time= 15 Minutes

z (cm)	Delta T (C)	z (cm)	Delta T (C)	z (cm)	Delta T (C)
.2	48.62	1.0	55.67	2.0	54.01
4.0	48.06	6.0	42.73	8.0	39.43
11.0	37.47	15.0	37.02	20.0	36.56
25.0	36.36	35.0	34.44	40.0	33.25
45.0	29.01	48.0	13.24	50.0	5.24
52.0	4.00				

Maximum Delta T (C)= 55.67 Position of maximum (cm)= 1.0
Data Set I.D.: 02H1R26T15M

Time= 20 Minutes

z (cm)	Delta T (C)	z (cm)	Delta T (C)	z (cm)	Delta T (C)
.2	49.89	1.0	56.63	2.0	55.78
4.0	50.37	6.0	44.50	8.0	40.68
11.0	38.65	15.0	37.93	20.0	37.60
25.0	37.37	35.0	35.41	40.0	34.24
45.0	29.44	48.0	15.55	50.0	5.46
52.0	4.13				

Maximum Delta T (C)= 56.63 Position of maximum (cm)= 1.0
Data Set I.D.: 02H1R26T20M

Time= 22 Minutes

z (cm)	Delta T (C)	z (cm)	Delta T (C)	z (cm)	Delta T (C)
.2	50.20	1.0	56.65	2.0	54.95
4.0	49.70	6.0	44.41	8.0	40.74
11.0	38.78	15.0	38.29	20.0	37.77
25.0	37.58	35.0	35.91	40.0	34.66
45.0	30.28	48.0	12.71	50.0	5.16
52.0	4.20				

Maximum Delta T (C)= 56.65 Position of maximum (cm)= 1.0
Data Set I.D.: Q2H1R26T22M

Time= 28 Minutes

z (cm)	Delta T (C)	z (cm)	Delta T (C)	z (cm)	Delta T (C)
.2	51.32	1.0	57.10	2.0	55.61
4.0	50.53	6.0	45.90	8.0	41.59
11.0	39.45	15.0	38.68	20.0	38.08
25.0	37.82	35.0	36.11	40.0	34.86
45.0	29.41	48.0	11.47	50.0	5.83
52.0	4.77				

Maximum Delta T (C)= 57.10 Position of maximum (cm)= 1.0
Data Set I.D.: Q2H1R26T28M

Time= 32 Minutes

z (cm)	Delta T (C)	z (cm)	Delta T (C)	z (cm)	Delta T (C)
.2	52.44	1.0	58.08	2.0	56.79
4.0	51.47	6.0	45.71	8.0	41.64
11.0	39.81	15.0	39.16	20.0	38.70
25.0	38.44	35.0	36.81	40.0	35.34
45.0	30.56	48.0	9.79	50.0	5.56
52.0	4.70				

Maximum Delta T (C)= 58.08 Position of maximum (cm)= 1.0
Data Set I.D.: Q2H1R26T32M

Time= 35 Minutes

z (cm)	Delta T (C)	z (cm)	Delta T (C)	z (cm)	Delta T (C)
.2	51.91	1.0	57.45	2.0	55.96
4.0	50.64	6.0	45.15	8.0	41.75
11.0	39.96	15.0	39.42	20.0	38.86
25.0	38.68	35.0	36.74	40.0	35.44
45.0	30.76	48.0	10.91	50.0	5.08
52.0	4.66				

Maximum Delta T (C)= 57.45 Position of maximum (cm)= 1.0
Data Set I.D.: B2H1R26T35M

Time= 38 Minutes

z (cm)	Delta T (C)	z (cm)	Delta T (C)	z (cm)	Delta T (C)
.2	52.89	1.0	58.07	2.0	56.57
4.0	51.34	6.0	46.24	8.0	42.08
11.0	39.86	15.0	39.35	20.0	38.90
25.0	38.66	35.0	36.92	40.0	35.72
45.0	28.89	48.0	10.04	50.0	5.69
52.0	4.92				

Maximum Delta T (C)= 58.07 Position of maximum (cm)= 1.0
Data Set I.D.: B2H1R26T38M

Ceiling Type Fiberboard
Fire Strength= 2.0 kW
Ceiling to Floor Height, H: 1.0 m
Probe Location (r/H): 0.75

Time= 2.5 Seconds

z (cm)	Delta T (C)	z (cm)	Delta T (C)	z (cm)	Delta T (C)
.2	.64	1.0	2.98	2.0	4.10
4.0	3.39	6.0	3.62	8.0	2.41
11.0	1.63	15.0	3.89	20.0	.35
25.0	.23	35.0	-.16	40.0	-.20
45.0	-.27	48.0	-.16	50.0	-.24
52.0	-.17				

Maximum Delta T (C)= 4.10 Position of maximum (cm)= 2.0
Data Set I.D.: Q2H1R75T2S

Time= 10 Seconds

z (cm)	Delta T (C)	z (cm)	Delta T (C)	z (cm)	Delta T (C)
.2	2.25	1.0	8.51	2.0	10.65
4.0	9.38	6.0	8.80	8.0	6.48
11.0	4.95	15.0	7.19	20.0	3.52
25.0	3.79	35.0	.67	40.0	.18
45.0	-.19	48.0	-.06	50.0	-.17
52.0	-.09				

Maximum Delta T (C)= 10.65 Position of maximum (cm)= 2.0
Data Set I.D.: Q2H1R75T10S

Time= 30 Seconds

z (cm)	Delta T (C)	z (cm)	Delta T (C)	z (cm)	Delta T (C)
.2	5.28	1.0	16.90	2.0	20.11
4.0	19.32	6.0	18.53	8.0	15.42
11.0	11.99	15.0	14.21	20.0	10.60
25.0	9.44	35.0	5.18	40.0	3.42
45.0	2.29	48.0	1.16	50.0	.35
52.0	.28				

Maximum Delta T (C)= 20.11 Position of maximum (cm)= 2.0
Data Set I.D.: Q2H1R75T30S

Time= 1 Minute

z (cm)	Delta T (C)	z (cm)	Delta T (C)	z (cm)	Delta T (C)
.2	8.84	1.0	24.83	2.0	28.41
4.0	28.21	6.0	27.36	8.0	24.10
11.0	20.90	15.0	23.11	20.0	18.59
25.0	17.03	35.0	12.60	40.0	10.54
45.0	8.66	48.0	6.46	50.0	3.69
52.0	2.64				

Maximum Delta T (C)= 28.41 Position of maximum (cm)= 2.0
Data Set I.D.: Q2H1R75T1M

Time= 2 Minutes

z (cm)	Delta T (C)	z (cm)	Delta T (C)	z (cm)	Delta T (C)
.2	13.90	1.0	32.08	2.0	35.16
4.0	35.82	6.0	35.39	8.0	33.63
11.0	30.53	15.0	32.70	20.0	26.84
25.0	25.71	35.0	20.92	40.0	19.38
45.0	17.38	48.0	14.36	50.0	9.92
52.0	6.24				

Maximum Delta T (C)= 35.83 Position of maximum (cm)= 4.0
Data Set I.D.: Q2H1R75T2M

Time= 3 Minutes

z (cm)	Delta T (C)	z (cm)	Delta T (C)	z (cm)	Delta T (C)
.2	16.73	1.0	34.41	2.0	37.43
4.0	38.24	6.0	38.06	8.0	36.68
11.0	33.96	15.0	35.98	20.0	30.32
25.0	29.66	35.0	25.42	40.0	24.11
45.0	22.06	48.0	18.36	50.0	12.97
52.0	7.48				

Maximum Delta T (C)= 38.25 Position of maximum (cm)= 4.0
Data Set I.D.: B2H1R75T3M

Time= 4 Minutes

z (cm)	Delta T (C)	z (cm)	Delta T (C)	z (cm)	Delta T (C)
.2	19.08	1.0	36.93	2.0	39.84
4.0	40.73	6.0	40.61	8.0	39.13
11.0	36.70	15.0	38.69	20.0	32.36
25.0	31.63	35.0	27.74	40.0	26.90
45.0	24.84	48.0	20.62	50.0	13.87
52.0	7.62				

Maximum Delta T (C)= 40.74 Position of maximum (cm)= 4.0
Data Set I.D.: B2H1R75T4M

Time= 5 Minutes

z (cm)	Delta T (C)	z (cm)	Delta T (C)	z (cm)	Delta T (C)
.2	20.68	1.0	38.25	2.0	41.39
4.0	42.17	6.0	41.61	8.0	40.03
11.0	37.67	15.0	39.65	20.0	33.89
25.0	33.11	35.0	29.52	40.0	28.42
45.0	25.92	48.0	22.02	50.0	14.78
52.0	8.29				

Maximum Delta T (C)= 42.17 Position of maximum (cm)= 4.0
Data Set I.D.: B2H1R75T5M

Time= 6 Minutes

z (cm)	Delta T (C)	z (cm)	Delta T (C)	z (cm)	Delta T (C)
.2	22.00	1.0	38.49	2.0	41.35
4.0	42.28	6.0	42.01	8.0	40.48
11.0	38.03	15.0	40.02	20.0	34.67
25.0	34.01	35.0	30.74	40.0	29.77
45.0	27.51	48.0	23.38	50.0	16.01
52.0	8.93				

Maximum Delta T (C)= 42.29 Position of maximum (cm)= 4.0
Data Set I.D.: B2H1R75T6M

Time= 7 Minutes

z (cm)	Delta T (C)	z (cm)	Delta T (C)	z (cm)	Delta T (C)
.2	22.68	1.0	38.65	2.0	41.72
4.0	42.51	6.0	42.42	8.0	41.31
11.0	38.98	15.0	40.94	20.0	35.42
25.0	34.70	35.0	31.79	40.0	30.87
45.0	28.53	48.0	23.95	50.0	16.21
52.0	8.91				

Maximum Delta T (C)= 42.51 Position of maximum (cm)= 4.0
Data Set I.D.: B2H1R75T7M

Time= 8 Minutes

z (cm)	Delta T (C)	z (cm)	Delta T (C)	z (cm)	Delta T (C)
.2	23.83	1.0	39.82	2.0	42.69
4.0	43.51	6.0	43.14	8.0	42.04
11.0	40.00	15.0	41.97	20.0	36.22
25.0	35.46	35.0	32.76	40.0	31.14
45.0	28.94	48.0	24.75	50.0	16.59
52.0	9.18				

Maximum Delta T (C)= 43.51 Position of maximum (cm)= 4.0
Data Set I.D.: B2H1R75T8M

Time= 10 Minutes

z (cm)	Delta T (C)	z (cm)	Delta T (C)	z (cm)	Delta T (C)
.2	25.37	1.0	40.89	2.0	43.59
4.0	44.35	6.0	44.52	8.0	43.43
11.0	40.89	15.0	42.84	20.0	37.40
25.0	36.57	35.0	33.59	40.0	32.45
45.0	30.35	48.0	26.02	50.0	17.41
52.0	9.19				

Maximum Delta T (C)= 44.52 Position of maximum (cm)= 6.0
Data Set I.D.: Q2H1R75T10M

Time= 15 Minutes

z (cm)	Delta T (C)	z (cm)	Delta T (C)	z (cm)	Delta T (C)
.2	28.27	1.0	42.63	2.0	45.57
4.0	46.36	6.0	46.32	8.0	45.07
11.0	42.57	15.0	44.52	20.0	39.21
25.0	38.34	35.0	35.52	40.0	34.65
45.0	32.67	48.0	27.36	50.0	18.17
52.0	3.52				

Maximum Delta T (C)= 46.36 Position of maximum (cm)= 4.0
Data Set I.D.: Q2H1R75T15M

Time= 20 Minutes

z (cm)	Delta T (C)	z (cm)	Delta T (C)	z (cm)	Delta T (C)
.2	29.91	1.0	43.87	2.0	46.37
4.0	47.22	6.0	47.04	8.0	45.98
11.0	44.15	15.0	46.10	20.0	40.50
25.0	39.62	35.0	36.46	40.0	35.67
45.0	33.52	48.0	28.33	50.0	19.03
52.0	2.37				

Maximum Delta T (C)= 47.22 Position of maximum (cm)= 4.0
Data Set I.D.: Q2H1R75T20M

Time= 22 Minutes

z (cm)	Delta T (C)	z (cm)	Delta T (C)	z (cm)	Delta T (C)
.2	29.77	1.0	42.67	2.0	45.29
4.0	46.20	6.0	46.15	8.0	45.01
11.0	43.14	15.0	45.10	20.0	39.89
25.0	39.35	35.0	36.58	40.0	35.79
45.0	33.60	48.0	28.96	50.0	18.75
52.0	2.33				

Maximum Delta T (C)= 46.20 Position of maximum (cm)= 4.0
Data Set I.D.: Q2H1R75T22M

Time= 28 Minutes

z (cm)	Delta T (C)	z (cm)	Delta T (C)	z (cm)	Delta T (C)
.2	30.60	1.0	42.76	2.0	45.52
4.0	46.29	6.0	46.48	8.0	45.53
11.0	43.68	15.0	45.61	20.0	40.68
25.0	40.09	35.0	36.89	40.0	35.97
45.0	34.26	48.0	29.59	50.0	18.75
52.0	2.38				

Maximum Delta T (C)= 46.48 Position of maximum (cm)= 6.0
Data Set I.D.: Q2H1R75T28M

Time= 32 Minutes

z (cm)	Delta T (C)	z (cm)	Delta T (C)	z (cm)	Delta T (C)
.2	31.54	1.0	43.98	2.0	46.84
4.0	47.56	6.0	47.36	8.0	46.35
11.0	44.60	15.0	46.51	20.0	41.00
25.0	40.04	35.0	37.09	40.0	36.20
45.0	34.27	48.0	29.56	50.0	19.00
52.0	2.15				

Maximum Delta T (C)= 47.56 Position of maximum (cm)= 4.0
Data Set I.D.: Q2H1R75T32M

Time= 35 Minutes

z (cm)	Delta T (C)	z (cm)	Delta T (C)	z (cm)	Delta T (C)
.2	31.87	1.0	44.11	2.0	46.67
4.0	47.62	6.0	47.49	8.0	46.45
11.0	44.27	15.0	46.21	20.0	41.06
25.0	40.16	35.0	37.38	40.0	36.79
45.0	34.78	48.0	29.01	50.0	18.15
52.0	2.07				

Maximum Delta T (C)= 47.62 Position of maximum (cm)= 4.0
Data Set I.D.: Q2H1R75T35M

Time= 38 Minutes

z (cm)	Delta T (C)	z (cm)	Delta T (C)	z (cm)	Delta T (C)
.2	32.00	1.0	43.69	2.0	46.29
4.0	47.24	6.0	47.11	8.0	46.08
11.0	44.13	15.0	42.72	20.0	41.10
25.0	40.30	35.0	37.43	40.0	36.70
45.0	34.88	48.0	29.80	50.0	19.25
52.0	1.77				

Maximum Delta T (C)= 47.24 Position of maximum (cm)= 4.0
Data Set I.D.: Q2H1R75T38M

Ceiling Type Fiberboard
Fire Strength= 0.75 kW
Ceiling to Floor Height, H: 1.0 m
Probe Location (r/H): 0.26

Time= 2.5 Seconds

z (cm)	Delta T (C)	z (cm)	Delta T (C)	z (cm)	Delta T (C)
.2	3.12	1.0	5.47	2.0	6.57
4.0	2.93	6.0	.76	8.0	.59
11.0	.32	15.0	.61	20.0	-.01
25.0	-.12	35.0	-.02	40.0	.06
45.0	.02	48.0	.22	50.0	.04
52.0	.16				

Maximum Delta T (C)= 6.57 Position of maximum (cm)= 2.0
Data Set I.D.: Q7H1R26T2S

Time= 10 Seconds

z (cm)	Delta T (C)	z (cm)	Delta T (C)	z (cm)	Delta T (C)
.2	8.11	1.0	12.11	2.0	11.72
4.0	6.54	6.0	.95	8.0	1.32
11.0	.54	15.0	.85	20.0	.16
25.0	.05	35.0	.13	40.0	.09
45.0	-.01	48.0	.10	50.0	.07
52.0	.13				

Maximum Delta T (C)= 12.11 Position of maximum (cm)= 1.0
Data Set I.D.: Q7H1R26T10S

Time= 30 Seconds

z (cm)	Delta T (C)	z (cm)	Delta T (C)	z (cm)	Delta T (C)
.2	14.13	1.0	18.43	2.0	16.94
4.0	9.82	6.0	2.90	8.0	3.59
11.0	2.97	15.0	3.27	20.0	2.08
25.0	1.80	35.0	1.35	40.0	.60
45.0	.31	48.0	.39	50.0	.31
52.0	.31				

Maximum Delta T (C)= 18.43 Position of maximum (cm)= 1.0
Data Set I.D.: Q7H1R26T30S

Time= 1 Minute

z (cm)	Delta T (C)	z (cm)	Delta T (C)	z (cm)	Delta T (C)
.2	17.57	1.0	22.24	2.0	20.77
4.0	14.52	6.0	6.24	8.0	7.47
11.0	6.55	15.0	6.85	20.0	5.47
25.0	5.08	35.0	3.70	40.0	2.16
45.0	1.28	48.0	1.04	50.0	.74
52.0	.71				

Maximum Delta T (C)= 22.24 Position of maximum (cm)= 1.0
Data Set I.D.: Q7H1R26T1M

Time= 2 Minutes

z (cm)	Delta T (C)	z (cm)	Delta T (C)	z (cm)	Delta T (C)
.2	20.53	1.0	25.47	2.0	24.18
4.0	19.14	6.0	10.56	8.0	11.85
11.0	11.03	15.0	11.32	20.0	9.96
25.0	9.41	35.0	7.87	40.0	6.20
45.0	4.87	48.0	3.93	50.0	2.76
52.0	1.39				

Maximum Delta T (C)= 25.47 Position of maximum (cm)= 1.0
Data Set I.D.: Q7H1R26T2M

Time= 3 Minutes

z (cm)	Delta T (C)	z (cm)	Delta T (C)	z (cm)	Delta T (C)
.2	21.39	1.0	26.55	2.0	25.30
4.0	20.77	6.0	13.01	8.0	14.20
11.0	13.28	15.0	13.57	20.0	12.34
25.0	11.89	35.0	10.52	40.0	9.26
45.0	7.41	48.0	5.97	50.0	4.43
52.0	1.38				

Maximum Delta T (C)= 26.55 Position of maximum (cm)= 1.0
Data Set I.D.: Q7H1R26T3M

Time= 4 Minutes

z (cm)	Delta T (C)	z (cm)	Delta T (C)	z (cm)	Delta T (C)
.2	21.92	1.0	26.37	2.0	25.34
4.0	21.73	6.0	14.52	8.0	15.15
11.0	14.40	15.0	14.73	20.0	13.60
25.0	13.25	35.0	11.89	40.0	10.70
45.0	8.90	48.0	6.98	50.0	5.08
52.0	1.38				

Maximum Delta T (C)= 26.37 Position of maximum (cm)= 1.0
Data Set I.D.: Q7H1R26T4M

Time= 5 Minutes

z (cm)	Delta T (C)	z (cm)	Delta T (C)	z (cm)	Delta T (C)
.2	22.75	1.0	27.77	2.0	26.57
4.0	22.39	6.0	15.17	8.0	15.85
11.0	15.08	15.0	15.39	20.0	14.35
25.0	14.00	35.0	12.63	40.0	11.71
45.0	10.01	48.0	7.77	50.0	5.30
52.0	1.37				

Maximum Delta T (C)= 27.77 Position of maximum (cm)= 1.0
Data Set I.D.: Q7H1R26T5M

Time= 6 Minutes

z (cm)	Delta T (C)	z (cm)	Delta T (C)	z (cm)	Delta T (C)
.2	23.18	1.0	27.83	2.0	26.86
4.0	23.26	6.0	15.68	8.0	16.46
11.0	15.69	15.0	15.99	20.0	14.93
25.0	14.49	35.0	13.35	40.0	12.22
45.0	10.35	48.0	8.29	50.0	5.71
52.0	1.36				

Maximum Delta T (C)= 27.83 Position of maximum (cm)= 1.0
Data Set I.D.: Q7H1R26T6M

Time= 7 Minutes

z (cm)	Delta T (C)	z (cm)	Delta T (C)	z (cm)	Delta T (C)
.2	23.27	1.0	27.78	2.0	26.83
4.0	23.29	6.0	16.08	8.0	17.13
11.0	16.19	15.0	16.49	20.0	15.39
25.0	15.07	35.0	13.95	40.0	13.04
45.0	10.82	48.0	8.73	50.0	5.84
52.0	1.36				

Maximum Delta T (C)= 27.78 Position of maximum (cm)= 1.0
Data Set I.D.: Q7H1R26T7M

Time= 8 Minutes

z (cm)	Delta T (C)	z (cm)	Delta T (C)	z (cm)	Delta T (C)
.2	24.24	1.0	28.67	2.0	27.46
4.0	23.64	6.0	16.61	8.0	17.58
11.0	16.68	15.0	16.96	20.0	15.84
25.0	15.46	35.0	14.28	40.0	13.32
45.0	11.29	48.0	9.02	50.0	6.15
52.0	1.35				

Maximum Delta T (C)= 28.67 Position of maximum (cm)= 1.0
Data Set I.D.: Q7H1R26T8M

Time= 10 Minutes

z (cm)	Delta T (C)	z (cm)	Delta T (C)	z (cm)	Delta T (C)
.2	23.96	1.0	28.62	2.0	27.74
4.0	24.14	6.0	17.32	8.0	18.32
11.0	17.15	15.0	17.43	20.0	16.30
25.0	15.97	35.0	15.00	40.0	14.33
45.0	12.11	48.0	9.26	50.0	5.55
52.0	1.33				

Maximum Delta T (C)= 28.62 Position of maximum (cm)= 1.0
Data Set I.D.: Q7H1R26T10M

Time= 15 Minutes

z (cm)	Delta T (C)	z (cm)	Delta T (C)	z (cm)	Delta T (C)
.2	24.60	1.0	29.03	2.0	27.85
4.0	24.33	6.0	18.02	8.0	18.71
11.0	17.71	15.0	17.97	20.0	17.07
25.0	16.79	35.0	15.88	40.0	15.42
45.0	13.10	48.0	9.95	50.0	5.42
52.0	1.29				

Maximum Delta T (C)= 29.03 Position of maximum (cm)= 1.0
Data Set I.D.: Q7H1R26T15M

Time= 20 Minutes

z (cm)	Delta T (C)	z (cm)	Delta T (C)	z (cm)	Delta T (C)
.2	25.18	1.0	29.07	2.0	27.97
4.0	25.05	6.0	18.77	8.0	19.49
11.0	18.45	15.0	18.70	20.0	17.81
25.0	17.54	35.0	16.54	40.0	16.04
45.0	13.77	48.0	9.98	50.0	4.78
52.0	1.26				

Maximum Delta T (C)= 29.07 Position of maximum (cm)= 1.0
Data Set I.D.: Q7H1R26T20M

Time= 22 Minutes

z (cm)	Delta T (C)	z (cm)	Delta T (C)	z (cm)	Delta T (C)
.2	24.70	1.0	28.55	2.0	27.98
4.0	25.47	6.0	18.88	8.0	20.61
11.0	18.79	15.0	19.06	20.0	18.00
25.0	17.76	35.0	16.77	40.0	16.26
45.0	13.93	48.0	10.06	50.0	4.75
52.0	1.24				

Maximum Delta T (C)= 28.55 Position of maximum (cm)= 1.0
Data Set I.D.: Q7H1R26T22M

Time= 25 Minutes

z (cm)	Delta T (C)	z (cm)	Delta T (C)	z (cm)	Delta T (C)
.2	24.80	1.0	28.10	2.0	27.17
4.0	24.67	6.0	19.00	8.0	19.95
11.0	18.86	15.0	19.12	20.0	18.14
25.0	17.87	35.0	16.93	40.0	16.31
45.0	13.03	48.0	7.01	50.0	3.67
52.0	1.23				

Maximum Delta T (C)= 28.10 Position of maximum (cm)= 1.0
Data Set I.D.: Q7H1R26T25M

Time= 28 Minutes

z (cm)	Delta T (C)	z (cm)	Delta T (C)	z (cm)	Delta T (C)
.2	24.76	1.0	28.19	2.0	27.25
4.0	25.24	6.0	19.43	8.0	20.26
11.0	18.87	15.0	19.13	20.0	18.32
25.0	18.10	35.0	17.23	40.0	16.61
45.0	14.36	48.0	7.85	50.0	3.78
52.0	1.22				

Maximum Delta T (C)= 28.19 Position of maximum (cm)= 1.0
Data Set I.D.: Q7H1R26T28M

Time= 32 Minutes

z (cm)	Delta T (C)	z (cm)	Delta T (C)	z (cm)	Delta T (C)
.2	25.37	1.0	29.06	2.0	28.04
4.0	25.32	6.0	19.83	8.0	20.32
11.0	19.30	15.0	19.54	20.0	18.56
25.0	18.25	35.0	17.36	40.0	16.89
45.0	14.79	48.0	9.75	50.0	3.91
52.0	1.21				

Maximum Delta T (C)= 29.06 Position of maximum (cm)= 1.0
Data Set I.D.: G7H1R26T32M

Time= 35 Minutes

z (cm)	Delta T (C)	z (cm)	Delta T (C)	z (cm)	Delta T (C)
.2	25.96	1.0	29.47	2.0	28.65
4.0	25.45	6.0	19.95	8.0	20.18
11.0	19.40	15.0	19.65	20.0	18.69
25.0	18.49	35.0	17.46	40.0	17.08
45.0	14.28	48.0	8.05	50.0	3.71
52.0	1.20				

Maximum Delta T (C)= 29.47 Position of maximum (cm)= 1.0
Data Set I.D.: G7H1R26T35M

Time= 38 Minutes

z (cm)	Delta T (C)	z (cm)	Delta T (C)	z (cm)	Delta T (C)
.2	26.04	1.0	29.23	2.0	28.29
4.0	25.61	6.0	20.11	8.0	20.56
11.0	19.59	15.0	19.84	20.0	19.02
25.0	18.75	35.0	17.86	40.0	17.29
45.0	14.77	48.0	7.95	50.0	3.22
52.0	1.20				

Maximum Delta T (C)= 29.24 Position of maximum (cm)= 1.0
Data Set I.D.: G7H1R26T38M

Ceiling Type Fiberboard
Fire Strength= 0.75 kW
Ceiling to Floor Height, H: 1.0 m
Probe Location (r/H): 0.75

Time= 2.5 Seconds

z (cm)	Delta T (C)	z (cm)	Delta T (C)	z (cm)	Delta T (C)
.2	.57	1.0	1.90	2.0	2.27
4.0	2.08	6.0	2.20	8.0	1.59
11.0	.98	15.0	.72	20.0	.51
25.0	.64	35.0	.35	40.0	.30
45.0	.21	48.0	.24	50.0	.15
52.0	.20				

Maximum Delta T (C)= 2.27 Position of maximum (cm)= 2.0
Data Set I.D.: 07H1R75T2S

Time= 10 Seconds

z (cm)	Delta T (C)	z (cm)	Delta T (C)	z (cm)	Delta T (C)
.2	.66	1.0	3.75	2.0	4.62
4.0	4.19	6.0	3.89	8.0	3.08
11.0	2.26	15.0	1.79	20.0	1.47
25.0	1.27	35.0	.59	40.0	.44
45.0	.35	48.0	.35	50.0	.18
52.0	.23				

Maximum Delta T (C)= 4.62 Position of maximum (cm)= 2.0
Data Set I.D.: 07H1R75T10S

Time= 30 Seconds

z (cm)	Delta T (C)	z (cm)	Delta T (C)	z (cm)	Delta T (C)
.2	.66	1.0	6.71	2.0	7.91
4.0	7.96	6.0	7.65	8.0	6.42
11.0	5.05	15.0	4.27	20.0	4.00
25.0	3.76	35.0	1.82	40.0	1.46
45.0	.78	48.0	.54	50.0	.35
52.0	.37				

Maximum Delta T (C)= 7.96 Position of maximum (cm)= 4.0
Data Set I.D.: Q7H1R75T30S

Time= 1 Minute

z (cm)	Delta T (C)	z (cm)	Delta T (C)	z (cm)	Delta T (C)
.2	.86	1.0	9.94	2.0	11.49
4.0	11.53	6.0	11.31	8.0	9.97
11.0	8.21	15.0	7.45	20.0	7.20
25.0	6.64	35.0	4.34	40.0	3.77
45.0	2.77	48.0	2.13	50.0	1.22
52.0	.89				

Maximum Delta T (C)= 11.53 Position of maximum (cm)= 4.0
Data Set I.D.: Q7H1R75T1M

Time= 2 Minutes

z (cm)	Delta T (C)	z (cm)	Delta T (C)	z (cm)	Delta T (C)
.2	.64	1.0	13.52	2.0	15.19
4.0	15.65	6.0	15.48	8.0	14.40
11.0	12.75	15.0	11.59	20.0	11.05
25.0	10.41	35.0	8.31	40.0	7.43
45.0	6.13	48.0	4.93	50.0	3.49
52.0	2.10				

Maximum Delta T (C)= 15.65 Position of maximum (cm)= 4.0
Data Set I.D.: Q7H1R75T2M

Time= 3 Minutes

z (cm)	Delta T (C)	z (cm)	Delta T (C)	z (cm)	Delta T (C)
.2	.64	1.0	14.86	2.0	16.60
4.0	17.26	6.0	17.11	8.0	16.24
11.0	14.81	15.0	13.76	20.0	12.99
25.0	12.56	35.0	10.63	40.0	9.66
45.0	8.38	48.0	7.19	50.0	5.31
52.0	1.50				

Maximum Delta T (C)= 17.26 Position of maximum (cm)= 4.0
Data Set I.D.: Q7H1R75T3M

Time= 4 Minutes

z (cm)	Delta T (C)	z (cm)	Delta T (C)	z (cm)	Delta T (C)
.2	8.45	1.0	16.37	2.0	17.85
4.0	18.39	6.0	18.26	8.0	17.62
11.0	16.18	15.0	15.05	20.0	14.16
25.0	13.40	35.0	11.92	40.0	11.11
45.0	9.83	48.0	8.37	50.0	6.34
52.0	4.47				

Maximum Delta T (C)= 18.39 Position of maximum (cm)= 4.0
Data Set I.D.: Q7H1R75T4M

Time= 5 Minutes

z (cm)	Delta T (C)	z (cm)	Delta T (C)	z (cm)	Delta T (C)
.2	8.86	1.0	16.55	2.0	18.02
4.0	18.70	6.0	18.64	8.0	18.16
11.0	16.89	15.0	15.67	20.0	14.76
25.0	14.26	35.0	12.44	40.0	11.68
45.0	10.39	48.0	8.77	50.0	6.73
52.0	4.61				

Maximum Delta T (C)= 18.70 Position of maximum (cm)= 4.0
Data Set I.D.: Q7H1R75T5M

Time= 6 Minutes

z (cm)	Delta T (C)	z (cm)	Delta T (C)	z (cm)	Delta T (C)
.2	9.32	1.0	17.05	2.0	18.62
4.0	19.26	6.0	19.12	8.0	18.55
11.0	17.32	15.0	16.12	20.0	15.23
25.0	14.82	35.0	13.18	40.0	12.29
45.0	10.99	48.0	9.18	50.0	7.01
52.0	4.61				

Maximum Delta T (C)= 19.26 Position of maximum (cm)= 4.0
Data Set I.D.: 07H1R75T6M

Time= 7 Minutes

z (cm)	Delta T (C)	z (cm)	Delta T (C)	z (cm)	Delta T (C)
.2	9.83	1.0	17.41	2.0	19.01
4.0	19.62	6.0	19.55	8.0	19.03
11.0	17.32	15.0	16.76	20.0	15.84
25.0	15.46	35.0	13.62	40.0	12.93
45.0	11.53	48.0	9.74	50.0	7.32
52.0	4.86				

Maximum Delta T (C)= 19.62 Position of maximum (cm)= 4.0
Data Set I.D.: 07H1R75T7M

Time= 8 Minutes

z (cm)	Delta T (C)	z (cm)	Delta T (C)	z (cm)	Delta T (C)
.2	10.35	1.0	17.92	2.0	19.41
4.0	19.98	6.0	19.88	8.0	19.51
11.0	18.26	15.0	16.91	20.0	16.11
25.0	15.68	35.0	13.83	40.0	13.12
45.0	11.87	48.0	10.04	50.0	7.55
52.0	5.09				

Maximum Delta T (C)= 19.98 Position of maximum (cm)= 4.0
Data Set I.D.: 07H1R75T8M

Time= 10 Minutes

z (cm)	Delta T (C)	z (cm)	Delta T (C)	z (cm)	Delta T (C)
.2	11.18	1.0	18.59	2.0	20.16
4.0	20.58	6.0	20.44	8.0	19.88
11.0	18.72	15.0	17.70	20.0	17.00
25.0	16.19	35.0	14.69	40.0	13.90
45.0	12.64	48.0	10.87	50.0	8.09
52.0	5.23				

Maximum Delta T (C)= 20.59 Position of maximum (cm)= 4.0
Data Set I.D.: Q7H1R75T10M

Time= 15 Minutes

z (cm)	Delta T (C)	z (cm)	Delta T (C)	z (cm)	Delta T (C)
.2	12.49	1.0	19.70	2.0	21.27
4.0	21.71	6.0	21.52	8.0	21.00
11.0	19.60	15.0	18.46	20.0	17.85
25.0	17.34	35.0	15.70	40.0	15.04
45.0	13.84	48.0	11.60	50.0	8.51
52.0	5.06				

Maximum Delta T (C)= 21.71 Position of maximum (cm)= 4.0
Data Set I.D.: Q7H1R75T15M

Time= 20 Minutes

z (cm)	Delta T (C)	z (cm)	Delta T (C)	z (cm)	Delta T (C)
.2	13.19	1.0	20.14	2.0	21.59
4.0	22.16	6.0	22.18	8.0	21.67
11.0	20.28	15.0	19.17	20.0	18.59
25.0	18.32	35.0	16.33	40.0	15.79
45.0	14.48	48.0	12.17	50.0	8.61
52.0	4.65				

Maximum Delta T (C)= 22.18 Position of maximum (cm)= 6.0
Data Set I.D.: Q7H1R75T20M

Time= 22 Minutes

z (cm)	Delta T (C)	z (cm)	Delta T (C)	z (cm)	Delta T (C)
.2	13.45	1.0	20.30	2.0	21.68
4.0	22.28	6.0	22.36	8.0	21.88
11.0	20.76	15.0	19.67	20.0	18.81
25.0	18.16	35.0	16.61	40.0	15.99
45.0	14.72	48.0	12.31	50.0	8.79
52.0	5.04				

Maximum Delta T (C)= 22.36 Position of maximum (cm)= 6.0
Data Set I.D.: Q7H1R75T22M

Time= 25 Minutes

z (cm)	Delta T (C)	z (cm)	Delta T (C)	z (cm)	Delta T (C)
.2	13.78	1.0	20.53	2.0	22.05
4.0	22.77	6.0	22.75	8.0	22.28
11.0	21.03	15.0	19.89	20.0	19.09
25.0	18.42	35.0	16.81	40.0	16.32
45.0	15.02	48.0	12.54	50.0	9.03
52.0	.75				

Maximum Delta T (C)= 22.77 Position of maximum (cm)= 4.0
Data Set I.D.: Q7H1R75T25M

Time= 28 Minutes

z (cm)	Delta T (C)	z (cm)	Delta T (C)	z (cm)	Delta T (C)
.2	13.91	1.0	20.39	2.0	21.86
4.0	22.52	6.0	22.63	8.0	22.27
11.0	21.00	15.0	20.11	20.0	19.31
25.0	18.89	35.0	17.18	40.0	16.55
45.0	15.29	48.0	12.80	50.0	9.11
52.0	.75				

Maximum Delta T (C)= 22.63 Position of maximum (cm)= 6.0
Data Set I.D.: Q7H1R75T28M

Time= 32 Minutes

z (cm)	Delta T (C)	z (cm)	Delta T (C)	z (cm)	Delta T (C)
.2	14.47	1.0	21.01	2.0	22.25
4.0	22.81	6.0	22.82	8.0	22.37
11.0	21.18	15.0	20.24	20.0	19.52
25.0	18.88	35.0	17.41	40.0	16.68
45.0	15.41	48.0	12.99	50.0	9.36
52.0	.75				

Maximum Delta T (C)= 22.82 Position of maximum (cm)= 6.0
Data Set I.D.: G7H1R75T32M

Time= 35 Minutes

z (cm)	Delta T (C)	z (cm)	Delta T (C)	z (cm)	Delta T (C)
.2	14.51	1.0	20.78	2.0	22.10
4.0	22.74	6.0	22.79	8.0	22.47
11.0	21.45	15.0	20.52	20.0	19.65
25.0	19.11	35.0	17.38	40.0	16.81
45.0	15.59	48.0	13.28	50.0	9.20
52.0	.75				

Maximum Delta T (C)= 22.79 Position of maximum (cm)= 6.0
Data Set I.D.: G7H1R75T35M

Time= 38 Minutes

z (cm)	Delta T (C)	z (cm)	Delta T (C)	z (cm)	Delta T (C)
.2	14.59	1.0	20.80	2.0	22.29
4.0	22.90	6.0	22.94	8.0	22.49
11.0	21.28	15.0	20.35	20.0	19.41
25.0	19.00	35.0	17.52	40.0	16.97
45.0	15.60	48.0	13.44	50.0	9.80
52.0	.76				

Maximum Delta T (C)= 22.94 Position of maximum (cm)= 6.0
Data Set I.D.: G7H1R75T38M

Appendix C
Test Conditions and Constants

Ceiling Properties

Material: Fiberboard

δ_c = 0.0127 m
α = 1.2E-07 m²/s
C_p = 1485 J/KgK
k_c = 0.0485 W/mK
ϵ = 0.91
ρ_c = 272 Kg/m³
d = 2.13 m

Insulation Properties

Material: Fiberglass #12

δ_i = 0.0826 m

Air Properties

C_p = 1004 J/kg K
ρ_∞ = 1.1 kg/m³
μ = 1.84E-05 Ns/m²
υ = 1.67E-05 m²/s

Nondimensional Q and Reynolds Number

	r/H Location			
	0.26		0.75	
Fire Size	Q^*	Re_{max}	Q^*	Re_{max}
2.0 kW	.00189	14300	.00189	28292
0.75 kW	.00069	---	.00071	---

Lavent Room Parameters

Ceiling Height = 1.0 m
Room length = 1.89m
Room Width = 1.89m
Curtian Length = 7.56m

Appendix D
Heat Conduction Program - ASCL[1]

```
Program Transient Conduction
Initial
      Constant alpha = 1.7E-7          $ "Thermal Diffusivity (m^2/s)"
      Constant delta = 0.000635          $ "Delta X (m)"
      Constant k = 0.0485                $ "Conductivity (W/m.K) "

End $ ' of Initial '

Dynamic
      Cinterval Cint = 60.
      Constant  Tstp = 2300.
      Termt(T .ge. Tstp)
      Table T0, 1, 18 /0.,2.5,12.5,32.5,62.5,92.5,122.5,152.5,...
      182.5,212.5,242.5,272.5,302.5,462.5,602.5,902.5,1202.5,2382.5,...
      293.,293.1,293.5,293.7,294.9,295.7,296.3,296.7,297.,297.3,...
      297.5,297.8,298.,299.,299.7,301.,301.5,303./
Derivative
      Algorithm Ialg = 5
      Nsteps    Nstp = 10
      Maxterval Maxt = .1
      Minterval Mint = .00001

      T00 = T0(T)
      T1d = alpha*(T0(T) - 2*T1 + T2)/(delta*delta)
      T1 = integ(t1d,293.)
      T2d = alpha*(T1 - 2*T2 + T3)/(delta*delta)
      T2 = integ(t2d,293.)
      T3d = alpha*(T2 - 2*T3 + T4)/(delta*delta)
      T3 = integ(t3d,293.)
      T4d = alpha*(T3 - 2*T4 + T5)/(delta*delta)
      T4 = integ(t4d,293.)
      T5d = alpha*(T4 - 2*T5 + T6)/(delta*delta)
      T5 = integ(t5d,293.)
      T6d = alpha*(T5 - 2*T6 + T7)/(delta*delta)
      T6 = integ(t6d,293.)
      T7d = alpha*(T6 - 2*T7 + T8)/(delta*delta)
      T7 = integ(t7d,293.)
      T8d = alpha*(T7 - 2*T8 + T9)/(delta*delta)
      T8 = integ(t8d,293.)
      T9d = alpha*(T8 - 2*T9 + T10)/(delta*delta)
      T9 = integ(t9d,293.)
```

```
      T10d = alpha*(T9 - 2*T10 + T11)/(delta*delta)
      T10 = integ(t10d,293.)
      T11d = alpha*(T10 - 2*T11 + T12)/(delta*delta)
      T11 = integ(t11d,293.)
      T12d = alpha*(T11 - 2* T12 + T13)/(delta*delta)
      T12 = integ(t12d,293.)
      T13d = alpha*(T12 - 2*T13 + T14)/(delta*delta)
      T13 = integ(t13d,293.)
      T14d = alpha*(T13 - 2*T14 + T15)/(delta*delta)
      T14 = integ(t14d,293.)
      T15d = alpha*(T14 - 2*T15 + T16)/(delta*delta)
      T15 = integ(t15d,293.)
      T16d = alpha*(T15 - 2*T16 + T17)/(delta*delta)
      T16 = integ(t16d,293.)
      T17d = alpha*(T16 - 2*T17 + T18)/(delta*delta)
      T17 = integ(t17d,293.)
      T18d = alpha*(T17 - 2*T18 + T19)/(delta*delta)
      T18 = integ(t18d,293.)
      T19d = alpha*(T18 - 2*T19 + T20)/(delta*delta)
      T19 = integ(t19d,293.)
      T20d = alpha*(T19 - 2*T20 + T21)/(delta*delta)
      T20 = integ(t20d,293.)
      T21 = T20
      flux1 = -k*(T1-T0(T))/delta
      flux2 =-k*(T2-T1)/delta

End $ ' of Derivative '
End $ ' of Dynamic '

Terminal

End $ ' of Terminal '
End $ ' of Program '
```

1 Advanced Continuous Simulation Model - Reference Manual, Mitchell and Gauthier Associates, Concord, MA, 1986.

APPENDIX E

Ceiling Surface Temperature, ΔT_c (K)

Fire Size	2.0 kW		0.75 kW	
Time\ r/H	0.26	0.75	0.26	0.75
12.5 sec	298.5	297.0	296.8	293.4
32.5 sec	302.5	299.0	298.7	293.7
1 Minute	305.8	300.8	300.5	294.8
2 Minutes	309.9	303.9	302.5	296.3
3 Minutes	312.4	305.5	303.8	297.0
4 Minutes	314.0	306.8	304.5	297.5
5 Minutes	315.5	308.3	305.4	298.0
7 Minutes	317.1	309.9	306.2	298.7
10 Minutes	319.0	312.2	307.0	299.7
15 Minutes	321.4	314.4	308.3	301.0
20 Minutes	322.0	315.6	309.0	301.5
25 Minutes	322.1	316.2	309.6	301.9
35 Minutes	322.4	317.4	310.7	302.6
Steady State	322.5	317.9	311.2	302.9

NOTE

ΔT_{amb} = 296 K 296 K 296 K 293 K

NIST-114A
(REV. 3-90)

U.S. DEPARTMENT OF COMMERCE
NATIONAL INSTITUTE OF STANDARDS AND TECHNOLOGY

BIBLIOGRAPHIC DATA SHEET

1. PUBLICATION OR REPORT NUMBER
NIST-GCR-92-613

2. PERFORMING ORGANIZATION REPORT NUMBER

3. PUBLICATION DATE
August 1992

4. TITLE AND SUBTITLE

Characterization of the Confined Ceiling Jet in the Presence of an Upper Layer in Transient and Steady-State Conditions

5. AUTHOR(S)

Vahid Motevalli and Christina Ricciuti

6. PERFORMING ORGANIZATION (IF JOINT OR OTHER THAN NIST, SEE INSTRUCTIONS)

Worcester Polytechnic Institute
Center for Firesafety Studies
Worcester, MA 01609

7. CONTRACT/GRANT NUMBER
NIST Grant 60NANBOD1049

8. TYPE OF REPORT AND PERIOD COVERED
Final Rept. Aug. 1990 - July 1991

9. SPONSORING ORGANIZATION NAME AND COMPLETE ADDRESS (STREET, CITY, STATE, ZIP)

U.S. Department of Commerce
National Institute of Standards & Technology
Gaithersburg, MD 20899

10. SUPPLEMENTARY NOTES

11. ABSTRACT (A 200-WORD OR LESS FACTUAL SUMMARY OF MOST SIGNIFICANT INFORMATION. IF DOCUMENT INCLUDES A SIGNIFICANT BIBLIOGRAPHY OR LITERATURE SURVEY, MENTION IT HERE.)

Although both confined and unconfined smooth ceiling jets have been previously studied, the data from small-scale experiments evaluated in this report provided a unique opportunity to characterize the transience of a ceiling jet in the presence of a developing upper layer. The development of an upper layer in an enclosure fire has notable effects on the ceiling jet. The presence of this hot gas layer increases the temperature in the ceiling jet and the heat transfer to the ceiling. Accurate prediction of the characteristics of the confined ceiling jet is important in calculating the response time of detection and suppression devices. This report examines data from a study of small-scale fire induced ceiling jet in a confined situation for a smooth horizontal ceiling. These results were obtained from experiments conducted at the Nattional Institute of Standards and Technology, Center fro Fire Research using 2.0 and 0.75 kW fires at r/H locations of 0.26 and 0.75. The data gathered from these experiments represents a collection of transient and steady-state temperature and velocity measurements of a confined ceiling jet and upper layer. The results from this data were compared to similar experimental data collected in a previous study for unconfined ceiling jet using the same apparatus. Comparison of the confined and unconfined ceiling jet data, quantifincation of the developing upper layer and analysis of heat transfer to the ceiling, are presented in this report. Despite the limited data, it is concluded that the unconfined ceiling jet correlations may only be valid at the very early time, prior to development of the upper layer and that steady-state unconfined correlations are certainly invalid for confined conditions. The velocity of the confined ceiling jet within the upper layer is 20-25% less than the unconfined case affecting the heat transfer coefficient.

12. KEY WORDS (6 TO 12 ENTRIES; ALPHABETICAL ORDER; CAPITALIZE ONLY PROPER NAMES; AND SEPARATE KEY WORDS BY SEMICOLONS)

ceiling jets; ceilings; fire plumes; heat transfer; temperature; walls

13. AVAILABILITY

[X] UNLIMITED

[ ] FOR OFFICIAL DISTRIBUTION. DO NOT RELEASE TO NATIONAL TECHNICAL INFORMATION SERVICE (NTIS).

[ ] ORDER FROM SUPERINTENDENT OF DOCUMENTS, U.S. GOVERNMENT PRINTING OFFICE, WASHINGTON, DC 20402.

[X] ORDER FROM NATIONAL TECHNICAL INFORMATION SERVICE (NTIS), SPRINGFIELD, VA 22161.

14. NUMBER OF PRINTED PAGES
151

15. PRICE
A08

ELECTRONIC FORM